

Summer School 2014: **Inverse Problem and Image Processing**

**Inverse modeling in inverse problems  
using optimization**

Mila Nikolova

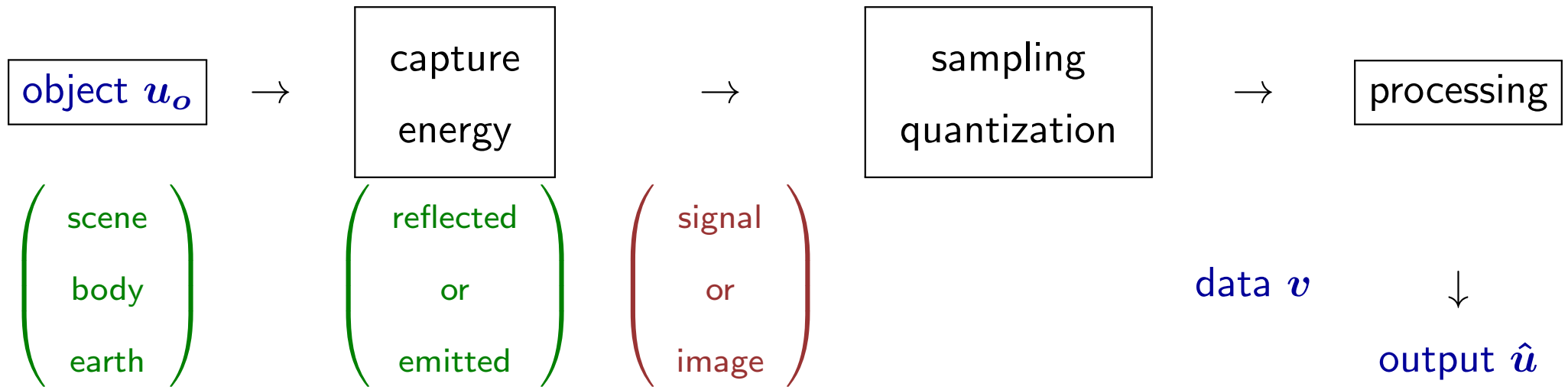
CMLA – CNRS, ENS Cachan, France

`nikolova@cmla.ens-cachan.fr`

`http://mnikolova.perso.math.cnrs.fr`

**Institute of Applied Physics and Computational Mathematics, Old yard**

**Beijing, 14-17 July, 2014**



**Mathematical model:**  $v = \text{Transform}(u_o) \bullet (\text{Perturbations})$

Some transforms: loss of pixels, blur, FT, Radon T., frame T. ( $\dots$ )

**Processing tasks:**  $\begin{cases} \hat{u} = \text{recover}(u_o) \\ \hat{u} = \text{objects of interest}(u_o) \end{cases} (\dots)$

Mathematical tools: PDEs, Statistics, Functional anal., Matrix anal., ( $\dots$ )

Example due to R.S. Wilson

$u_o$  (unknown-signal, picture, density map)

$v$  (data, degraded) = Transform( $u_o$ ) +  $n$  (noise)

An ill-posed inverse problem

$$u_o = [1 \ 1 \ 1 \ 1]^T$$

Transform:

$$A = \begin{bmatrix} 10 & 7 & 8 & 7 \\ 7 & 5 & 6 & 5 \\ 8 & 6 & 10 & 9 \\ 7 & 5 & 9 & 10 \end{bmatrix}$$

$$\text{rank}(A) = 4$$

• no noise:  $v = Au_o = [32 \ 23 \ 33 \ 31]^T \Rightarrow \hat{u} = A^{-1}v = u_o$

• with noise:  $v = Au_o + n = [32.1 \ 22.9 \ 33.1 \ 30.9]^T$

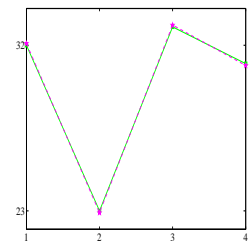
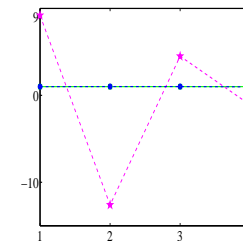
Least-squares solution:  $\hat{u} = \arg \min_{u \in \mathbb{R}^4} \{ \|Au - v\|^2 \} = A^{-1}v$

$$\Rightarrow \hat{u} = [9.2 \ -12.6 \ 4.5 \ -1.1]^T$$

Tikhonov regularization:  $\hat{u} = \arg \min_{u \in \mathbb{R}^4} \mathcal{F}_v(u)$

$$\mathcal{F}_v(u) \stackrel{\text{def}}{=} \|Au - v\|^2 + \beta \sum_{i=1}^3 (u[i+1] - u[i])^2$$

$$\beta = 1 \Rightarrow \hat{u} = [1 \ 1.01 \ 1.02 \ 0.98]^T$$



Image/signal processing tasks often require to solve **ill-posed inverse problems**

Out-of-focus picture:  $v = a * u_o + \text{noise} = Au_o + \text{noise}$

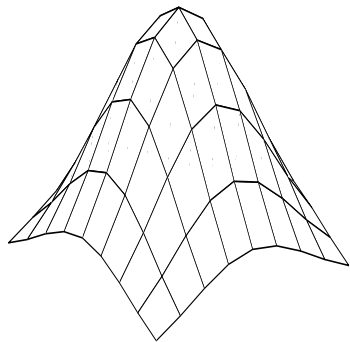
$A$  is ill-conditioned  $\equiv$  (nearly) noninvertible

Least-squares solution:  $\hat{u} = \arg \min_u \{ \|Au - v\|^2 \}$

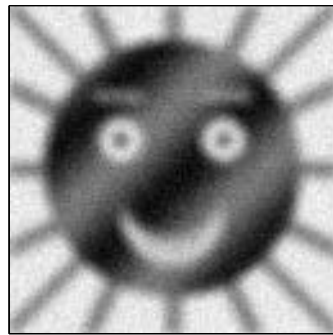
Tikhonov regularization:  $\hat{u} := \arg \min_u \{ \|Au - v\|^2 + \beta \sum_i \|G_i u\|^2 \}$  for  $\{G_i\} \approx \nabla$ ,  $\beta > 0$



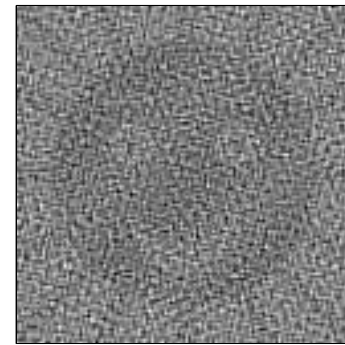
Original  $u_o$



Blur  $a$



Data  $v$

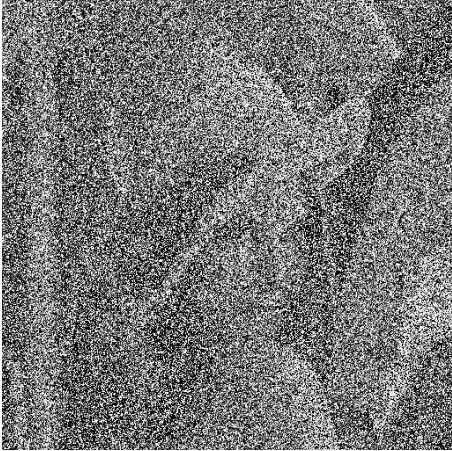


$\hat{u}$ : Least-squares



$\hat{u}$ : Tikhonov

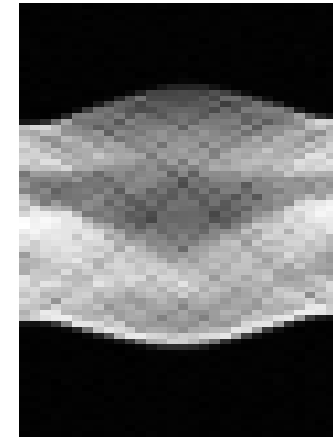
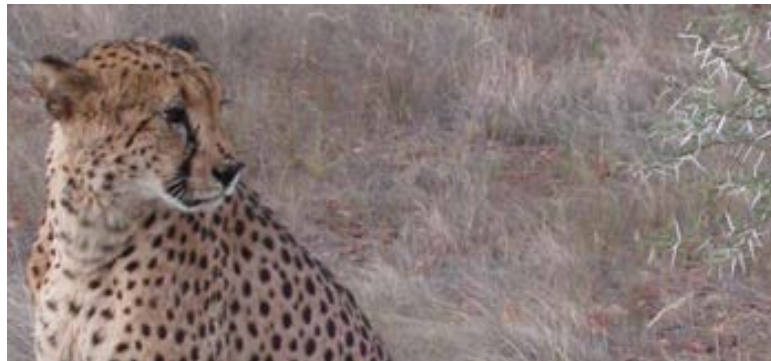




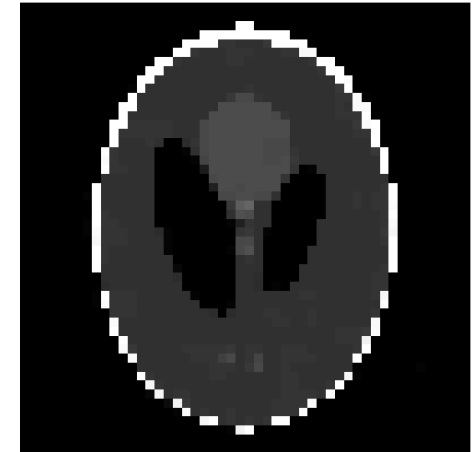
Impulse noise



Jitter (video)



Radon (tomography)



Formulate your problem as the minimization (maximization) of a functional (an energy) whose solution is the sought after signal/image

Goal of this tutorial: How to choose your energy  $\mathcal{F}_v$ ?

Approach: Salient features of the minimizers of classes of energies  $\mathcal{F}_v$

## Outline

1. Energy minimization methods (p. 7)
2. Regularity results (p. 17)
3. Non-smooth regularization – minimizers are sparse in a given subspace (p. 26)
4. Non-smooth data-fidelity – minimizers fit exactly some data entries (p. 35)
5. Comparison with Fully Smooth Energies (p. 51)
6. Non-convex regularization – edges are sharp (p. 54)
7. Nonsmooth data-fidelity and regularization – peculiar features (p. 62)
8. Fully smoothed  $\ell_1$ –TV models – bounding the residual (p. 83)
9. Inverse modeling and Bayesian MAP – there is distortion (p. 98)
10. Some References (p. 103)

# 1. Energy minimization methods

$$u_o \text{ (unknown)} \quad v \text{ (data)} = \text{Transform}(u_o) \bullet \text{(Perturbations)}$$

solution  $\hat{u}$

$$\hat{u} \begin{cases} \nearrow & \text{close to data production model } \Psi(u, v) \quad \text{(data-fidelity)} \\ \searrow & \text{coherent with priors and desiderata } \Phi(u) \quad \text{(prior – functional, constraint )} \end{cases}$$

Combining models:  $\hat{u} := \arg \min_{u \in \Omega} \mathcal{F}_v(u) \quad (\mathcal{P})$

$$\mathcal{F}_v(u) := \Psi(u, v) + \beta \Phi(u), \quad \beta > 0$$

How to choose  $(\mathcal{P})$  to get a good  $\hat{u}$  ?

Applications: Denoising, Segmentation, Deblurring, Tomography, Seismic imaging, Zoom, Superresolution, Compression, Learning, Motion estimation, Pattern recognition ( $\dots$ )

The  $m \times n$  image  $u$  is stored in a  $p = mn$ -length vector,  $u \in \mathbb{R}^p$ , data  $v \in \mathbb{R}^q$

$\Psi$  usually models the production of data  $\mathbf{v}$   $\Rightarrow \Psi = -\log(\text{Likelihood}(\mathbf{v}|\mathbf{u}))$

$$v = Au_o + n \text{ for } n \text{ white Gaussian noise} \Rightarrow \boxed{\Psi(u, v) \propto \|Au - v\|_2^2}$$

The information on  $\mathbf{u}$  we have is implicitly contained in  $\Psi$ . It is scarcely enough.

A good prior  $\Phi$  is needed to solve our task.

$\Phi$  model for the unknown  $\mathbf{u}$  (statistics, smoothness, edges, textures, expected features)

- Bayesian approach
- Variational approach

Both approaches lead to similar energies

$$\text{Prior via regularization term} \quad \Phi(\mathbf{u}) = \sum_i \varphi(\|G_i \mathbf{u}\|)$$

$\varphi : \mathbb{R}_+ \rightarrow \mathbb{R}_+$  potential function (PF)

$\{G_i\}$  — linear operators. Examples : Id,  $\nabla$ ,  $\nabla^2$ ,  $\nabla \widetilde{W}$  for  $\widetilde{W}$  left inverse of a frame if  $u = W(\text{image})$

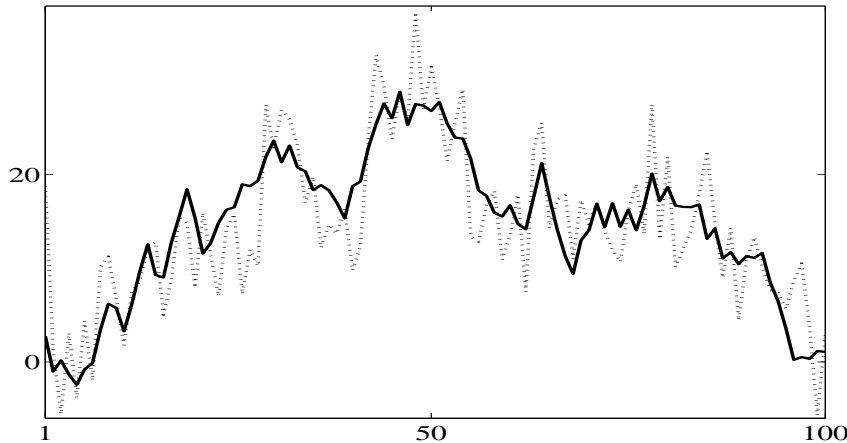
Bayes:  $U, V$  random variables, Likelihood  $f_{V|U}(v|u)$ , Prior  $f_U(u) \propto \exp\{-\lambda\Phi(u)\}$

Maximum a Posteriori (MAP) yields the most likely solution  $\hat{u}$  given the data  $V = v$ :

$$\begin{aligned}\hat{u} = \arg \max_u f_{U|V}(u|v) &= \arg \min_u \left( -\ln f_{V|U}(v|u) - \ln f_U(u) \right) \\ &= \arg \min_u \left( \Psi(u, v) + \beta\Phi(u) \right) = \arg \min_u \mathcal{F}_v(u)\end{aligned}$$

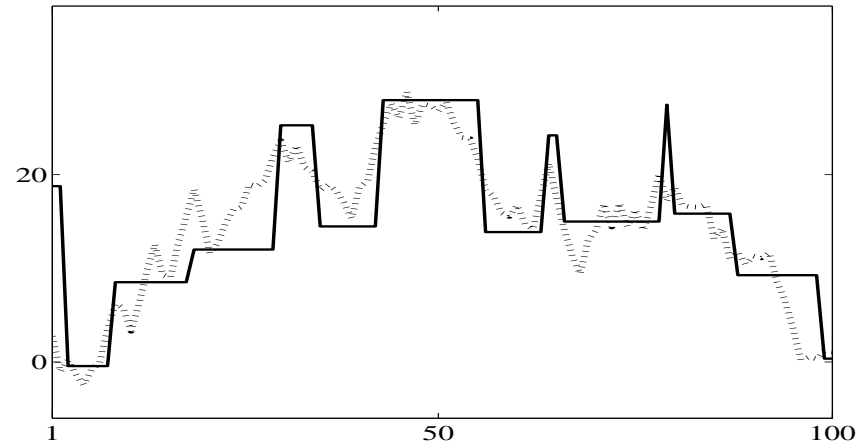
MAP is a very usual way to combine models on data-acquisition and priors

Realist models for data-acquisition  $f_{V|U}$  and prior  $f_U$  is still an open question



Original  $u_o \sim f_U$  (—)

Data  $v = u_o + \text{noise}$  ( $\cdots$ ), noise  $\sim f_{V|U}$



The true MAP  $\hat{u}$  (—)

The original  $u_o$  ( $\cdots$ )

Are you satisfied with the solution?

- **Minimizer approach** (the core of our tutorials)
  - Analyze the main properties exhibited by the (local) minimizers  $\hat{u}$  of  $\mathcal{F}_v$  as a function of the shape of  $\mathcal{F}_v$

Strong results.

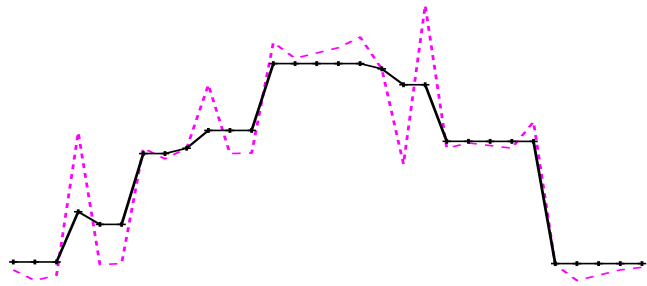
**Rigorous tools for modelling**

- Conceive  $\mathcal{F}_v$  so that the properties of  $\hat{u}$  satisfy your requirements.

(a “chicken and egg” problem?)

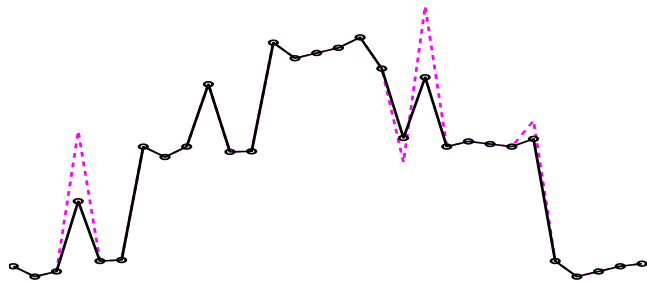
*“There is nothing quite as practical as a good theory.” Kurt Lewin*

## Illustration: the role of the smoothness of $\mathcal{F}_v$



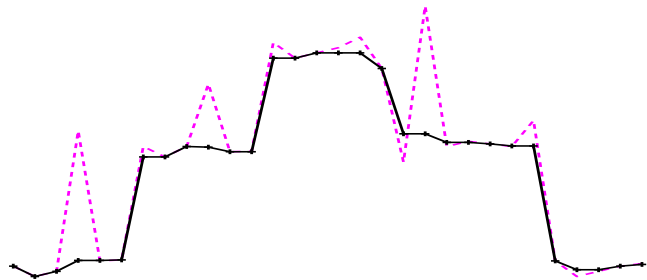
STAIR-CASING

$$\mathcal{F}_v(u) = \underbrace{\sum_{i=1}^p (u_i - v_i)^2}_{\text{smooth}} + \beta \underbrace{\sum_{i=1}^{p-1} |u_i - u_{i+1}|}_{\text{non-smooth}}$$



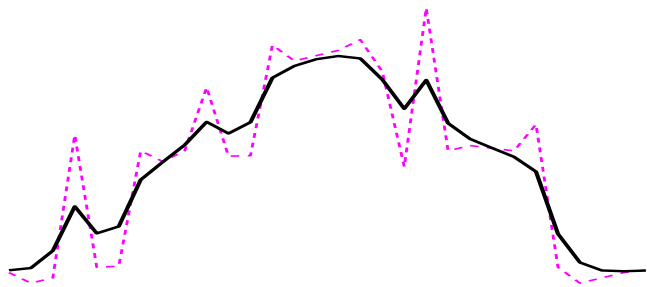
EXACT DATA-FIT

$$\mathcal{F}_v(u) = \underbrace{\sum_{i=1}^p |u_i - v_i|}_{\text{non-smooth}} + \beta \underbrace{\sum_{i=1}^{p-1} (u_i - u_{i+1})^2}_{\text{smooth}}$$



BOTH EFFECTS

$$\mathcal{F}_v(u) = \underbrace{\sum_{i=1}^p |u_i - v_i|}_{\text{non-smooth}} + \beta \underbrace{\sum_{i=1}^{p-1} |u_i - u_{i+1}|}_{\text{non-smooth}}$$



$$\mathcal{F}_v(u) = \underbrace{\sum_{i=1}^p (u_i - v_i)^2}_{\text{smooth}} + \beta \underbrace{\sum_{i=1}^{p-1} (u_i - u_{i+1})^2}_{\text{smooth}}$$

Data (---), Minimizer (—)

We shall explain why and how to use

## Some energy functions

Regularization [Tikhonov, Arsenin 77]:  $\mathcal{F}_v(u) = \|Au - v\|^2 + \beta \|Gu\|^2$ ,  $G = I$  or  $G \approx \nabla$

Focus on edges, contours, segmentation, labeling

Statistical framework

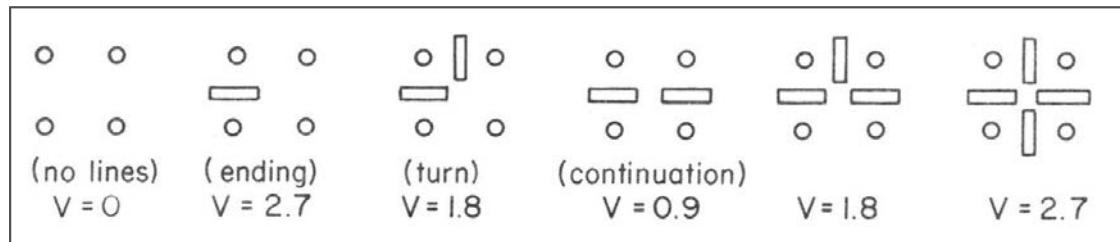
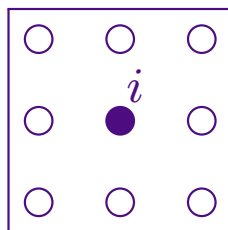
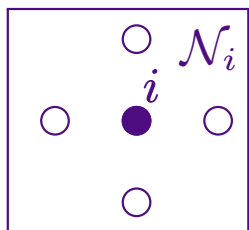
Potts model [Potts 52] ( $\ell_0$  semi-norm applied to differences):

$$\mathcal{F}_v(u) = \Psi(u, v) + \beta \sum_{i,j} \phi(u[i] - u[j]) \quad \phi(t) := \begin{cases} 0 & \text{if } t = 0 \\ 1 & \text{if } t \neq 0 \end{cases}$$

Line process in Markov random field priors [Geman, Geman 84]:  $(\hat{u}, \hat{\ell}) = \arg \min_{u, \ell} \mathcal{F}_v(u, \ell)$

$$\mathcal{F}_v(u, \ell) = \Psi(u, v) + \beta \sum_i \left( \sum_{j \in \mathcal{N}_i} \varphi(u[i] - u[j]) (1 - \ell_{i,j}) + \sum_{(k,n) \in \mathcal{N}_{i,j}} V(\ell_{i,j}, \ell_{k,n}) \right)$$

$[\ell_{i,j} = 0 \Leftrightarrow \text{no edge}]$ ,  $[\ell_{i,j} = 1 \Leftrightarrow \text{edge between } i \text{ and } j]$ ,  $\varphi(t) = 1$





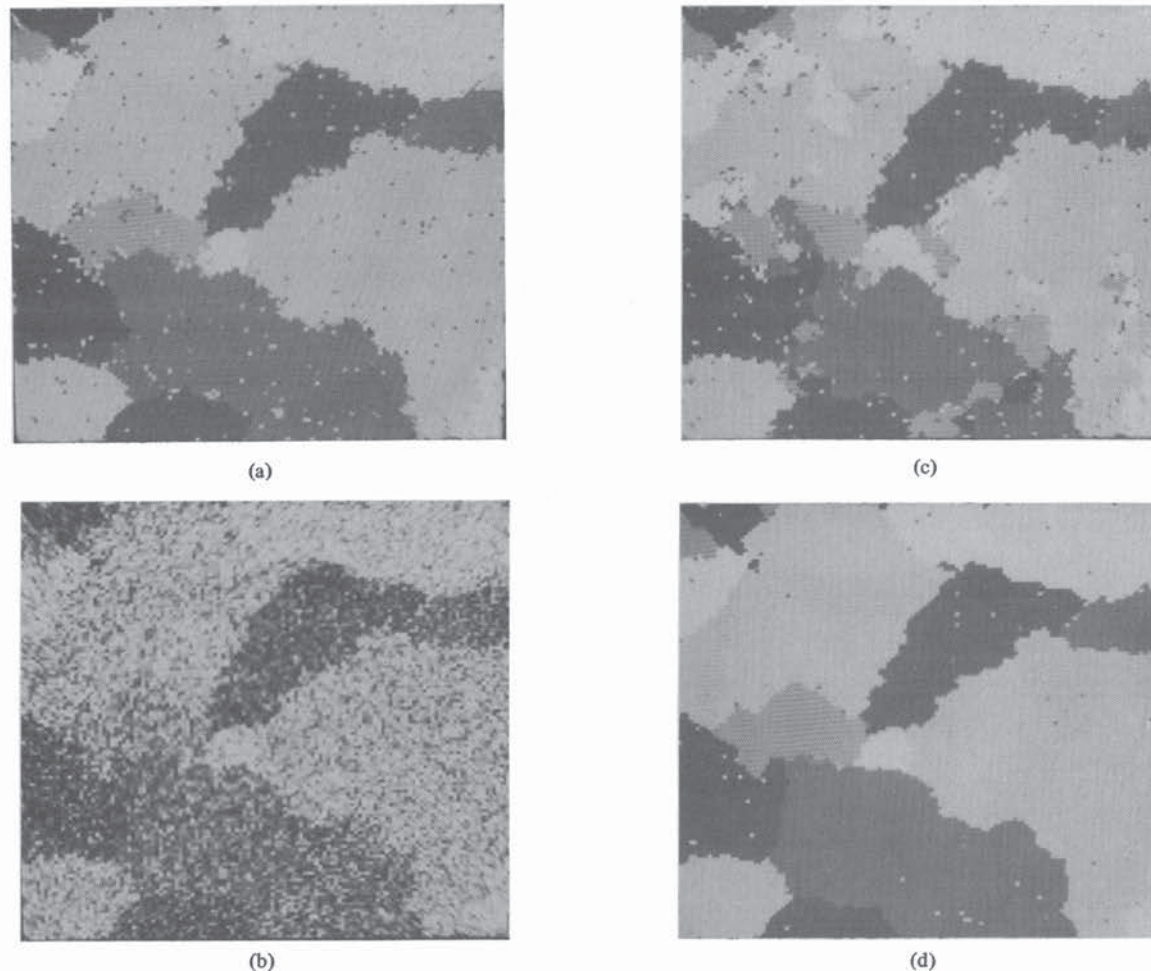


Fig. 2. (a) Original image: Sample from MRF. (b) Degraded image: Additive noise. (c) Restoration: 25 iterations. (d) Restoration: 300 iterations.

Image credits: S. Geman and D. Geman 1984. Restoration with 5 labels using Gibbs sampler

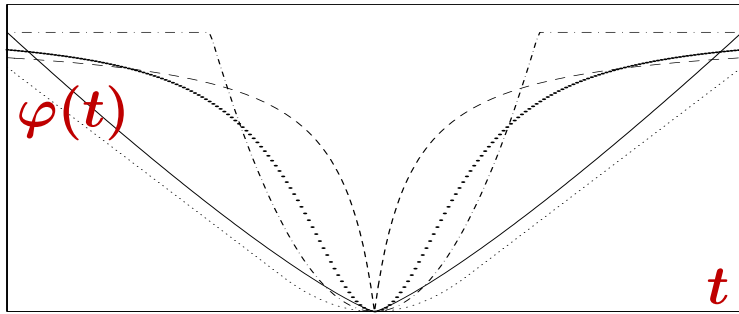
*“We make an analogy between images and statistical mechanics systems. Pixel gray levels and the presence and orientation of edges are viewed as states of atoms or molecules in a lattice-like physical system. The assignment of an energy function in the physical system determines its Gibbs distribution. Because of the Gibbs distribution, Markov random field (MRF) equivalence, this assignment also determines an MRF image model.” [S. Geman, D. Geman 84]*

M.-S. functional [Mumford, Shah 89]:  $\mathcal{F}_v(u, L) = \int_{\Omega} (u - v)^2 dx + \beta \left( \int_{\Omega \setminus L} \|\nabla u\|^2 dx + \alpha |L| \right)$

discrete version:  $\Phi(u) = \sum_i \varphi(\|G_i u\|), \quad \varphi(t) = \min\{t^2, \alpha\}, \quad \{G_i\} \approx \nabla$

Total Variation (TV) [Rudin, Osher, Fatemi 92]:  $\mathcal{F}_v(u) = \|u - v\|_2^2 + \beta \mathbf{TV}(u)$

$$\mathbf{TV}(u) = \int \|\nabla u\|_2 dx \approx \sum_i \|G_i u\|_2$$



Various edge-preserving functions  $\varphi$  to define  $\Phi$

$\varphi$  is edge-preserving if  $\lim_{t \rightarrow \infty} \frac{\varphi'(t)}{t} = 0$

[Charbonnier, Blanc-Féraud, Aubert, Barlaud 97 ...]

Minimizer approach

$\ell_1$  – Data fidelity [Nikolova 02]:  $\mathcal{F}_v(u) = \|Au - v\|_1 + \beta \Phi(u)$

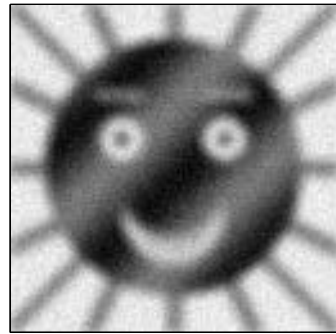
$L_1$  – TV model [T. Chan, Esedoglu 05]:  $\mathcal{F}_v(u) = \|u - v\|_1 + \beta \mathbf{TV}(u)$

CPU time ! Computers ↑↑

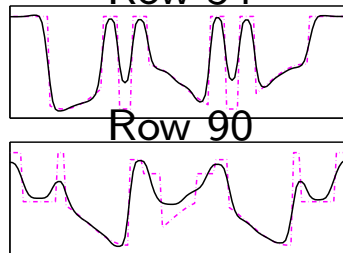
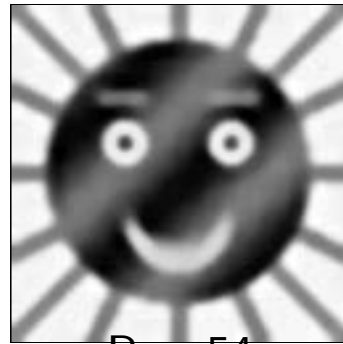
Original  $u_o$



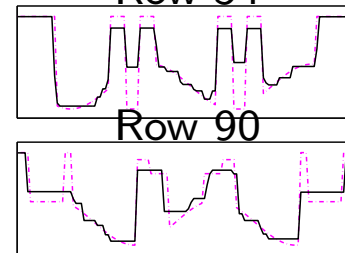
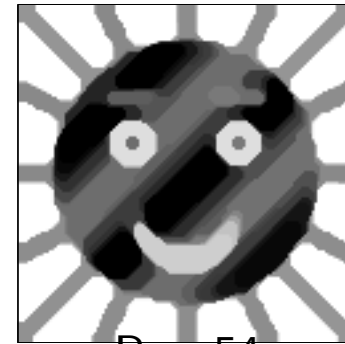
Data  $v = a * u_o + n$



$\varphi(t) = |t|^{\alpha \in (1,2)}$



$\varphi(t) = |t|$



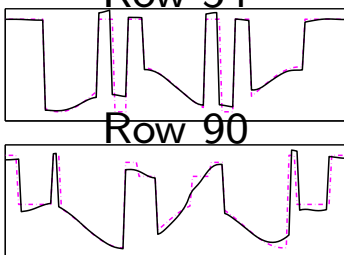
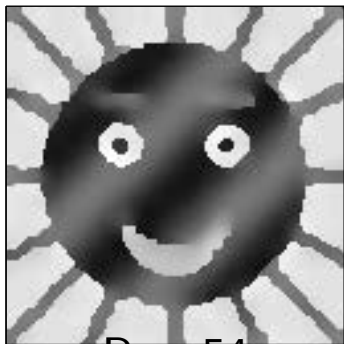
$$\mathcal{F}_v(u) = \|Au - v\|^2 + \beta \sum_i \varphi((\nabla u)[i])$$

$\varphi$  smooth at 0

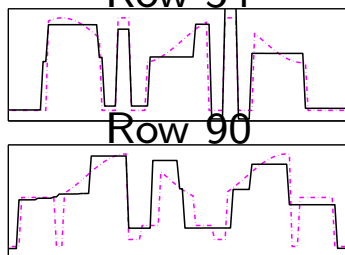
$\varphi$  nonsmooth at 0

$\varphi$   
c  
o  
n  
v  
e  
x

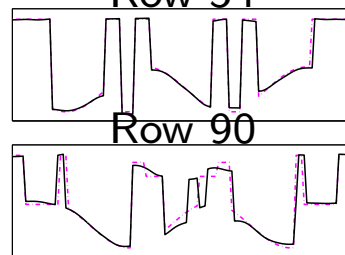
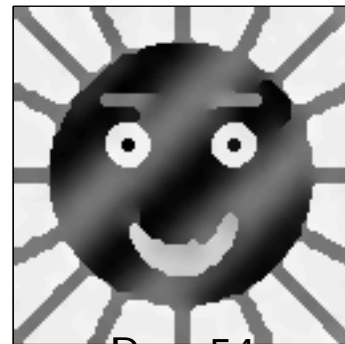
$\varphi(t) = at^2/(1 + at^2)$



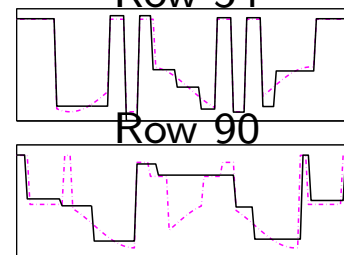
$\varphi(t) = \alpha|t|/(1 + \alpha|t|)$



$\varphi(t) = \min\{at^2, 1\}$



$\varphi(t) = 1 - \mathbb{1}_{(t=0)}$



n  
o  
n  
c  
o  
n  
v  
e  
x

## Summer School 2014: Inverse Problem and Image Processing

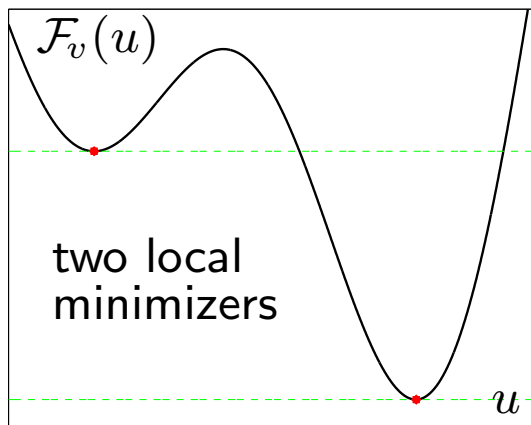
### Tutorial: Inverse modeling in inverse problems using optimization

#### Outline

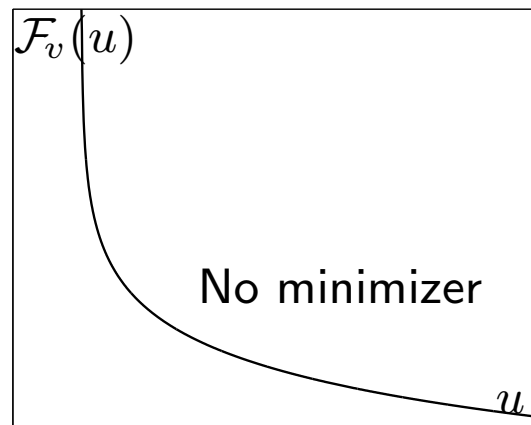
1. Energy minimization methods (p. 7)
2. Regularity results
3. Non-smooth regularization – minimizers are sparse in a given subspace (p. 26)
4. Non-smooth data-fidelity – minimizers fit exactly some data entries (p. 35)
5. Comparison with Fully Smooth Energies (p. 51)
6. Non-convex regularization – edges are sharp (p. 54)
7. Nonsmooth data-fidelity and regularization – peculiar features (p. 62)
8. Fully smoothed  $\ell_1$ –TV models – bounding the residual (p. 83)
9. Inverse modeling and Bayesian MAP – there is distortion (p. 98)
10. Some References (p. 103)

## 2 Regularity Results

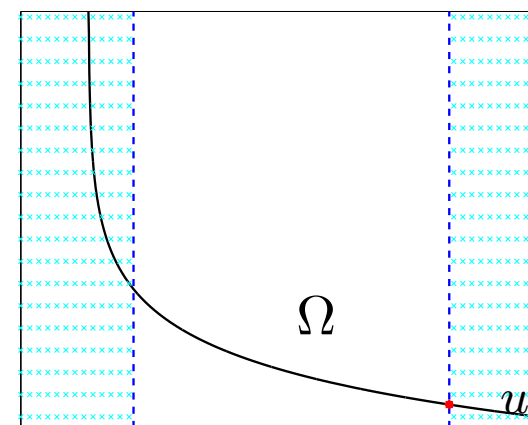
### Optimization problems



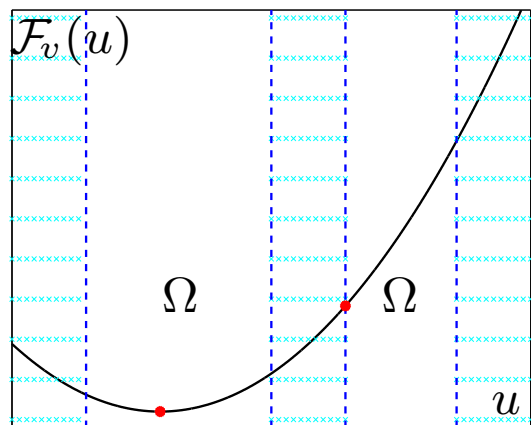
$\mathcal{F}_v$  nonconvex



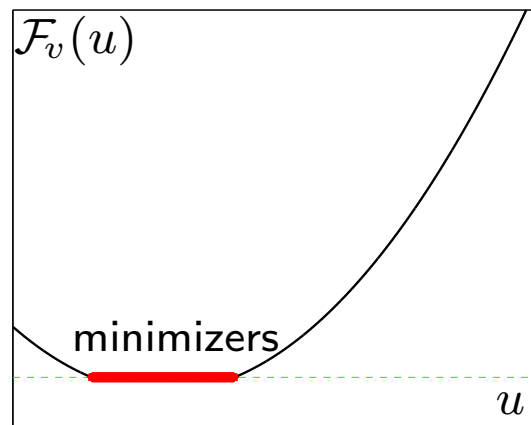
$\mathcal{F}_v$  convex non coercive  $\Omega = \mathbb{R}$



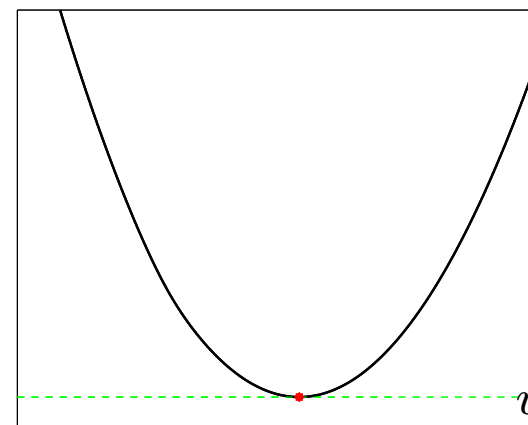
$\mathcal{F}_v$  convex non coercive  $\Omega$  compact



$\mathcal{F}_v$  strictly convex,  $\Omega$  nonconvex



$\mathcal{F}_v$  non strictly convex



$\mathcal{F}_v$  strictly convex on  $\mathbb{R}$

$$\mathcal{F}_v : \Omega \rightarrow \mathbb{R} \quad \Omega \subset \mathbb{R}^p$$

- Set of optimal solutions  $\hat{U} = \{\hat{u} \in \Omega : \mathcal{F}_v(\hat{u}) \leq \mathcal{F}_v(u) \quad \forall u \in \Omega\}$

$\hat{U} = \{u\}$  if  $\mathcal{F}_v$  strictly convex

$\hat{U} \neq \emptyset$  if  $\mathcal{F}_v$  coercive or if  $\mathcal{F}_v$  continuous and  $\Omega$  compact

Otherwise – check

(e.g. see if  $\mathcal{F}_v$  is asymptotically level stable [Auslender, Teboulle 03])

- Nonconvex problems:

Algorithms may get trapped in local minima

A “good” local minimizer can be satisfying

Global optimization – difficult, but progress, e.g. [Robini, Reissman JGO 13]

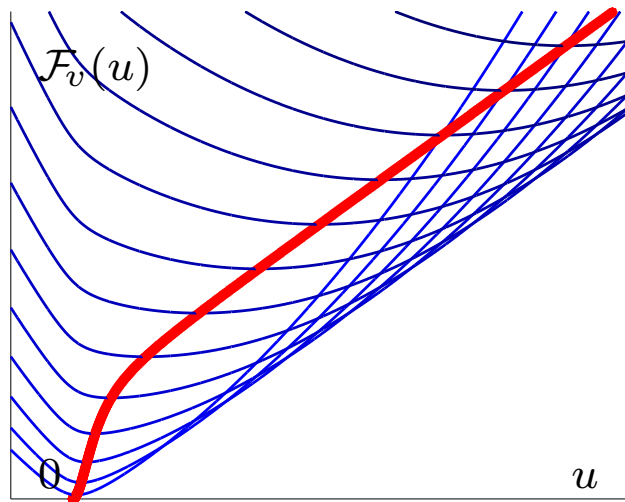
Convex relaxation methods, see, e.g., [Yuan, Bae, Tai CVPR 10]

- Attention to numerical errors

Definition:  $\mathcal{U} : \mathcal{O} \rightarrow \mathbb{R}^p$ ,  $\mathcal{O} \subset \mathbb{R}^q$  open, is a (local) minimizer function for

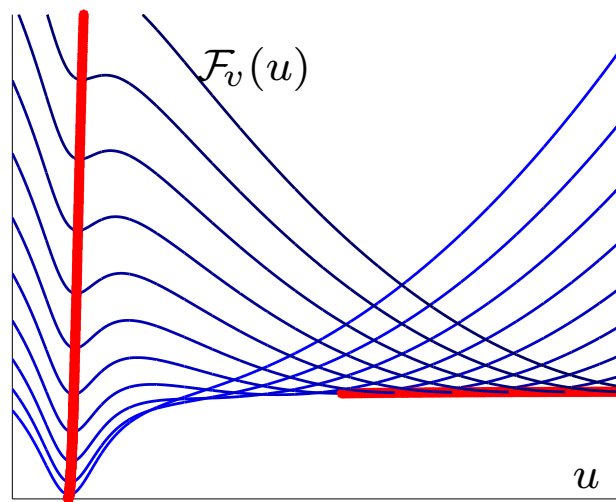
$\mathcal{F}_{\mathcal{O}} := \{\mathcal{F}_v : v \in \mathcal{O}\}$  if  $\mathcal{F}_v$  has a strict (local) minimum at  $\mathcal{U}(v)$ ,  $\forall v \in \mathcal{O}$

Minimizer functions – an useful tool to analyze the properties of minimizers...



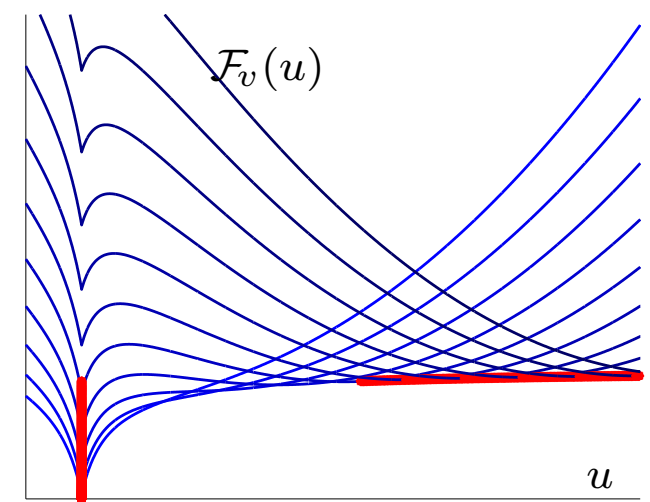
$$\mathcal{F}_v(u) = (u - v)^2 + \beta\sqrt{\alpha + u^2}$$

minimizer function (●●)



$$\mathcal{F}_v(u) = (u - v)^2 + \beta\frac{\alpha u^2}{1 + \alpha u^2}$$

local minimizer functions (●●)



$$\mathcal{F}_v(u) = (u - v)^2 + \beta\frac{\alpha|u|}{1 + \alpha|u|}$$

global minimizer function (●●)

Each blue curve curve:  $u \rightarrow \mathcal{F}_v(u)$  for  $v \in \{0, 2, \dots\}$

**Question 1** What these plots reveal about the local / global minimizer functions?

$$\mathcal{F}_v(u) = \|Au - v\|_2^2 + \beta\Phi(u)$$

$$\Phi(u) = \sum_i \varphi(\|G_i u\|_2)$$

$$u \in \mathbb{R}^p$$

$$v \in \mathbb{R}^q$$

$$\left\{ \begin{array}{l} \varphi : \mathbb{R}_+ \rightarrow \mathbb{R} \\ \varphi \text{ increasing, continuous} \\ \varphi(t) > \varphi(0), \quad \forall t > 0 \end{array} \right.$$

$\{G_i\}$  linear operators  $\mathbb{R}^p \rightarrow \mathbb{R}^s$ ,  $s \geq 1$

$\varphi'(0^+) > 0 \Rightarrow \Phi$  is nonsmooth on  $\bigcup_i \{u : G_i u = 0\}$

Systematically:  $\ker A \cap \ker G = \{0\}$

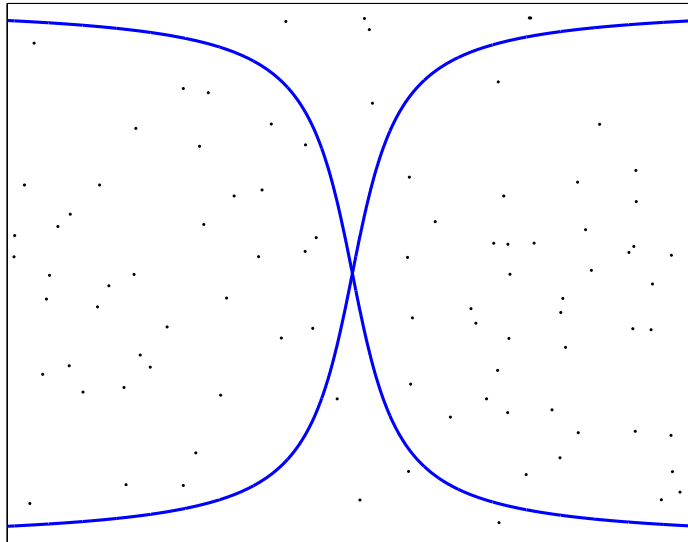
$$G := \begin{bmatrix} G_1 \\ G_2 \\ \dots \end{bmatrix}$$

Recall:

$\mathcal{F}_v$  has a (local) minimum at  $\hat{u} \Rightarrow \delta\mathcal{F}_v(\hat{u})(d) = \lim_{t \downarrow 0} \frac{\mathcal{F}_v(u+td) - \mathcal{F}_v(u)}{t} \geq 0, \quad \forall d \in \mathbb{R}^p$

$\mathcal{F}_v$  nonconvex  $\Rightarrow$  there may be many local minima





- $N = \{(s, t) : t = \pm \arctan(s)\}$
- $N$  is closed in  $\mathbb{R}^2$  and its Lebesgue measure in  $\mathbb{R}^2$  is  $\mathbb{L}^2(N) = 0$
- $(x, y) = \text{random } \mathbb{R}^2$

**Question 2** What is the chance that  $(x, y) \in N$ ?

## Stability of the minimizers of $\mathcal{F}_v$

[Durand & Nikolova 06]

*Assumptions:*  $\varphi : \mathbb{R}_+ \rightarrow \mathbb{R}$  is continuous and  $\mathcal{C}^{m \geq 2}$  on  $\mathbb{R}_+ \setminus \{\theta_1, \dots, \theta_n\}$ ,  
edge-preserving, possibly **non-convex** and  $\text{rank}(A) = p$

### A. LOCAL MINIMIZERS

(knowing local minimizers is important)

There is a **closed**  $N \subset \mathbb{R}^q$  with Lebesgue measure  $\mathbb{L}^q(N) = 0$  such that  $\forall v \in \mathbb{R}^q \setminus N$ , every (local) minimizer  $\hat{u}$  of  $\mathcal{F}_v$  is given by  $\hat{u} = \mathcal{U}(v)$  where  $\mathcal{U}$  is a  $\mathcal{C}^{m-1}$  (local) minimizer function.

**Question 3** For  $v \in \mathbb{R}^q \setminus N$ , compare  $\mathcal{U}(v)$  and  $\mathcal{U}(v + \varepsilon)$  where  $\varepsilon \in \mathbb{R}^q$  is small enough.

### B. GLOBAL MINIMIZERS

- $\exists \hat{N} \subset \mathbb{R}^q$  with  $\mathbb{L}^q(\hat{N}) = 0$  and  $\text{Int}(\mathbb{R}^q \setminus \hat{N})$  dense in  $\mathbb{R}^q$  such that  $\forall v \in \mathbb{R}^q \setminus \hat{N}$ ,  $\mathcal{F}_v$  has a **unique global minimizer**.
- There is an open subset of  $\mathbb{R}^q \setminus \hat{N}$ , dense in  $\mathbb{R}^q$ , where the global minimizer function  $\hat{\mathcal{U}}$  is  $\mathcal{C}^{m-1}$ -continuous.

**Question 4** What is the chance that  $v \in \hat{N}$ ? What can happen if  $v \in \hat{N}$ ?

# Nonasymptotic bounds on minimizers

[Nikolova 07]

Classical bounds for  $\beta \searrow 0$  or  $\beta \nearrow \infty$

Assumption:  $\varphi$  is piecewise  $\mathcal{C}^1$

- $\varphi$  is strictly increasing or  $\text{rank}(A) = p$

$$\hat{u} \text{ is a (local) minimizer of } \mathcal{F}_v \quad \Rightarrow \quad \|A\hat{u}\| \leq \|v\|$$

- $\|\varphi'\|_\infty = \text{constant}$  ( $\varphi$  is edge-preserving) and  $\text{rank}(A) = q \leq p$

$$\hat{u} \text{ is a (local) minimizer of } \mathcal{F}_v \quad \Rightarrow \quad \|v - A\hat{u}\|_\infty \leq \frac{\beta}{2} \|\varphi'\|_\infty \|(AA^*)^{-1}A\|_\infty \|G\|_1$$

$$\|\varphi'\|_\infty = 1, A = \text{Id and } G - 1^{\text{st}} \text{ order differences: } \begin{cases} \text{signal} & \Rightarrow \|v - \hat{u}\|_\infty \leq \beta \\ \text{image} & \Rightarrow \|v - \hat{u}\|_\infty \leq 2\beta \end{cases}$$

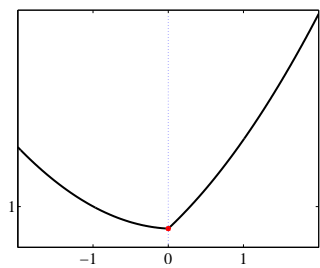
**Question 5** If  $v = u_o + n$  for  $n$  Gaussian noise, is it possible to clean  $v$  from this noise by minimizing  $\mathcal{F}_v$ ? (See  $\Psi$  on p. 8.)

# Non-Smooth Energies, Side Derivatives, Subdifferential

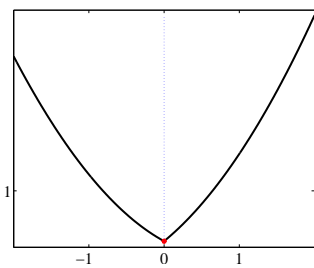
**Rademacher's theorem:** If  $\mathcal{F}_v : \mathbb{R}^p \rightarrow \mathbb{R}$  is Lipschitz continuous, then  $\mathcal{F}_v$  is differentiable (in the usual sense) almost everywhere in  $\mathbb{R}^p$ .

A *kink* is a point  $u$  where  $\nabla \mathcal{F}_v(u)$  is not defined (in the usual sense).

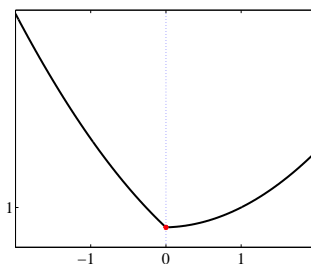
Example:  $\mathcal{F}_v(u) = \frac{1}{2}(u - v)^2 + \beta|u|$  for  $\beta = 1 > 0$  and  $u, v \in \mathbb{R}$



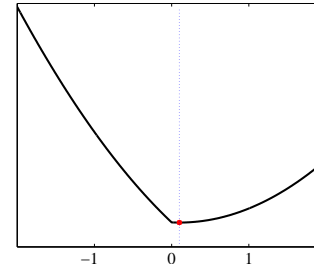
$$v = -0.9$$



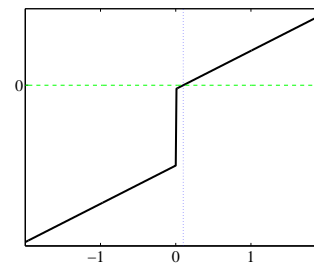
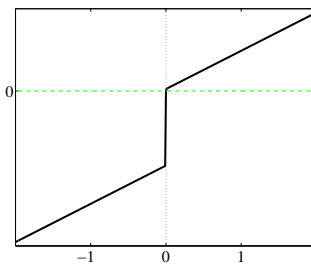
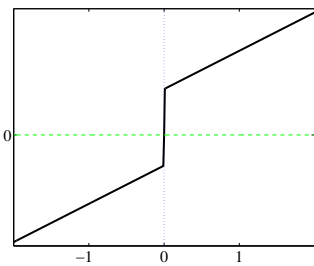
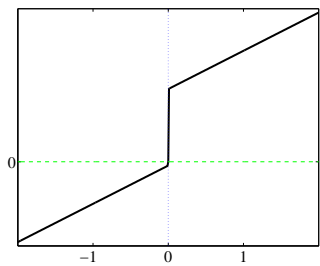
$$v = -0.2$$



$$v = 0.95$$



$$v = 1.1$$



$$\hat{u} = \begin{cases} v + \beta & \text{if } v < -\beta \\ 0 & \text{if } |v| \leq \beta \\ v - \beta & \text{if } v > \beta \end{cases}$$

**Question 6** Comment the minimizers on the 1st row. What is drawn on the 2nd row?

## Summer School 2014: Inverse Problem and Image Processing

### Tutorial: Inverse modeling in inverse problems using optimization

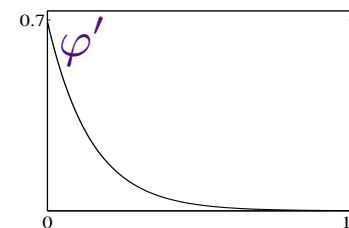
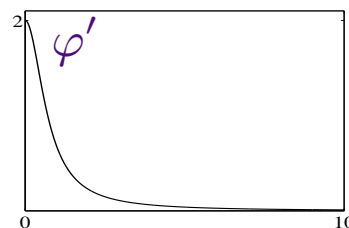
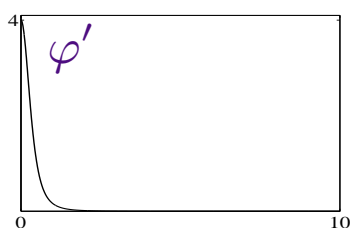
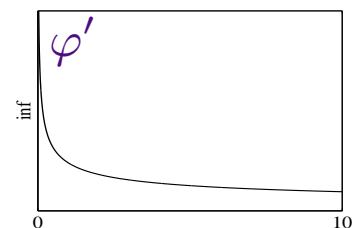
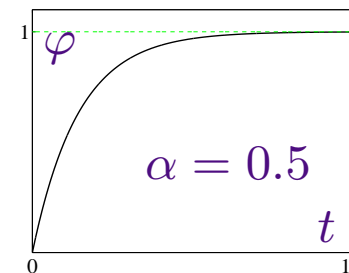
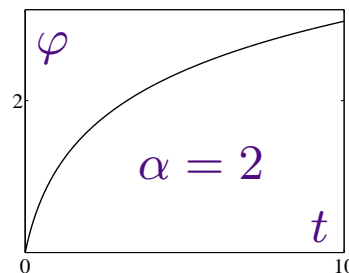
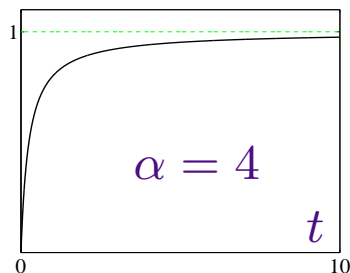
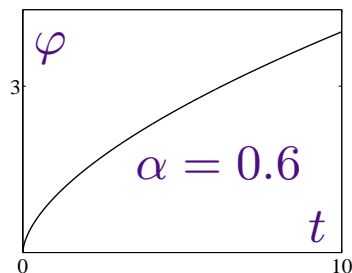
#### Outline

1. Energy minimization methods (p. 7)
2. Regularity results (p. 17)
3. Non-smooth regularization – minimizers are sparse in a given subspace
4. Non-smooth data-fidelity – minimizers fit exactly some data entries (p. 35)
5. Comparison with Fully Smooth Energies (p. 51)
6. Non-convex regularization – edges are sharp (p. 54)
7. Nonsmooth data-fidelity and regularization – peculiar features (p. 62)
8. Fully smoothed  $\ell_1$ –TV models – bounding the residual (p. 83)
9. Inverse modeling and Bayesian MAP – there is distortion (p. 98)
10. Some References (p. 103)

### 3 Minimizers under Non-Smooth Regularization

$$\mathcal{F}_v(u) = \Psi(u, v) + \beta \sum_{i=1}^r \varphi(\|G_i u\|), \quad \Psi \in \mathcal{C}^{m \geq 2}, \quad \varphi \in \mathcal{C}^m(\mathbb{R}_+^*), \quad 0 < \varphi'(0^+) \leq \infty$$

$$\varphi(t) \left\| \begin{array}{l} t^\alpha, \alpha \in (0, 1) \\ \frac{\alpha t}{\alpha t + 1} \\ \ln(\alpha t + 1) \\ 1 - \alpha^t, \alpha \in (0, 1) \\ (\dots), \alpha > 0 \end{array} \right.$$



$\varphi(t) = t$  and  $G_i u \approx (\nabla u)_i \Rightarrow \Phi(u) = \text{TV}(u)$  (total variation) [Rudin, Osher, Fatemi 92]

**General case**  $\mathcal{F}_v(u) = \Psi(u, v) + \beta \sum_{i=1}^r \varphi(\|G_i u\|)$   $\Psi \in \mathcal{C}^{m \geq 2}, \varphi'(0^+) > 0$

[Nikolova 97,00]

Let  $\hat{u}$  be a (local) minimizer of  $\mathcal{F}_v$ . Set  $\hat{h} := \{i : G_i \hat{u} = 0\}$

Then  $\exists \mathcal{O} \subset \mathbb{R}^q$  open,  $\exists \mathcal{U} \in \mathcal{C}^{m-1}$  (local) minimizer function so that

$$v' \in \mathcal{O}, \hat{u}' = \mathcal{U}(v') \Rightarrow G_i \hat{u}' = 0, \forall i \in \hat{h}$$

$$\hat{h} \subset \{1, \dots, r\} \quad \mathcal{O}_{\hat{h}} := \{v \in \mathbb{R}^q : G_i \mathcal{U}(v) = 0, \forall i \in \hat{h}\} \Rightarrow \mathbb{L}^q(\mathcal{O}_{\hat{h}}) > 0$$

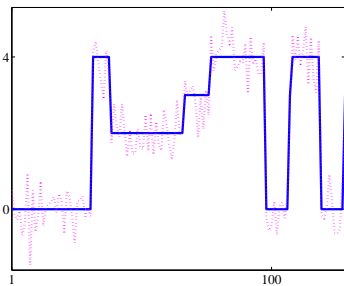
Data  $v$  yield (local) minimizers  $\hat{u}$  of  $\mathcal{F}_v$  such that  
 $G_i \hat{u} = 0$  for a set of indexes  $\hat{h}$

$G_i = \nabla_i \Rightarrow \hat{u}[i] = \hat{u}[j]$  for many neighbors  $(i, j)$  (the “stair-casing” effect)

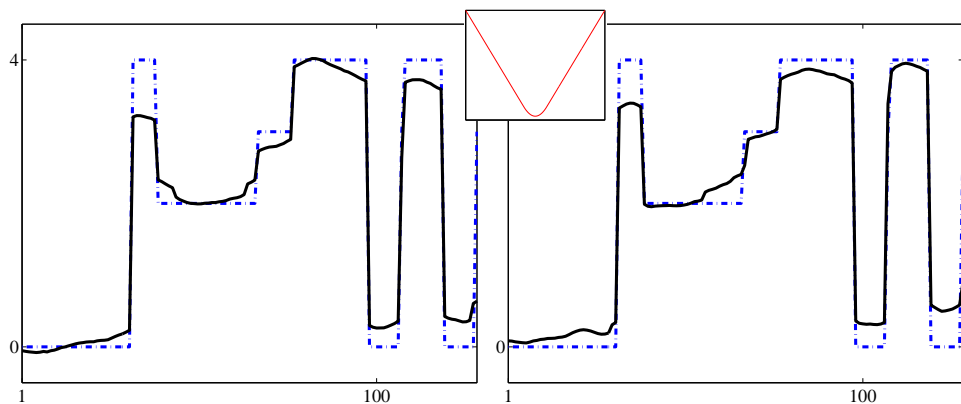
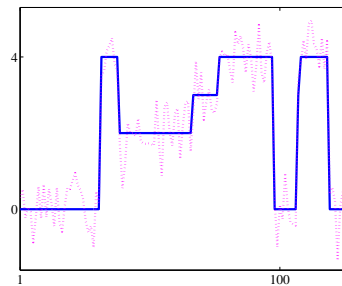
$G_i u = u[i] \Rightarrow$  many samples  $\hat{u}[i] = 0$  – highly used in Compressed Sensing

**Question 7** What happens if  $\{G_i\}$  yield second-order differences?

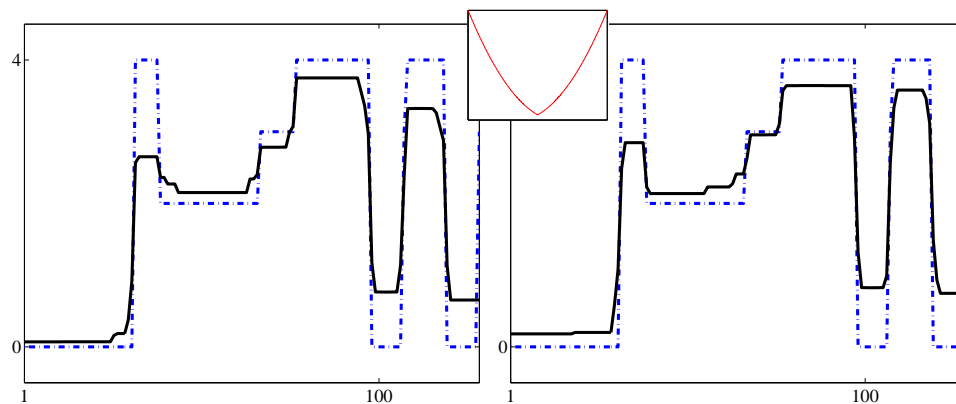
Property fails if  $\mathcal{F}_v$  is smooth, except for  $v \in N$  where  $N$  is closed and  $\mathbb{L}^q(N) = 0$ .



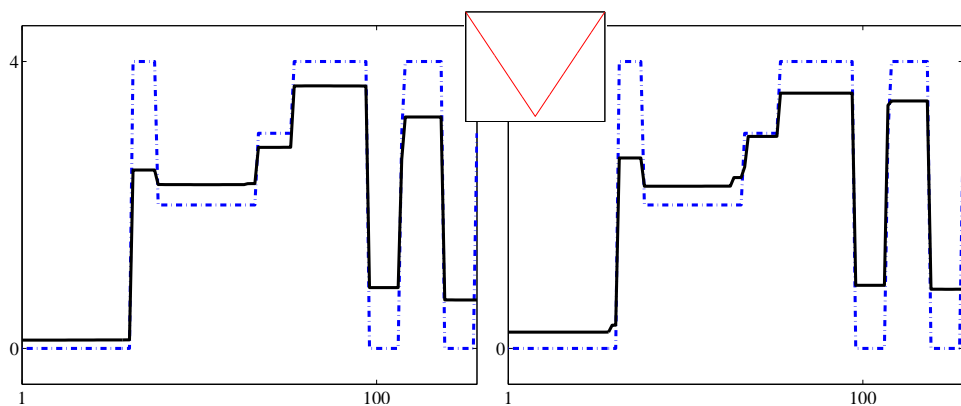
$$\mathcal{F}_v(u) = \|u - v\|^2 + \beta \sum \varphi(|u[i] - u[i-1]|)$$



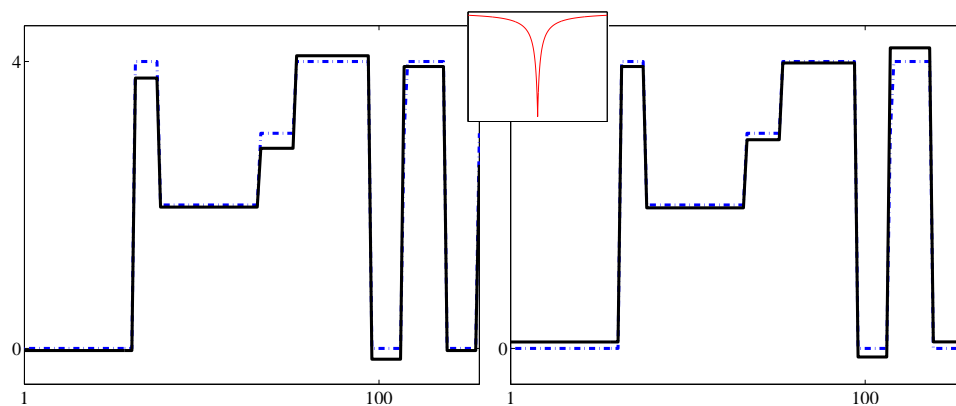
$$\varphi(t) = \sqrt{\alpha + t^2}, \quad \varphi'(0) = 0 \quad \text{(smooth at 0)}$$



$$\varphi(t) = (t + \alpha \text{sign}(t))^2, \quad \varphi'(0^+) = 2\alpha$$



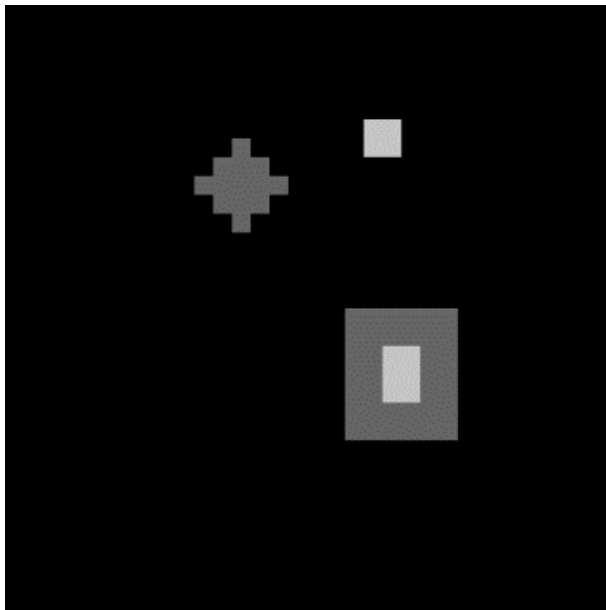
$$\varphi(t) = |t|, \quad \varphi'(0^+) = 1$$



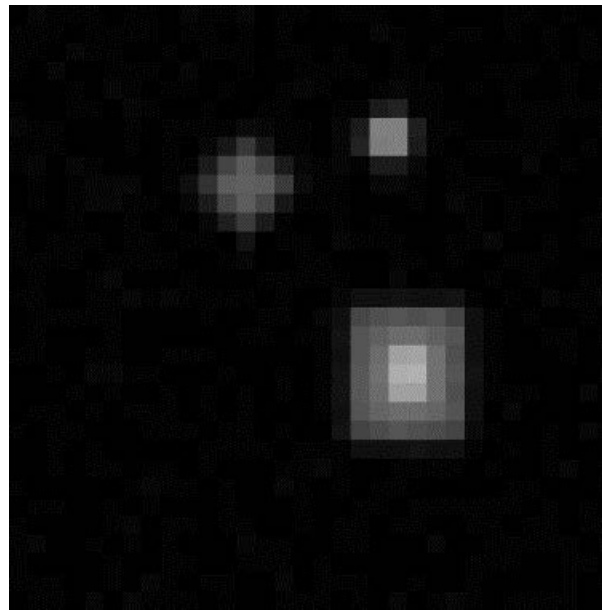
$$\varphi(t) = \alpha|t|/(1 + \alpha|t|), \quad \varphi'(0^+) = \alpha$$



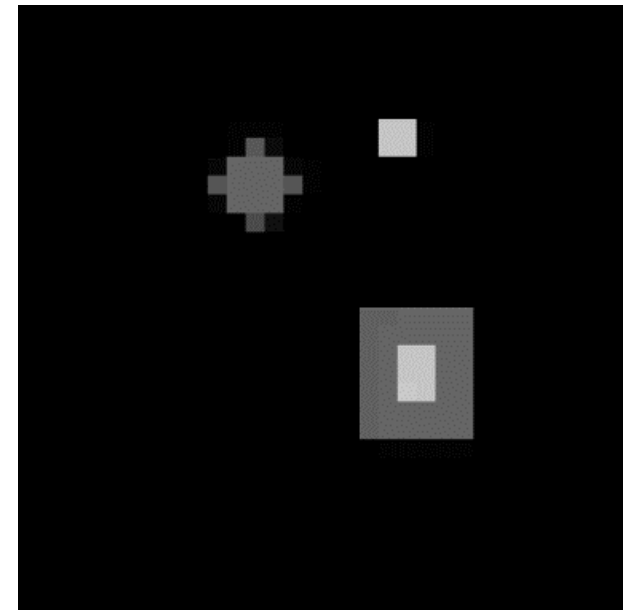
TV energy:  $\mathcal{F}_v(u) = \|Au - v\|^2 + \beta\text{TV}(u)$



Original



Data



Restored: TV energy

Image credit to the authors: D. C. Dobson and F. Santosa, "Recovery of blocky images from noisy and blurred data", SIAM J. Appl. Math., 56 (1996), pp. 1181-1199.

## Questions to clarify the main property

Let  $u_o \in \mathbb{R}$  and  $\text{pdf}(u_o) = \frac{1}{2}e^{-|u_o|}$  (Laplacian distribution)

**Question 8** Give  $\Pr(u_o = 0)$ .

Let  $v = u_o + n$  where  $\text{pdf}(n) = \frac{1}{\sigma\sqrt{2\pi}}e^{-\frac{n^2}{2\sigma^2}}$  (centered Gaussian distribution)

The corresponding MAP energy to recover  $u_o$  from  $v$  reads as

$$\mathcal{F}_v(u) = \frac{1}{2}(u - v)^2 + \beta|u| \quad \text{for} \quad \beta = \frac{1}{\sigma^2}$$

**Question 9** Give the minimizer function  $\mathcal{U}$  for  $\mathcal{F}_v$ .

Useful reminder on p. 24.

**Question 10** Determine the set  $\{\nu \in \mathbb{R} : \mathcal{U}(\nu) = 0\}$ . Comment the result.

## Disparity estimation

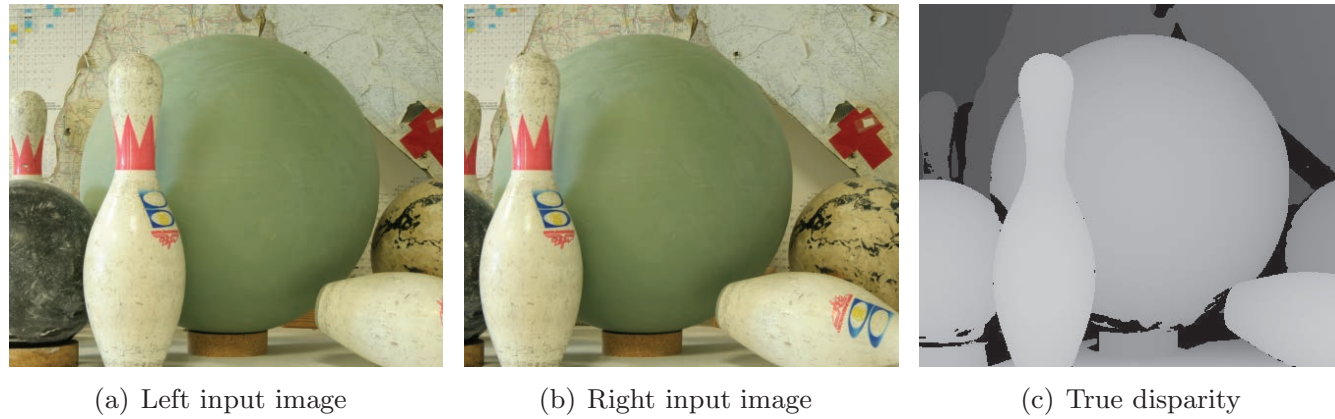


**Figure 7.** Rectified stereo image pair and the ground truth disparity. Light gray pixels indicate structures near to the camera, and black pixels correspond to unknown disparity values.

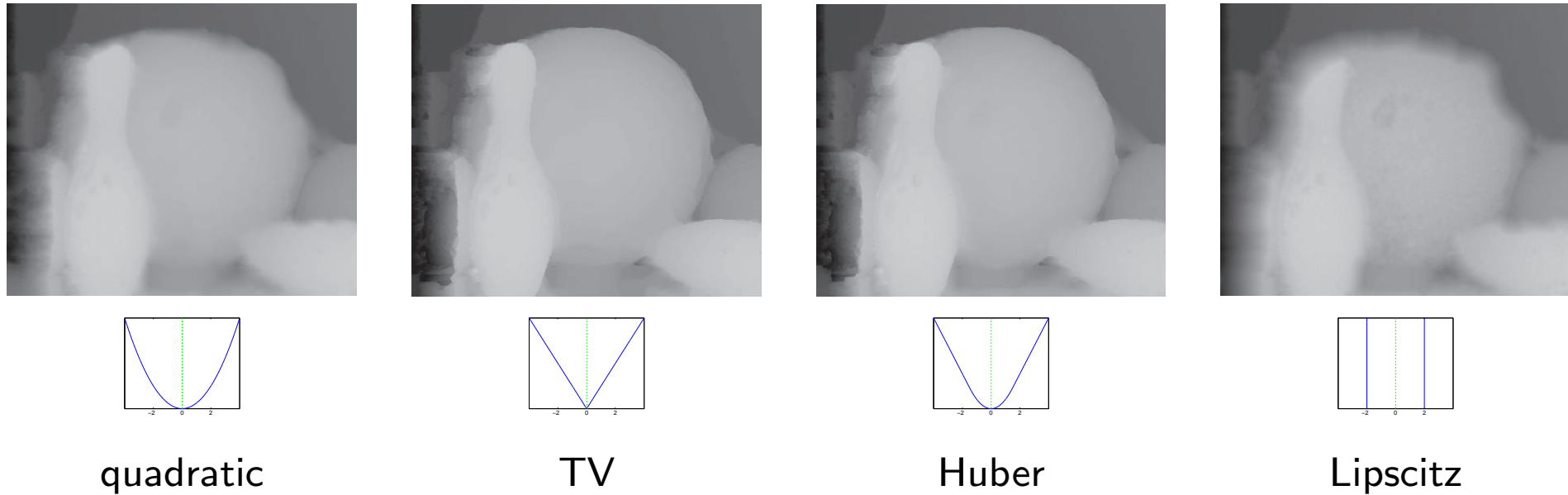
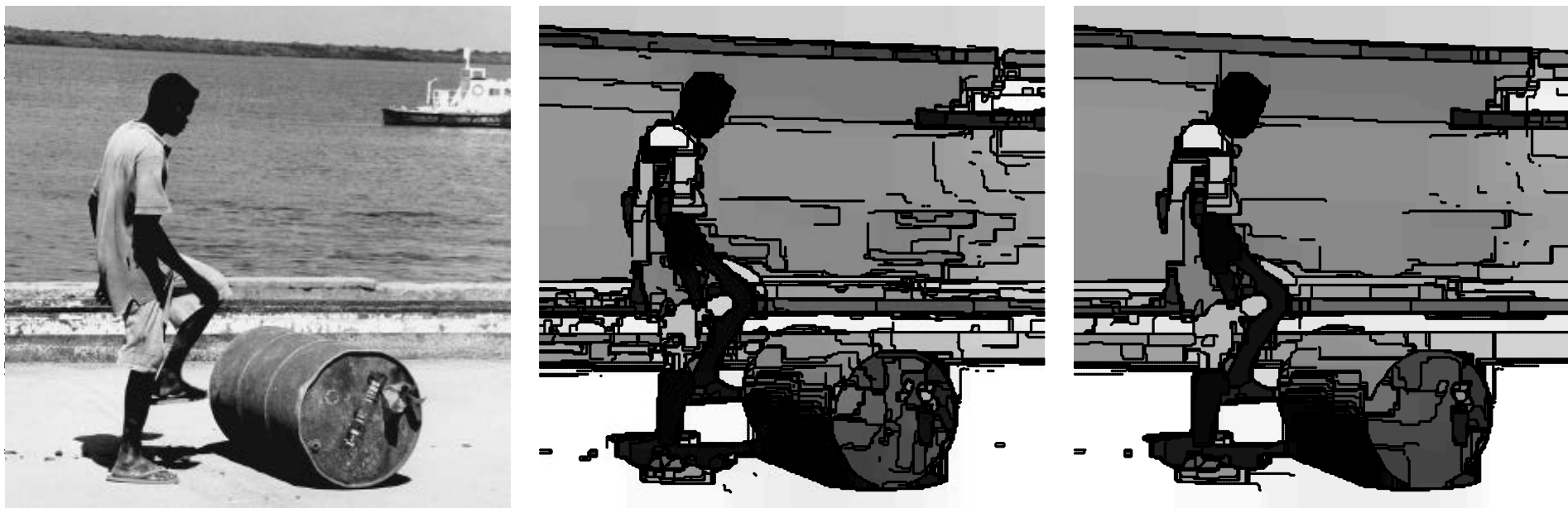


Image credits to the authors: Pock, Cremers, Bischof, and Chambolle “Global Solutions of Variational Models with Convex Regularization”, SIIMS 3(4) 2010, pp. 1122-1145



Minimization of  $\mathcal{F}_v(u) = \|u - v\|_2^2 + \beta \text{TV}(u)$ ,  $\beta = 100$  and  $\beta = 180$

## Questions relevant to the Potts model (see p. 12)

Here  $\varphi(t) = \begin{cases} 0 & \text{if } t = 0 \\ 1 & \text{if } t \neq 0 \end{cases}$

**Question 11** Compute the global minimizer of  $\mathcal{F}_v(u) = (u - v)^2 + \beta\varphi(u)$  for  $u, v \in \mathbb{R}$  and  $\beta > 0$ , according to the value of  $v$ .

Consider  $\mathcal{F}_v(\mathbf{u}) = \|\mathbf{u} - \mathbf{v}\|_2^2 + \beta \sum_{i=1}^p \varphi(u[i])$  for  $\beta > 0$  and  $u, v \in \mathbb{R}^p$ .

**Note:**  $\sum_{i=1}^p \varphi(u[i]) = \#\{i : u[i] \neq 0\} = \ell_0(u)$  is the counting norm.

The global minimizer function  $\mathcal{U} : \mathbb{R}^p \rightarrow \mathbb{R}^p$  for  $\mathcal{F}_v$  has  $p$  components which depend on  $v$ .

**Question 12** Compute each component  $\mathcal{U}_i$

**Question 13** Let  $h \subset \{1, \dots, p\}$ . Determine the subset  $\mathcal{O}_h \subset \mathbb{R}^p$  such that if  $v \in \mathcal{O}_h$  then the global minimizer  $\hat{u}$  of  $\mathcal{F}_v$  satisfies  $\hat{u}[i] = 0, \forall i \in h$  and  $\hat{u}[i] \neq 0$  if  $i \notin h$ .

## Summer School 2014: Inverse Problem and Image Processing

### Tutorial: Inverse modeling in inverse problems using optimization

#### Outline

1. Energy minimization methods (p. 7)
2. Regularity results (p. 17)
3. Non-smooth regularization – minimizers are sparse in a given subspace (p. 26)
4. Non-smooth data-fidelity – minimizers fit exactly some data entries
5. Comparison with Fully Smooth Energies (p. 51)
6. Non-convex regularization – edges are sharp (p. 54)
7. Nonsmooth data-fidelity and regularization – peculiar features (p. 62)
8. Fully smoothed  $\ell_1$ –TV models – bounding the residual (p. 83)
9. Inverse modeling and Bayesian MAP – there is distortion (p. 98)
10. Some References (p. 103)

## 4 Minimizers relevant to non-smooth data-fidelity

### General case

[Nikolova 02]

$$\mathcal{F}_v(u) = \sum_i \psi(|a_i u - v[i]|) + \beta \Phi(u), \quad a_i = A_{\text{row } i}, \Phi \in \mathcal{C}^m, \psi \in \mathcal{C}^m(\mathbb{R}_+^*), \psi'(0^+) > 0$$

Let  $\hat{u}$  be a (local) minimizer of  $\mathcal{F}_v$ . Set  $\hat{h} =: \{i : a_i \hat{u} = v[i]\}$ .

Then  $\exists \mathcal{O} \subset \mathbb{R}^q$  open,  $\exists \mathcal{U} \in \mathcal{C}^{m-1}$  (local) minimizer function so that

$$v' \in \mathcal{O}, \hat{u}' = \mathcal{U}(v') \Rightarrow a_i \hat{u}' = v[i], \quad \forall i \in \hat{h}$$

$$\hat{h} \subset \{1, \dots, q\} \quad \mathcal{O}_{\hat{h}} := \left\{ v \in \mathbb{R}^q : a_i \mathcal{U}(v) = v_i, \forall i \in \hat{h} \right\} \Rightarrow \mathbb{L}^q(\mathcal{O}_{\hat{h}}) > 0$$

(Local) minimizers  $\hat{u}$  of  $\mathcal{F}_v$  achieve an exact fit to (noisy) data  
 $a_i \hat{u} = v[i]$  for a certain number of indexes  $i$

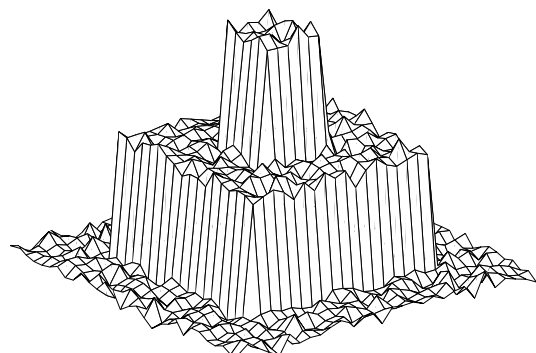
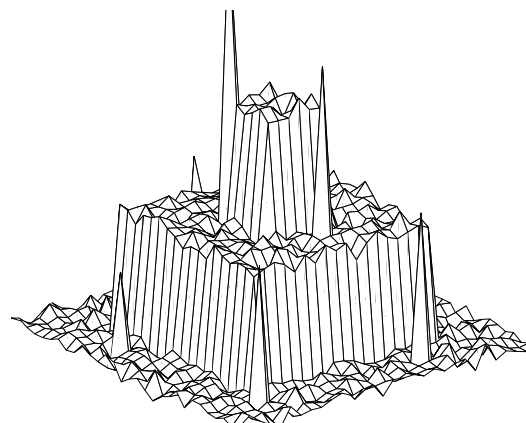
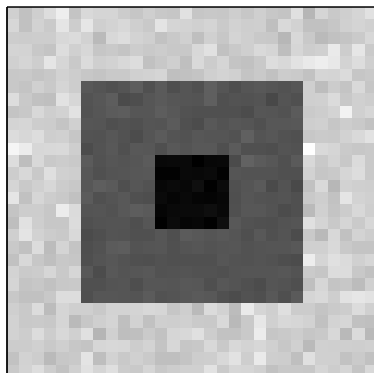
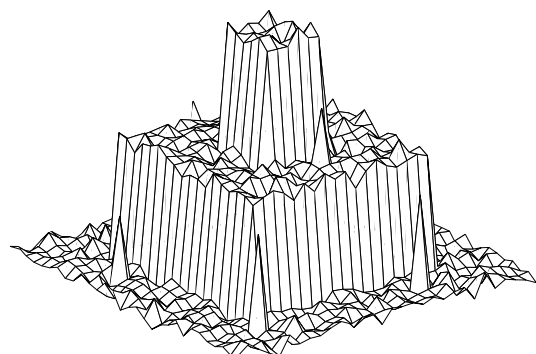
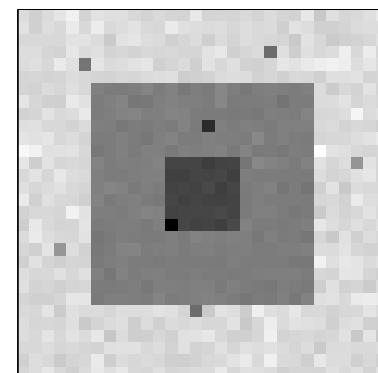
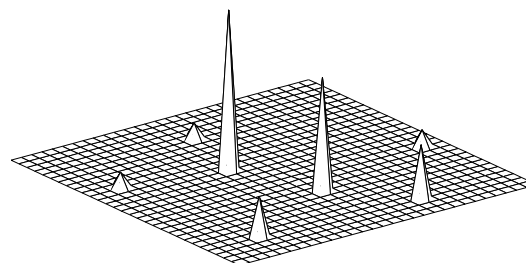
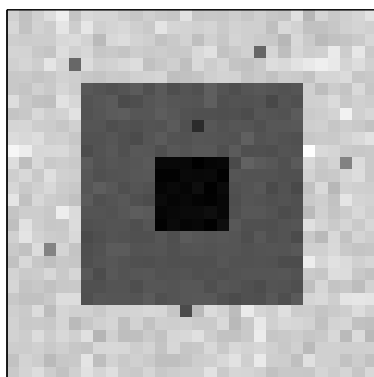
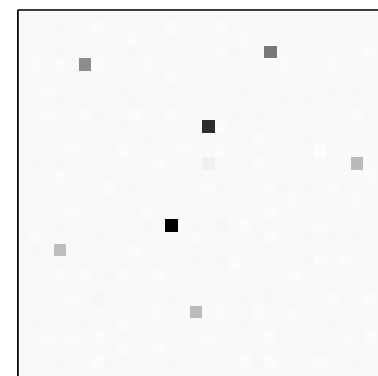
Property fails if  $\mathcal{F}$  is fully smooth, except for  $v \in N$  where  $N$  is closed and  $\mathbb{L}^q(N) = 0$ .

**Question 14** Suggest cases when you would like that your minimizer obeys this property.

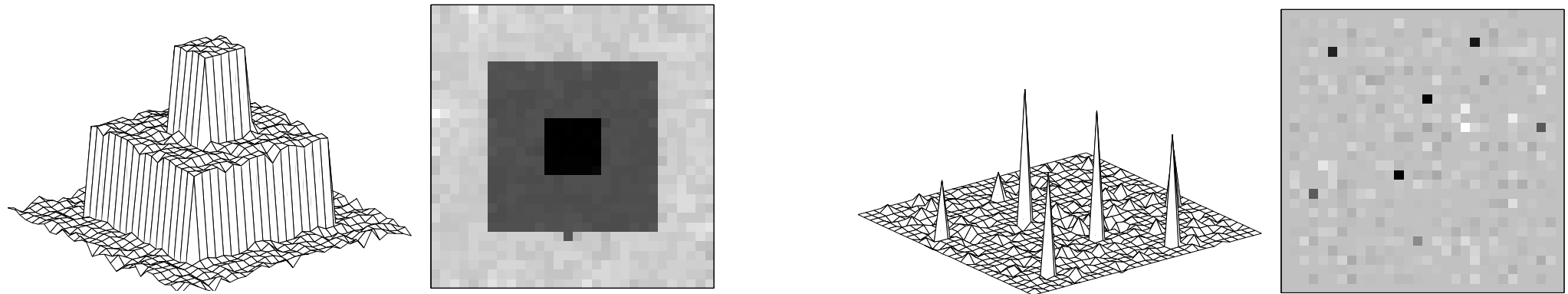
**Question 15** Compute the minimizer of  $\mathcal{F}_v(u) = |u - v| + \beta u^2$  for  $u, v \in \mathbb{R}$  and  $\beta > 0$ .

**Question 16** Can you find a relationship between the properties of the minimizer when  $\varphi'(0^+) > 0$  (chapter 3, p. 26) and when  $\psi'(0^+) > 0$  (chapter 4, p. 35)

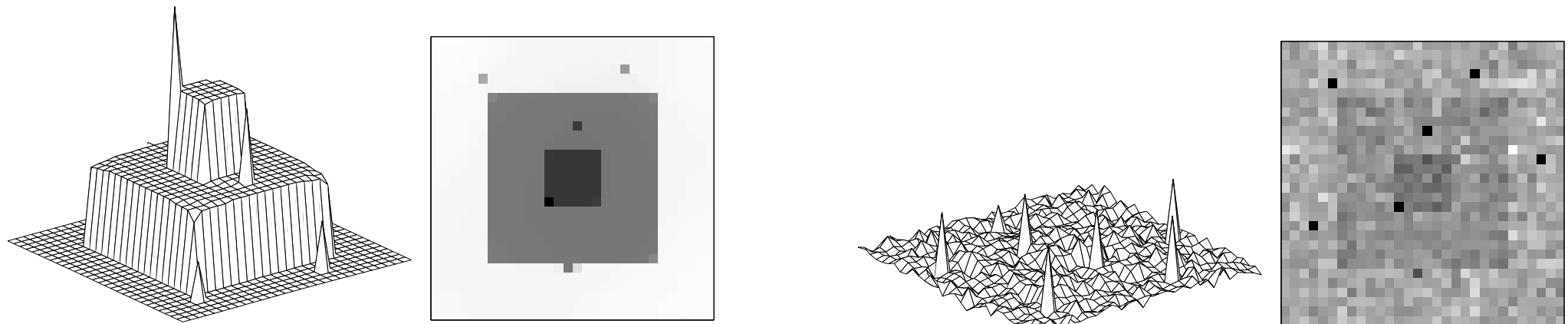


Original  $u_o$ Data  $v = u_o + \text{outliers}$ Restoration  $\hat{u}$  for  $\beta = 0.14$ Residuals  $v - \hat{u}$ 

$$\mathcal{F}_v(u) = \sum_i |u[i] - v[i]| + \beta \sum_{j \in \mathcal{N}_i} |u[i] - u[j]|^{1.1}$$

Restoration  $\hat{u}$  for  $\beta = 0.25$ Residuals  $v - \hat{u}$ 

$$\mathcal{F}_v(u) = \sum_i |u[i] - v[i]| + \beta \sum_{j \in \mathcal{N}_i} |u[i] - u[j]|^{1.1}$$

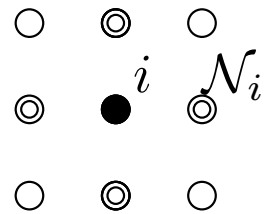
Restoration  $\hat{u}$  for  $\beta = 0.2$ Residuals  $v - \hat{u}$ 

TV-like energy: 
$$\mathcal{F}_v(u) = \sum_i (u[i] - v[i])^2 + \beta \sum_{j \in \mathcal{N}_i} |u[i] - u[j]|$$

## Detection and cleaning of outliers using $\ell_1$ data-fidelity

[Nikolova 04]

$$\mathcal{F}_v(u) = \sum_{i=1}^p |u[i] - v[i]| + \frac{\beta}{2} \sum_{i=1}^p \sum_{j \in \mathcal{N}_i} \varphi(|u[i] - u[j]|)$$



$\varphi$ : smooth, convex, edge-preserving

Assumptions:  $\left\{ \begin{array}{l} \text{data } v \text{ contain uncorrupted samples } v[i] \\ v[i] \text{ is outlier if } |v[i] - v[j]| \gg 0, \forall j \in \mathcal{N}_i \end{array} \right.$

$$v \in \mathbb{R}^p \Rightarrow \hat{u} = \arg \min_u \mathcal{F}_v(u) \quad \left\{ \begin{array}{l} v[i] \text{ is regular if } i \in \hat{h} \\ v[i] \text{ is outlier if } i \in \hat{h}^c \end{array} \right.$$

$$\hat{h} = \{i : \hat{u}[i] = v[i]\}$$

Outlier detector:  $v \rightarrow \hat{h}^c(v) = \{i : \hat{u}[i] \neq v[i]\}$   
 Smoothing:  $\hat{u}[i] \text{ for } i \in \hat{h}^c = \text{estimate of the outlier}$

Justification based on the properties of  $\hat{u}$

L. Bar, A. Brook, N. Sochen and N. Kiryati,  
“Deblurring of Color Images Corrupted by Impulsive Noise”,  
IEEE Trans. on Image Processing, 2007

$$\mathcal{F}_v(u) = \|Au - v\|_1 + \beta\Phi(u)$$



blurred, noisy (r.-v.)



zoom - restored

## Recovery of frame coefficients using $\ell_1$ data-fitting

[Durand, Nikolova 07]

- Data:  $\mathbf{v} = \mathbf{u}_o + \text{noise}$
- Frame coefficients:  $\mathbf{y} = \mathbf{W}\mathbf{v} = \mathbf{W}\mathbf{u}_o + \text{noise}$

$\widetilde{\mathbf{W}}$  =left inverse of  $\mathbf{W}$

- Hard thresholding 
$$\mathbf{y}_T[i] := \begin{cases} 0 & \text{if } |\mathbf{y}[i]| \leq T \\ \mathbf{y}[i] & \text{if } |\mathbf{y}[i]| > T \end{cases}$$

keeps relevant information if  $T$  small

- $\tilde{\mathbf{u}} = \widetilde{\mathbf{W}}\mathbf{y}_T$  — Gibbs oscillations and wavelet-shaped artifacts
- Hybrid energy methods—combine fitting to  $\mathbf{y}_T$  with prior  $\Phi(\mathbf{u})$

[Bobichon, Bijaoui 97], [Coifman, Sowa 00], [Durand, Froment 03]...

Desiderata:  $\mathcal{F}_y$  convex and

Keep  $\hat{x}[i] = y_T[i]$

Restore  $\hat{x}[i] \neq y_T[i]$

significant coefs:  $y[i] \approx (Wu_o)[i]$     outliers:  $|y[i]| \gg |(Wu_o)[i]|$  (frame-shaped artifacts)

thresholded coefs:  $(Wu_o)[i] \approx 0$     edge coefs:  $|(Wu_o)[i]| > |y_T[i]| = 0$  (“Gibbs” oscillations)

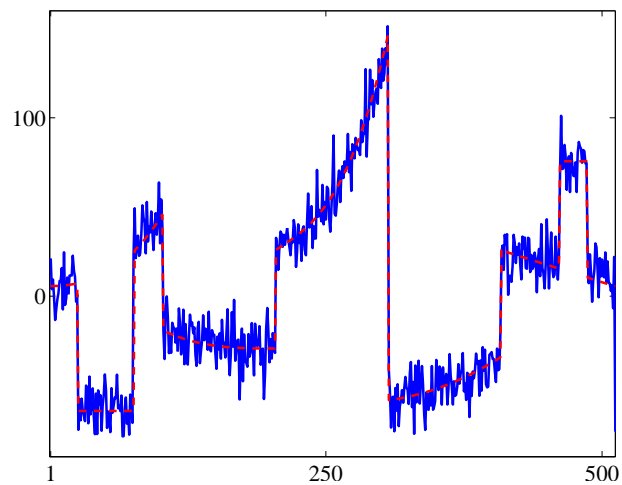
Then:

$$\text{minimize } \mathcal{F}_y(x) = \sum_i \lambda_i |(x - y_T)[i]| + \int_{\Omega} \varphi(|\nabla \tilde{W}x|) \Rightarrow \hat{x}$$

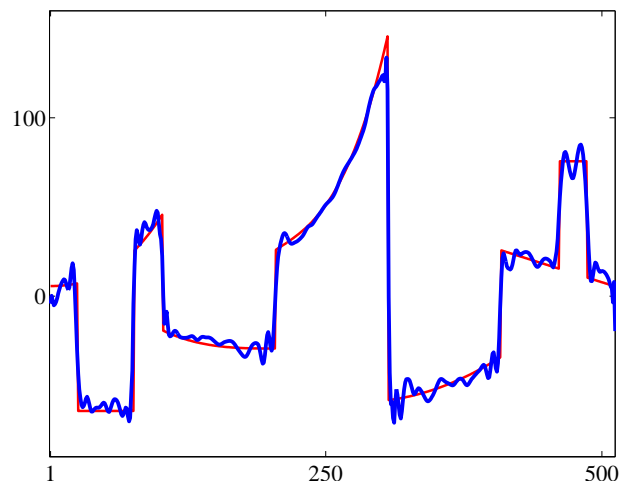
$$\hat{u} = \tilde{W} \hat{x} \text{ for } \tilde{W} \text{ left inverse, } \varphi \text{ edge-preserving}$$

Question 17 Explain why the minimizers of  $\mathcal{F}_y$  fulfill the desiderata.

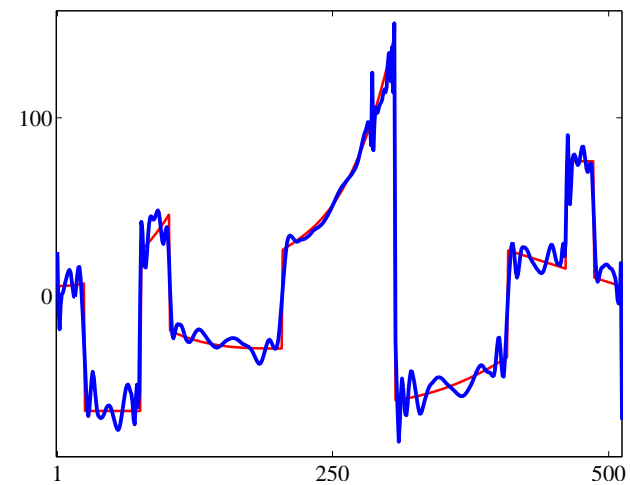
Hint: “good” coefficients fitted exactly, “bad” coefficients corrected according to the prior.



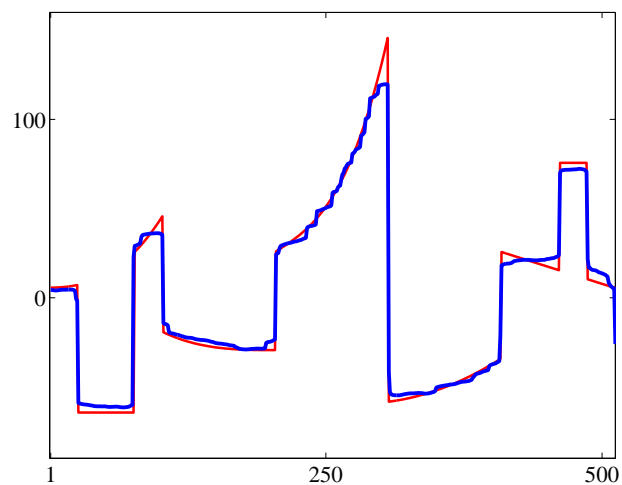
Original and data



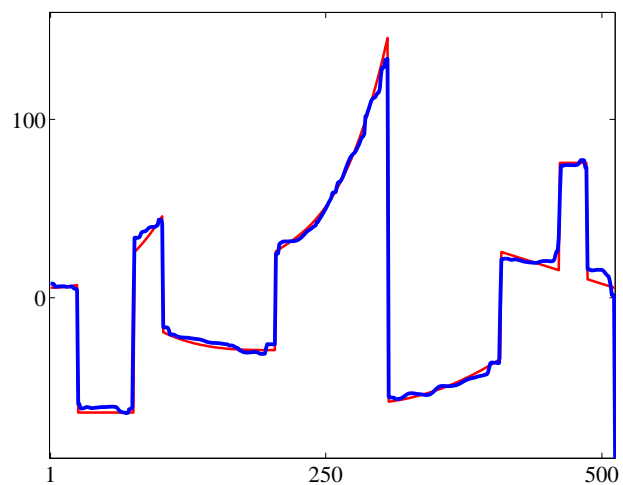
Sure-shrink method



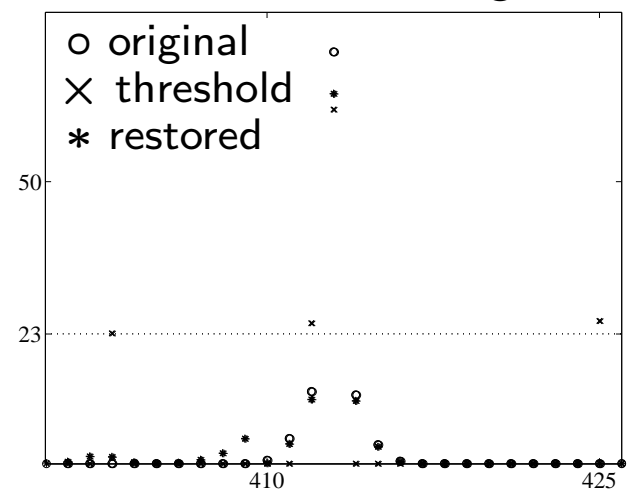
Hard thresholding



Total variation



The proposed method



Magnitude of coefficients

Restored signal (—), original signal (- -).

## Fast 2-stage restoration under impulse noise

[R.Chan, Nikolova et al. 04,05,08]

1. Approximate the outlier-detection stage by rank-order filter

(e.g. adaptive or center-weighted median)

Corrupted pixels  $\hat{h}^c = \{i : \hat{v}[i] \neq v[i]\}$  where  $\hat{v}$ =Rank-Order Filter ( $v$ )

$\Rightarrow$  improve speed and accuracy

2. Restore  $\hat{u}$  (denoise, deblur) using an edge-preserving energy method

subject to  $a_i \hat{u} = v[i]$  for all  $i \in \hat{h}$





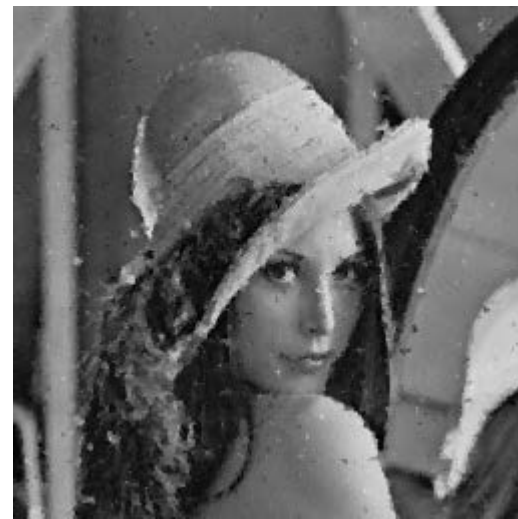
50% RV noise



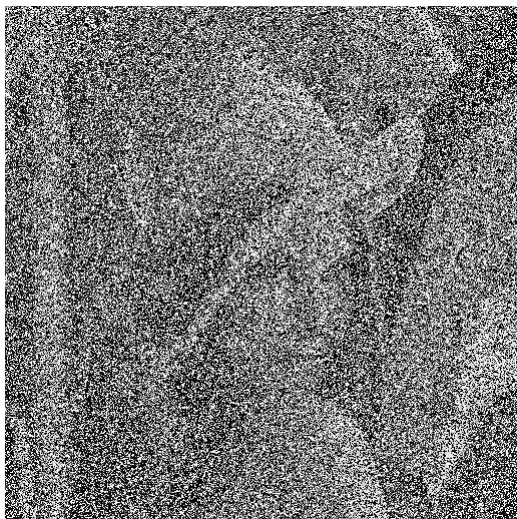
ACWMF



DPVM



Our method



70 % SP noise(6.7dB)



Adapt.med.(25.8dB)



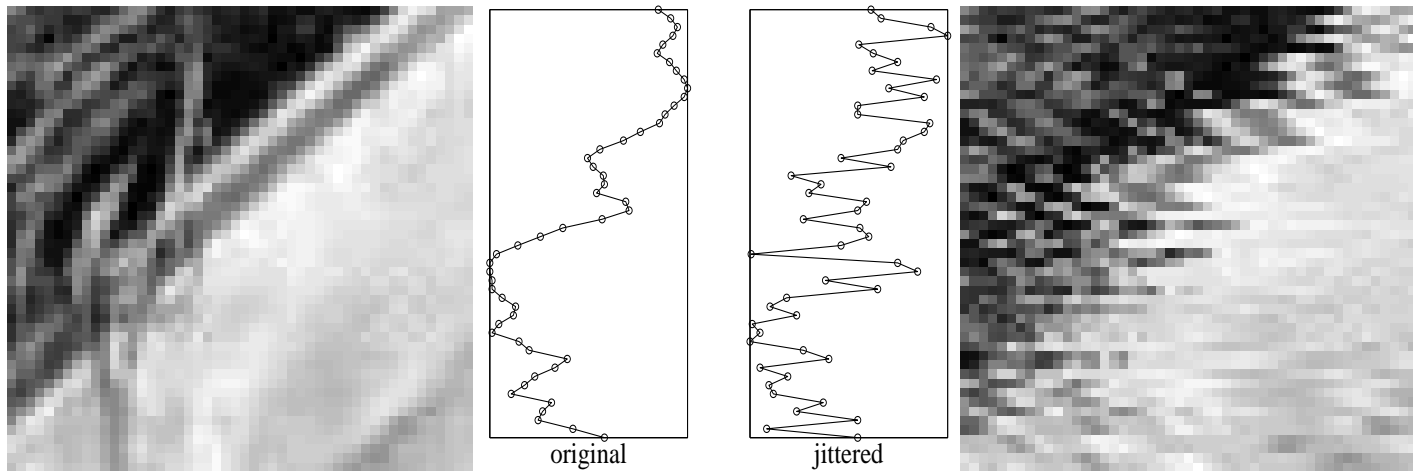
Our method(29.3dB)



Original Lena

# One-step real-time dejittering of digital video

- Image  $u \in \mathbb{R}^{m \times n}$ , rows  $u_i$ , its pixels  $u_i[j]$
- Data  $v_i[j] = u_i[j + d_i]$ ,  $d_i$  integer,  $|d_i| \leq M$ , typically  $M \leq 20$ .
- Restore  $\hat{u} \equiv \text{restore } \hat{d}_i, 1 \leq i \leq m$



Original

(b) One column

Jittered

(b) The same column in the original (left) and in the jittered (right) image

The gray-values of the columns of natural images can be seen as large pieces of 2<sup>nd</sup> (or 3<sup>rd</sup>) order polynomials which is false for their jittered versions.



Each column  $\hat{u}_i$  is restored using  $\hat{d}_i = \arg \min_{|d_i| \leq N} \mathcal{F}(d_i)$

$$\mathcal{F}(d_i) = \sum_{j=N+1}^{c-N} |v_i[j + d_i] - 2\hat{u}_{i-1}[j] + \hat{u}_{i-2}[j]|^\alpha, \quad \alpha \in \{0.5, 1\}, \quad N > M$$

**Question 18** Explain why the minimizers of  $\mathcal{F}$  can solve the problem as stated.

**Question 19** What changes if  $\alpha = 1$  or if  $\alpha = 0.5$ ?

**Question 20** Is it easy to solve the numerical problem?

A Monte-Carlo experiment shows that in almost all cases,  $\alpha = 0.5$  is better.

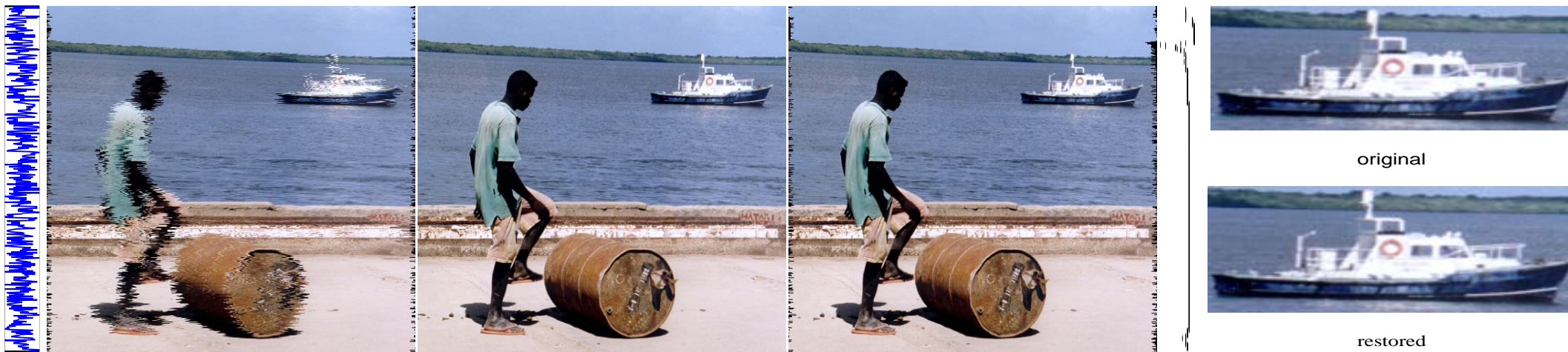


Jittered,  $[-20, 20]$

$\alpha = 1$

Jitter:  $6 \sin\left(\frac{n}{4}\right)$

$\alpha = 1 \equiv$  Original

Jittered  $\{-8, \dots, 8\}$ 

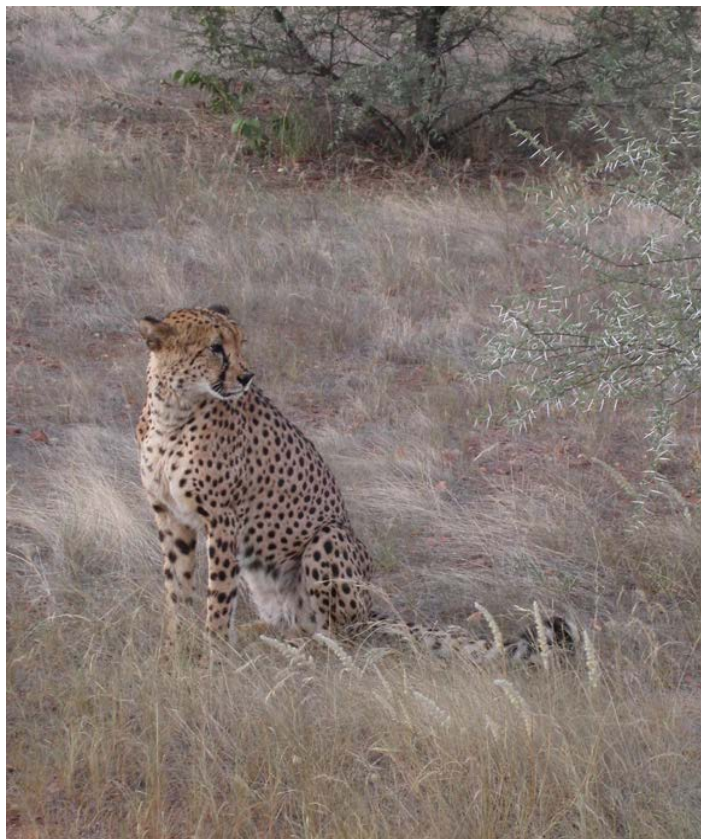
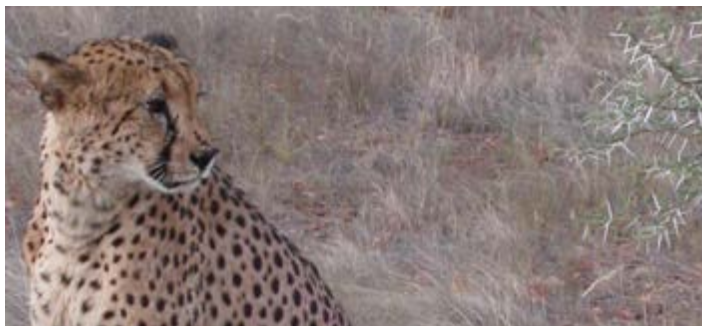
Original image

 $\alpha = 1$ 

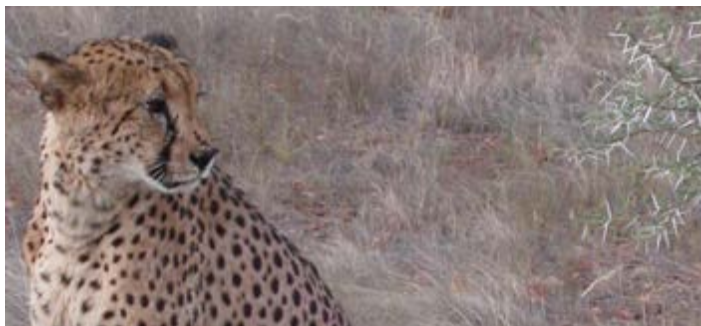
Zooms

 $(512 \times 512)$  Jitter  $M = 6$   $\alpha \in \{1, \frac{1}{2}\}$  = Original Lena  $(256 \times 256)$ Jitter  $\{-6, \dots, 6\}$  $\alpha \in \{1, \frac{1}{2}\}$

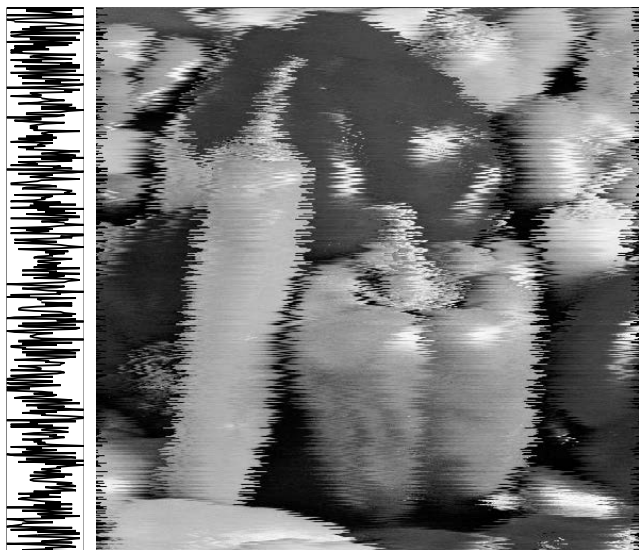


Jitter  $\{-15, \dots, 15\}$  $\alpha = 1, \alpha = 0.5$ 

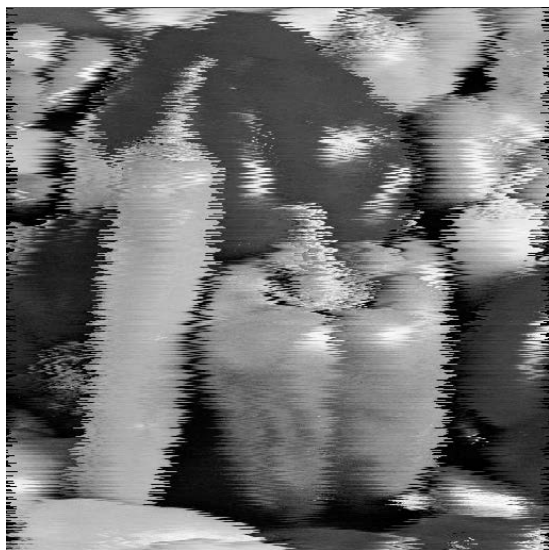
Original image



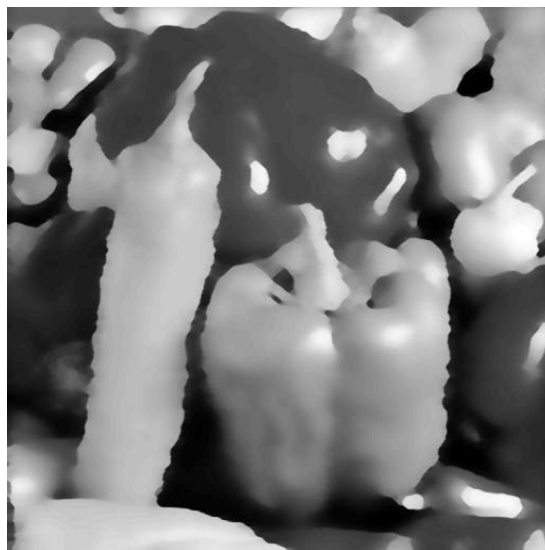




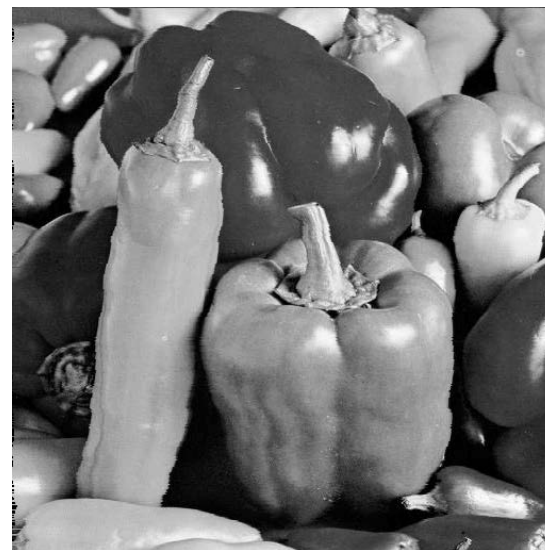
Jitter



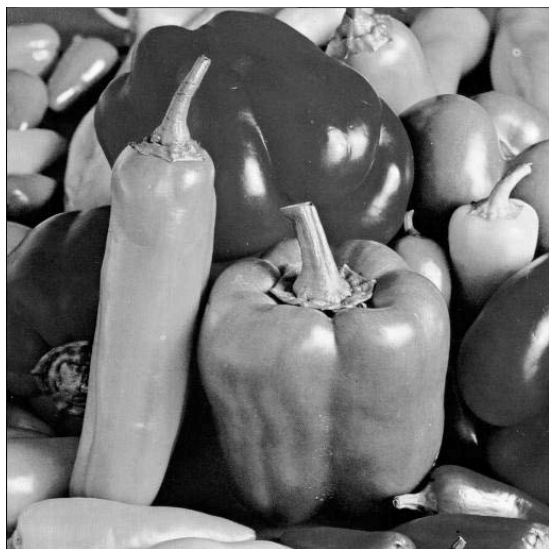
Jittered Image



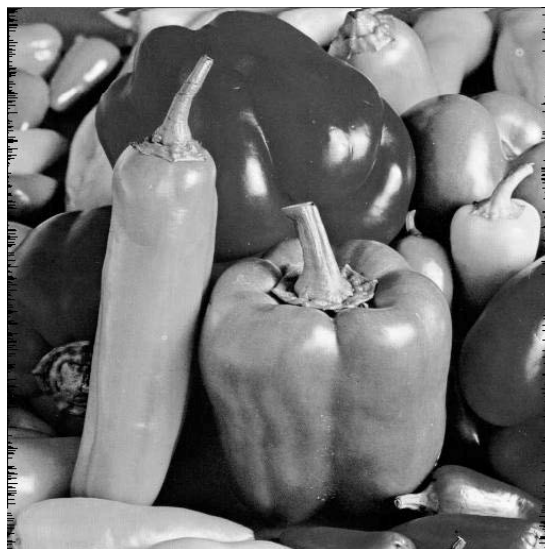
Bayesian TV



Bake &amp; Shake



Original

Our:  $\alpha=0.5$ Our: Error  $u_o - \hat{u}$

## 5. Comparison with Fully Smooth Energies

$\mathcal{F}_v(u) = \Psi(u, v) + \beta\Phi(u)$ ,  $\mathcal{F} \in \mathcal{C}^{m \geq 2}$  + easy assumptions. If  $h \neq \emptyset \Rightarrow$

$\{v \in \mathbb{R}^q : \mathcal{F}_v\text{-minimum at } \hat{u}, G_i \hat{u} = 0, \forall i \in h\}$       **closed and**  
 $\{v \in \mathbb{R}^q : \mathcal{F}_v\text{-minimum at } \hat{u}, a_i \hat{u} = v_i, \forall i \in h\}$       **negligible in  $\mathbb{R}^q$**

For  $\mathcal{F}_v$  smooth, the chance that noisy data  $v$  yield a minimizer  $\hat{u}$  of  $\mathcal{F}_v$  which for some  $i$  satisfies exactly  $G_i \hat{u} = 0$  or  $a_i \hat{u} = v_i$  is negligible

Nearly all  $v \in \mathbb{R}^q$  lead to  $\hat{u} = \mathcal{U}(v)$  satisfying  $G_i \hat{u} \neq 0, \forall i$  and  $a_i \hat{u} \neq v_i, \forall i$

**Question 21** What are the consequences if one approximates a nonsmooth energy by a smooth energy?

## Questions to clarify the theoretical results

Let  $u \in \mathbb{R}^p$  and  $v \in \mathbb{R}^q$ .

Consider that  $A \in \mathbb{R}^{q \times p}$  and  $G \in \mathbb{R}^{r \times p}$  satisfy  $\ker(A) \cap \ker(G) = \{0\}$ .

$$\mathcal{F}_v(u) = \|Au - v\|_2^2 + \beta \|Gu\|_2^2 \quad \text{for } \beta > 0$$

**Question 22** Calculate  $\nabla \mathcal{F}_v(u)$ .

**Question 23** Determine the minimizer function  $\mathcal{U}$ .

Let  $G_i \in \mathbb{R}^{1 \times p}$  denote the  $i$ th row of  $G$ .

**Question 24** Characterize the set  $\mathcal{K} = \{\nu \in \mathbb{R}^p : G_i \mathcal{U}(\nu) = 0\}$ .

Let  $a_i \in \mathbb{R}^{1 \times p}$  denote the  $i$ th row of  $A$ .

**Question 25** Characterize the set  $\mathcal{L} = \{\nu \in \mathbb{R}^p : a_i \mathcal{U}(\nu) = \nu[i]\}$ .



## Summer School 2014: Inverse Problem and Image Processing

### Tutorial: Inverse modeling in inverse problems using optimization

#### Outline

1. Energy minimization methods (p. 7)
2. Regularity results (p. 17)
3. Non-smooth regularization – minimizers are sparse in a given subspace (p. 26)
4. Non-smooth data-fidelity – minimizers fit exactly some data entries (p. 35)
5. Comparison with Fully Smooth Energies (p. 51)
6. Non-convex regularization – edges are sharp
7. Nonsmooth data-fidelity and regularization – peculiar features (p. 62)
8. Fully smoothed  $\ell_1$ –TV models – bounding the residual (p. 83)
9. Inverse modeling and Bayesian MAP – there is distortion (p. 98)
10. Some References (p. 103)

## 6 Nonconvex Regularization: Why Edges are Sharp?

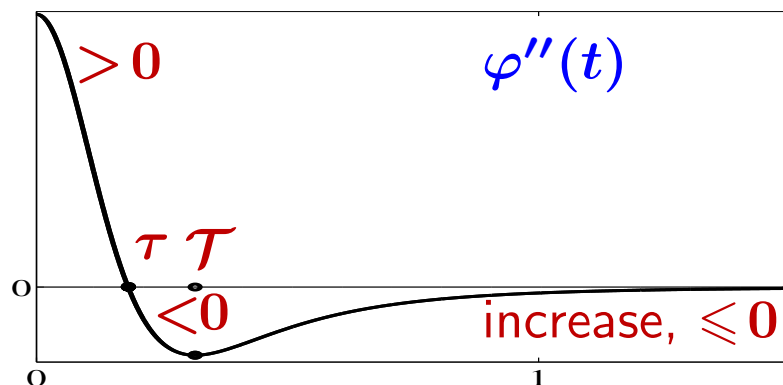
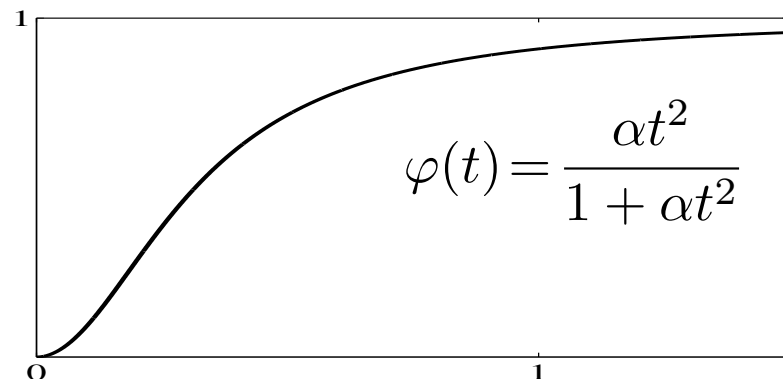
[Nikolova 04, 10]

$$\mathcal{F}_v(u) = \|Au - v\|^2 + \beta \sum_{i \in J} \varphi(\|G_i u\|)$$

$$J = \{1, \dots, r\}$$

Standard assumptions on  $\varphi$ :  $\mathcal{C}^2$  on  $\mathbb{R}_+$  and  $\lim_{t \rightarrow \infty} \varphi''(t) = 0$ , as well as:

$\varphi'(0) = 0$  ( $\Phi$  is smooth)



$\varphi'(0^+) > 0$  ( $\Phi$  is nonsmooth)

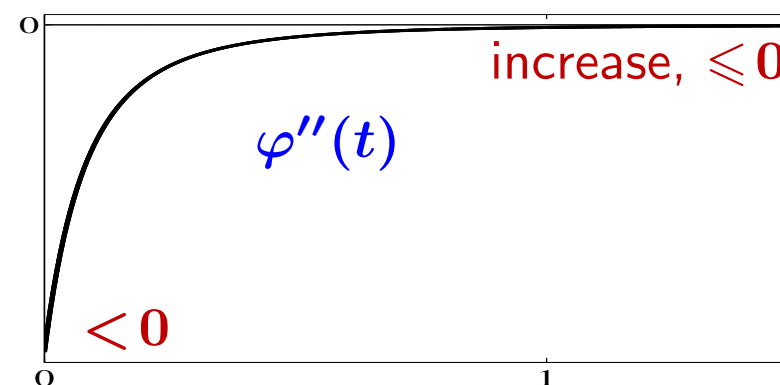
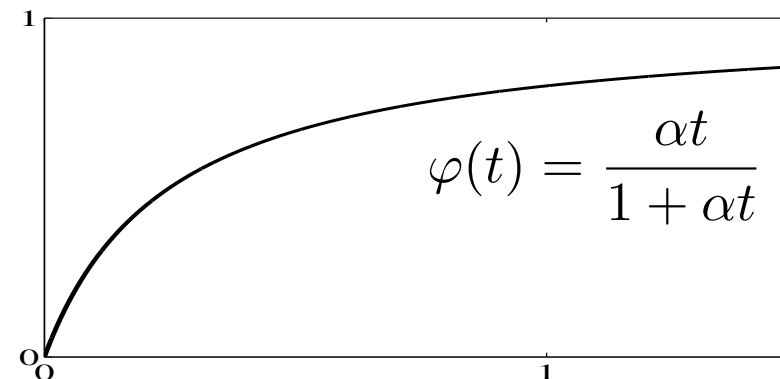
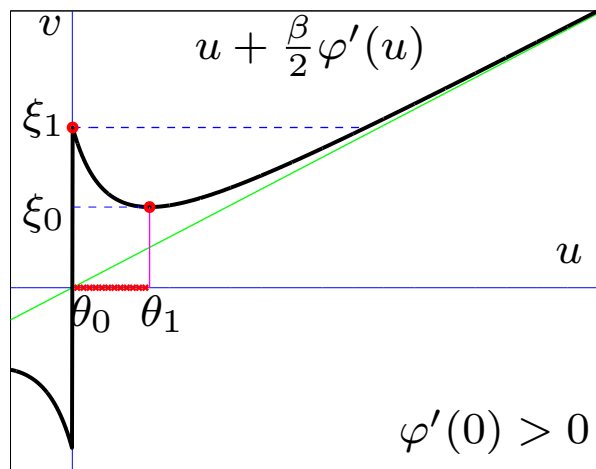
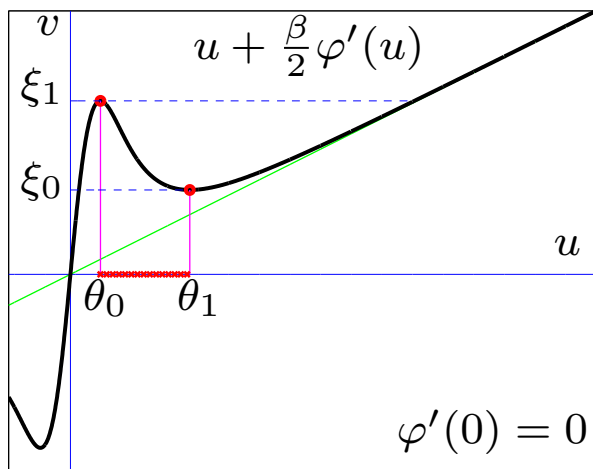


ILLUSTRATION ON  $\mathbb{R}$ 

$$\mathcal{F}_v(u) = (u - v)^2 + \beta\varphi(|u|), \quad u, v \in \mathbb{R}$$



*No local minimizer in  $(\theta_0, \theta_1)$*

$$\exists \xi_0 > 0, \quad \exists \xi_1 > \xi_0$$

$$|v| \leq \xi_1 \Rightarrow |\hat{u}_0| \leq \theta_0$$

strong smoothing

$$|v| \geq \xi_0 \Rightarrow |\hat{u}_1| \geq \theta_1$$

loose smoothing

$$\exists \xi \in (\xi_0, \xi_1) \quad |v| \leq \xi \Rightarrow \text{global minimizer} = \hat{u}_0 \quad (\text{strong smoothing})$$

$$|v| \geq \xi \Rightarrow \text{global minimizer} = \hat{u}_1 \quad (\text{loose smoothing})$$

For  $v = \xi$  the global minimizer jumps from  $\hat{u}_0$  to  $\hat{u}_1 \equiv$  decision for an “edge”

Since [Geman<sup>2</sup>1984] various nonconvex  $\Phi$  to produce minimizers with smooth regions and sharp edges

## Sharp edge property

There exist  $\theta_0 \geq 0$  and  $\theta_1 > \theta_0$  such that any (local) minimizer  $\hat{u}$  of  $\mathcal{F}_v$  satisfies

$$\text{either } \|G_i \hat{u}\| \leq \theta_0 \quad \text{or} \quad \|G_i \hat{u}\| \geq \theta_1 \quad \forall i \in J$$

$$\begin{aligned} \hat{h}_0 &= \{i : \|G_i \hat{u}\| \leq \theta_0\} && \text{homogeneous regions} \\ \hat{h}_1 &= \{i : \|G_i \hat{u}\| \geq \theta_1\} && \text{edges} \end{aligned}$$

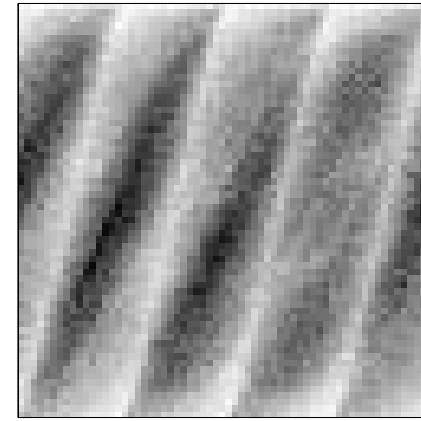
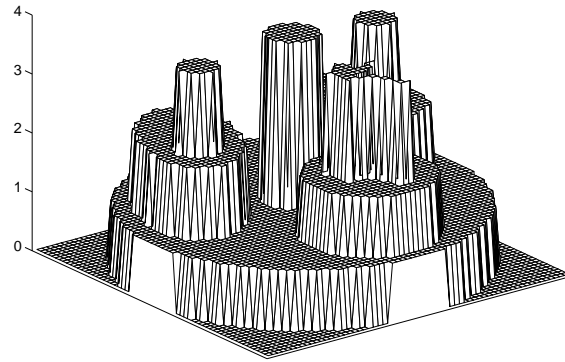
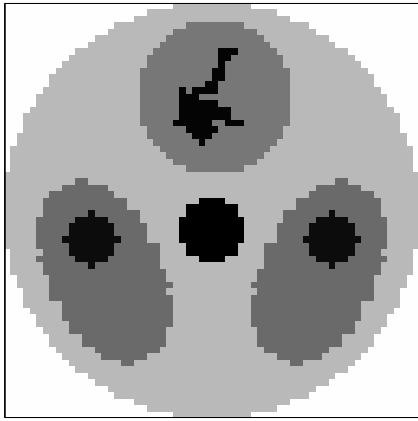
When  $\beta$  increases, then  $\theta_0$  decreases and  $\theta_1$  increases.

In particular

$$\varphi'(0^+) > 0 \quad \Rightarrow \quad \theta_0 = 0 \quad \text{fully segmented image} \quad (G_i \hat{u} = 0, \forall i \in \hat{h}_0)$$

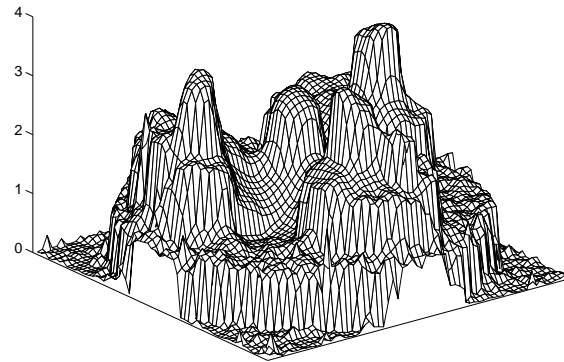
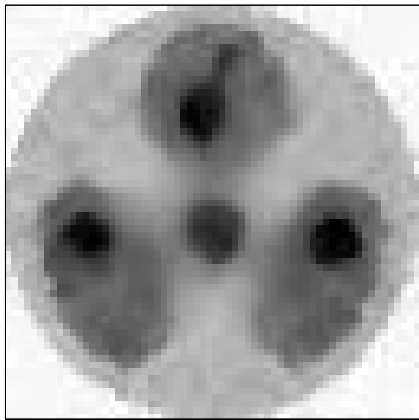
**Question 26** Explain the prior model involved in  $\mathcal{F}_v$  when  $\varphi$  is nonconvex with  $\varphi'(0) = 0$  and with  $\varphi'(0^+) > 0$ .

# IMAGE RECONSTRUCTION IN EMISSION TOMOGRAPHY

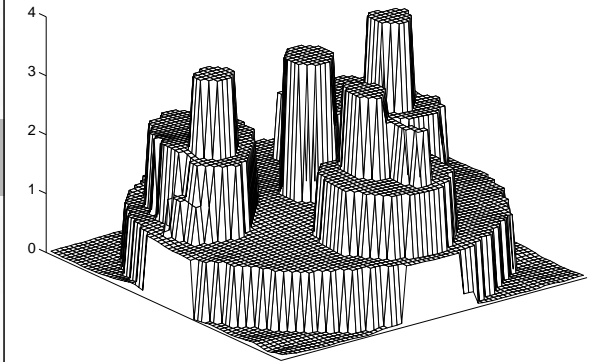
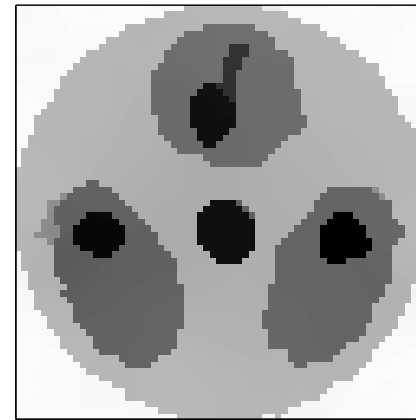


Original phantom

Emission tomography simulated data



$\varphi$  is smooth (Huber function)



$\varphi(t) = t/(\alpha + t)$  (non-smooth, non-convex)

Reconstructions using  $\mathcal{F}_v(u) = \Psi(u, v) + \beta \sum_{j \in \mathcal{N}_i} \varphi(|u[i] - u[j]|)$ ,  $\Psi = \text{smooth, convex}$

## Selection for the global minimizer

Additional assumptions:  $\|\varphi\|_\infty < \infty$ ,  $\{G_i\}$ —1<sup>st</sup>-order differences,  $A^*A$  invertible

$$\mathbf{1}_{\Sigma i} = \begin{cases} 1 & \text{if } i \in \Sigma \subset \{1, \dots, p\} \\ 0 & \text{else} \end{cases} \quad \begin{array}{l} \text{Original: } u_o = \xi \mathbf{1}_\Sigma, \quad \xi > 0 \\ \text{Data: } v = \xi A \mathbf{1}_\Sigma = Au_o \end{array}$$

$\hat{u}$  = global minimizer of  $\mathcal{F}_v$

## Sketch of the results

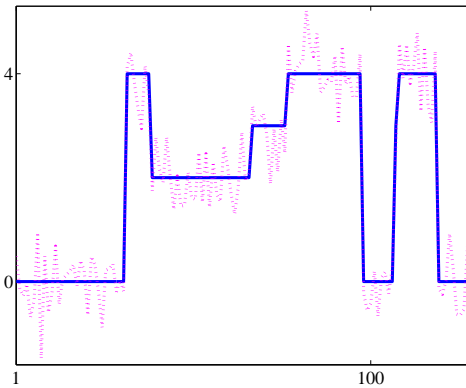
$\exists \xi_1 > 0$  such that  $\xi > \xi_1 \Rightarrow \hat{u}$ —perfect edges

Moreover:

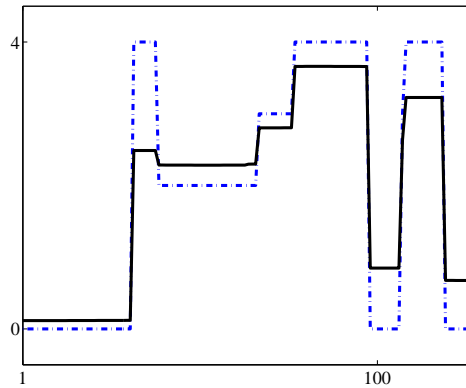
- $\Phi$  non smooth, then  $\xi > \xi_1 \Rightarrow \hat{u} = c u_o, \quad c < 1, \quad \lim_{\xi \rightarrow \infty} c = 1$
- $\varphi(t) = \eta, \quad t \geq \eta$ , then  $\xi > \xi_1 \Rightarrow \hat{u} = u_o$

This holds true also for  $\varphi(t) = \min\{\alpha t^2, 1\}$  and for  $\varphi(t) = \begin{cases} 0 & \text{if } t = 0 \\ 1 & \text{if } t \neq 0 \end{cases}$

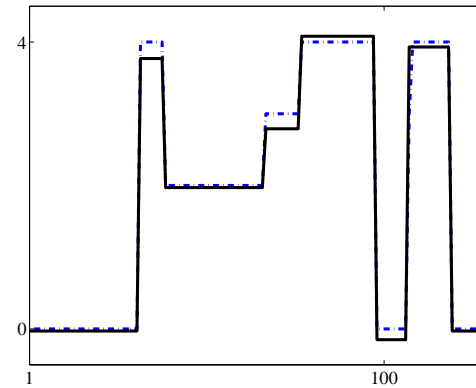
## Comparison with Convex Edge-Preserving Regularization



Data  $v = u_o + n$



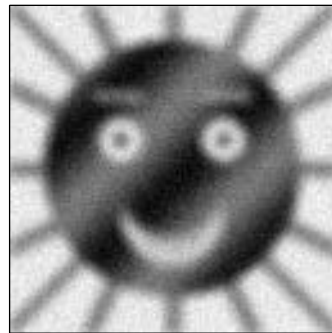
$\varphi(t) = |t|$



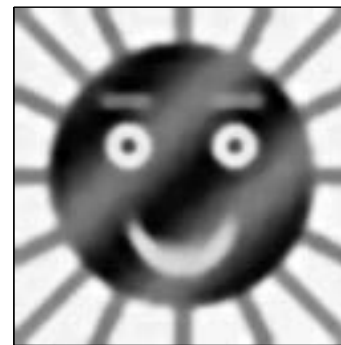
$\varphi(t) = \alpha|t|/(1 + \alpha|t|)$



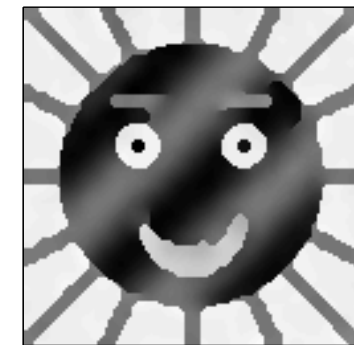
original



data

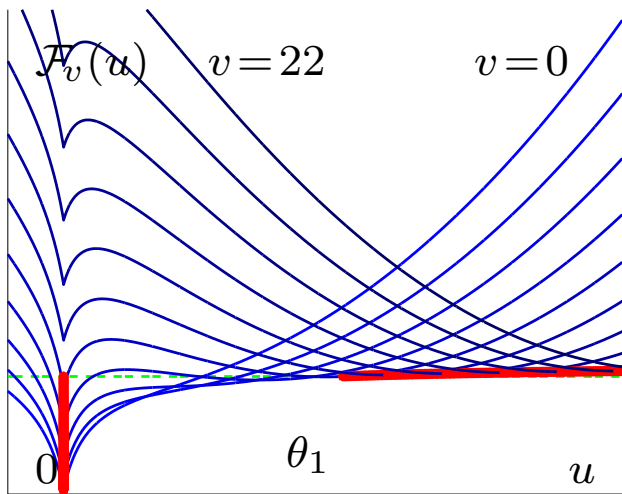


$\varphi(t) = |t|^{1.4}$



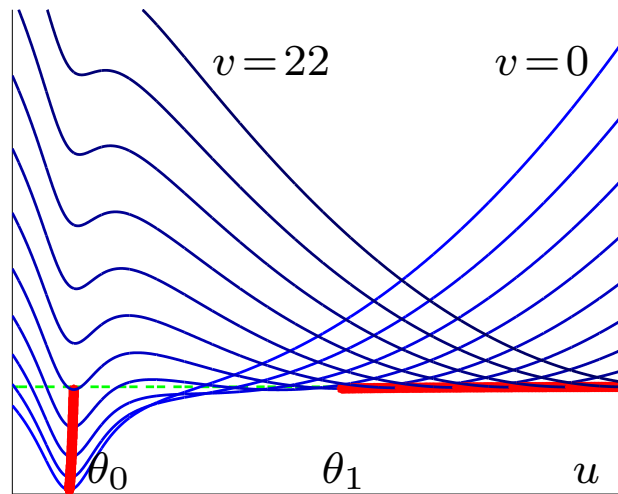
$\varphi(t) = \min\{\alpha t^2, 1\}$

**Question 27** Why edges are sharper when  $\varphi$  is nonconvex?



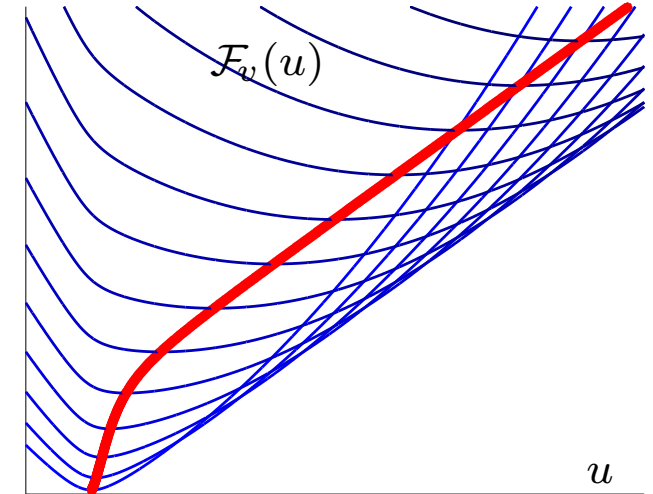
$$\mathcal{F}_v(u) = (u - v)^2 + \beta \frac{\alpha|u|}{(1 + \alpha|u|)}$$

global function (●●)



$$\mathcal{F}_v(u) = (u - v)^2 + \beta \frac{\alpha u^2}{(1 + \alpha u^2)}$$

global minimizer functions (●●)



$$\mathcal{F}_v(u) = (u - v)^2 + \beta \sqrt{\alpha + u^2}$$

unique minimizer function (●●)

Each blue curve:  $u \rightarrow \mathcal{F}_v(u)$  for  $v \in \{0, 2, \dots\}$

**Question 28** How to describe the global minimizer when  $v$  increases?



## Summer School 2014: Inverse Problem and Image Processing

### Tutorial: Inverse modeling in inverse problems using optimization

#### Outline

1. Energy minimization methods (p. 7)
2. Regularity results (p. 17)
3. Non-smooth regularization – minimizers are sparse in a given subspace (p. 26)
4. Non-smooth data-fidelity – minimizers fit exactly some data entries (p. 35)
5. Comparison with Fully Smooth Energies (p. 51)
6. Non-convex regularization – edges are sharp (p. 54)
7. Nonsmooth data-fidelity and regularization – peculiar features
8. Fully smoothed  $\ell_1$ –TV models – bounding the residual (p. 83)
9. Inverse modeling and Bayesian MAP – there is distortion (p. 98)
10. Some References (p. 103)

## 7. Nonsmooth data-fidelity and regularization

Consequence of §3 and §4: if  $\Phi$  and  $\Psi$  non-smooth, 
$$\begin{cases} G_i \hat{u} = 0 & \text{for } i \in \hat{h}_\varphi \neq \emptyset \\ a_i \hat{u} = v[i] & \text{for } i \in \hat{h}_\psi \neq \emptyset \end{cases}$$

### The $L_1$ -TV energy

T. F. Chan and S. Esedoglu, “Aspects of Total Variation Regularized  $L^1$  Function Approximation”, SIAM J. on Applied Mathematics, 2005

$$\mathcal{F}_v(u) = \|u - \mathbb{1}_\Omega\|_1 + \beta \int_{\mathbb{R}^d} \|\nabla u(x)\|_2 dx \quad \text{where} \quad \mathbb{1}_\Omega(x) := \begin{cases} 1 & \text{if } x \in \Omega \\ 0 & \text{else} \end{cases}$$

•  $\exists \hat{u} = \mathbb{1}_\Sigma$  ( $\Omega$  convex  $\Rightarrow \Sigma \subset \Omega$  and  $\hat{u}$  unique for almost every  $\beta > 0$ )

• **contrast invariance**: if  $\hat{u}$  minimizes for  $v = \mathbb{1}_\Omega$  then  $c\hat{u}$  minimizes  $\mathcal{F}_{cv}$

the contrast of image features is more important than their shapes

• critical values  $\beta^*$  
$$\begin{cases} \beta < \beta^* & \Rightarrow \text{objects in } \hat{u} \text{ with good contrast} \\ \beta > \beta^* & \Rightarrow \text{they suddenly disappear} \end{cases}$$

$\Rightarrow$  **data-driven scale selection**

## Binary images by L1 – TV

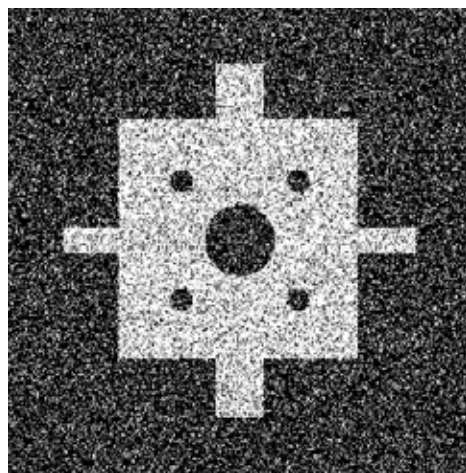
[T. Chan, S. Esedoglu, Nikolova 06]

Classical approach to find a binary image  $\hat{u} = \mathbf{1}_{\hat{\Sigma}}$  from binary data  $\mathbf{1}_{\Omega}$ ,  $\Omega \subset \mathbb{R}^2$

$$\hat{\Sigma} = \arg \min_{\Sigma} \{ \|\mathbf{1}_{\Sigma} - \mathbf{1}_{\Omega}\|_2^2 + \beta \text{TV}(\mathbf{1}_{\Sigma}) \} \quad \text{nonconvex problem} \quad (\star)$$

usual techniques (curve evolution, level-sets) fail

$$\hat{\Sigma} \text{ solves } (\star) \Leftrightarrow \hat{u} = \mathbf{1}_{\hat{\Sigma}} \text{ minimizes } \|u - \mathbf{1}_{\Omega}\|_1 + \beta \text{TV}(u) \quad (\text{convex})$$



Data

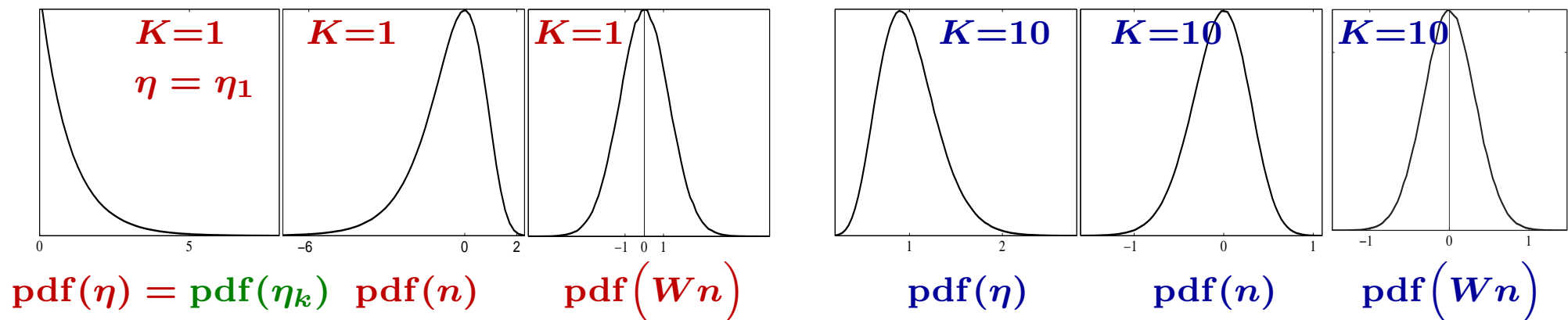


Restored

## Multiplicative noise removal on Frame coefficients [Durand, Fadili, Nikolova 09]

Multiplicative noise arises in various active imaging systems e.g. synthetic aperture radar

- Original image:  $S_o$
- One shot:  $\Sigma_k = S_o \eta_k$
- Data:  $\Sigma = \frac{1}{K} \sum_{k=1}^K \Sigma_k = S_o \frac{1}{K} \sum_{k=1}^K \eta_k = S_o \eta$  where  $\text{pdf}(\eta) = \text{Gamma density}$
- Log-data:  $v = \log \Sigma = \log S_o + \log \eta = u_0 + n$
- Frame Coefficients:  $y = Wv = Wu_0 + Wn$  ( $W$  curvelets)



**Question 29** Comment the noise distribution of  $Wn$

- Hard Thresholding:  $y_T[i] = \begin{cases} 0 & \text{if } |y[i]| \leq T, \\ y[i] & \text{otherwise} \end{cases} \quad \forall i \in I, \quad T > 0$  (suboptimal).

$$I_1 = \{i \in I : |y[i]| > T\} \quad \text{and} \quad I_0 = I \setminus I_1$$

- **Restored coefficients:**  $\hat{x} = \arg \min_x \mathcal{F}_y(x)$  ( $\ell_1 - \text{TV}$  energy)

$$\mathcal{F}_y(x) = \lambda_0 \sum_{i \in I_0} |x[i]| + \lambda_1 \sum_{i \in I_1} |x[i] - y[i]| + \|\widetilde{W}x\|_{\text{TV}}$$

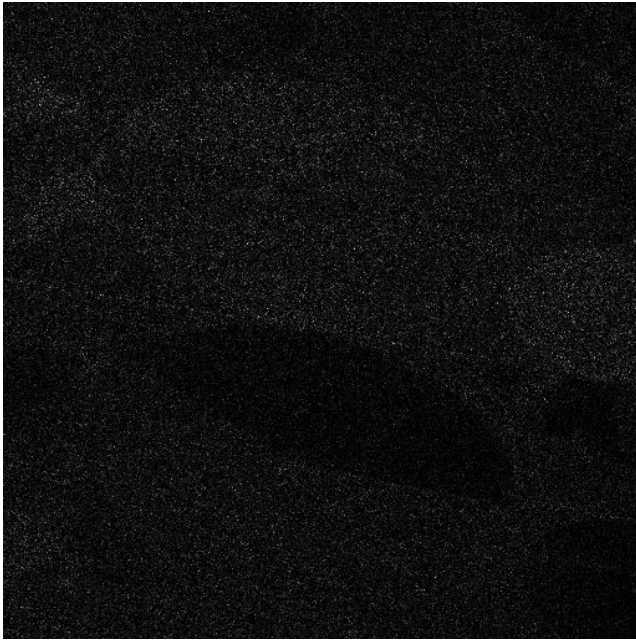
$$\hat{S} = B \exp(\widetilde{W} \hat{x}), \quad \text{where } \widetilde{W} \text{ left inverse, } B \text{ bias correction}$$

**Question 30** Explain the job the minimizer  $\hat{x}$  of  $\mathcal{F}_y$  should do.

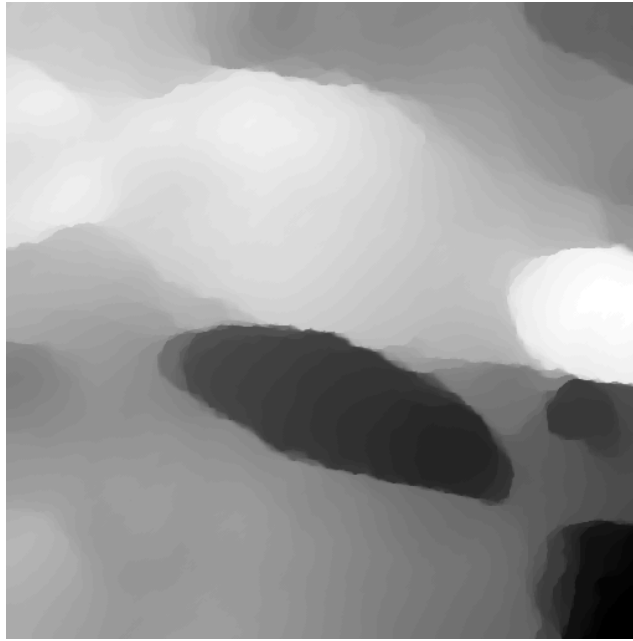
### Some comparisons

- **BS** [Chesneau, Fadili, Starck 08]: Block-Stein thresholds the curvelet coefficients,  $\approx$  minimax (large class of images with additive noises), optimal threshold  $\mathfrak{T} = 4.50524$
- **AA** [Aubert, Aujol 08]:  $\Psi = -\text{Log-Likelihood}(\Sigma)$ ,  $\Phi = \text{TV}(\Sigma)$  (i.e.  $\mathcal{F}_v \equiv \text{MAP}$  for  $\Sigma$ )
- **SO** [Shi, Osher 08]: relaxed inverse scale-space for  $\mathcal{F}_v(u) = \|v - u\|_2^2 + \beta \text{TV}(u) \approx \text{MAP}(u)$   
Stopping rule:  $k^* = \max\{k \in \mathbb{N} : \text{Var}(u^{(k)} - u_o) \geq \text{Var}(n)\}$ .

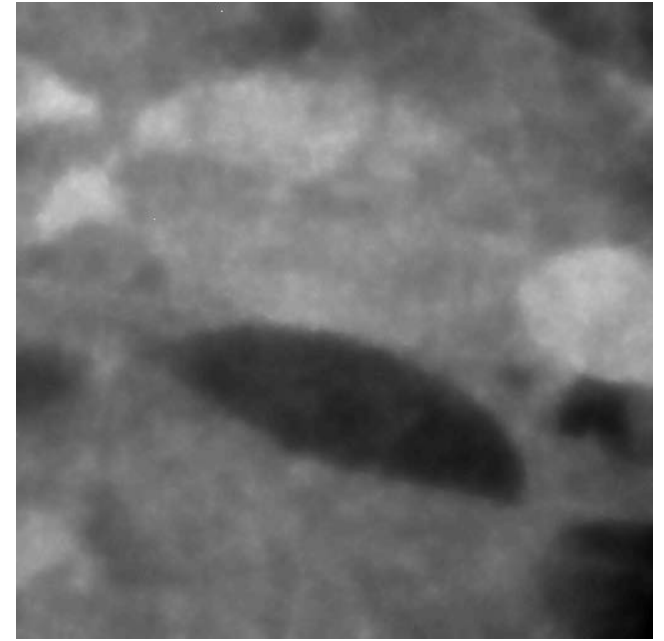
Monte-Carlo comparative experiment confirms the proposed method



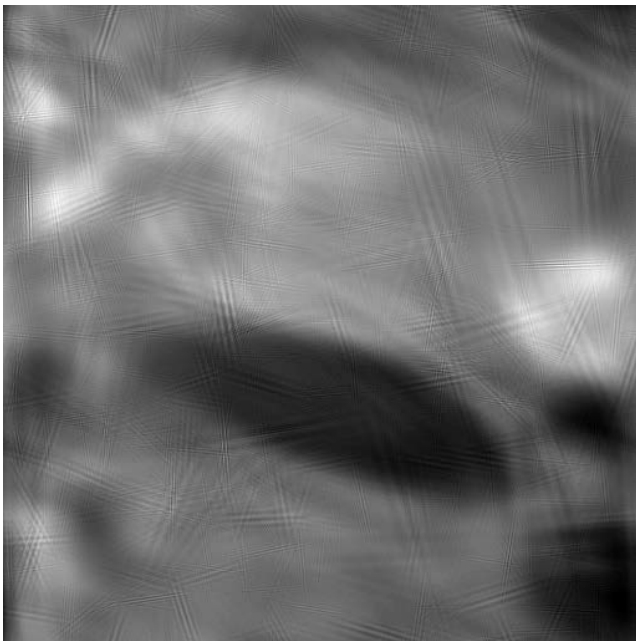
Noisy Fields  $K = 1$  (512×512)



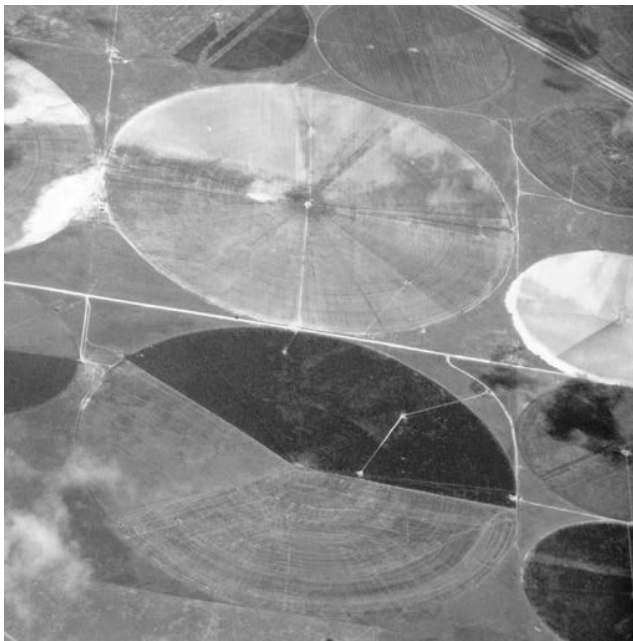
SO: PSNR=9.59, MAE=196



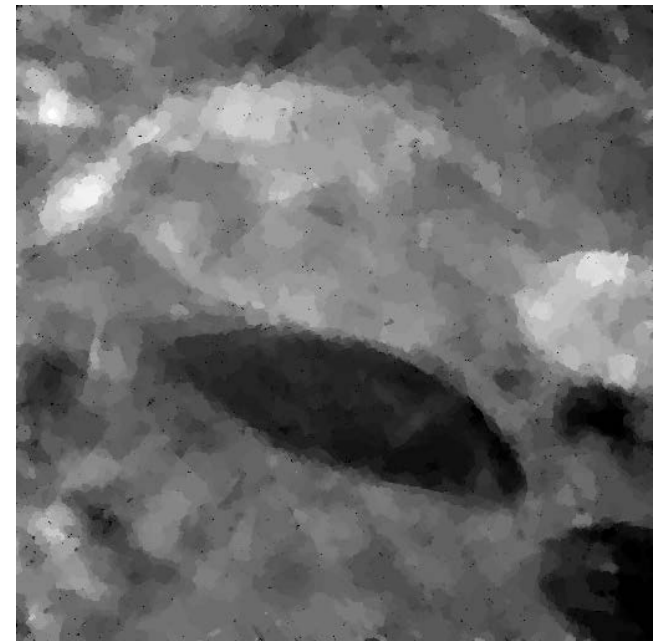
AA: PSNR=15.74, MAE=76.66



BS: PSNR=22.52, MAE=35.22

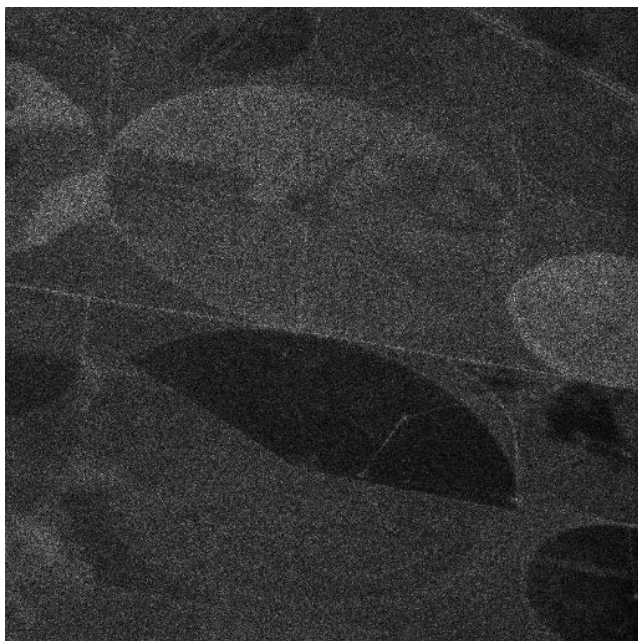


Fields (original)



Our: PSNR=22.89, MAE=33.67

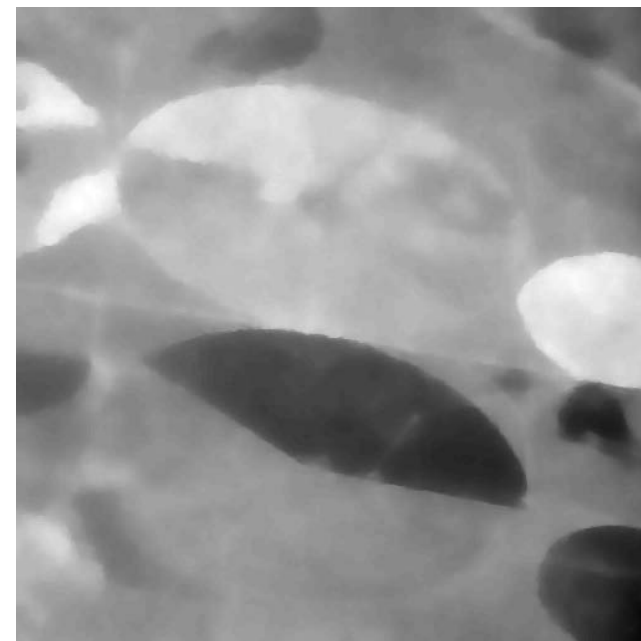




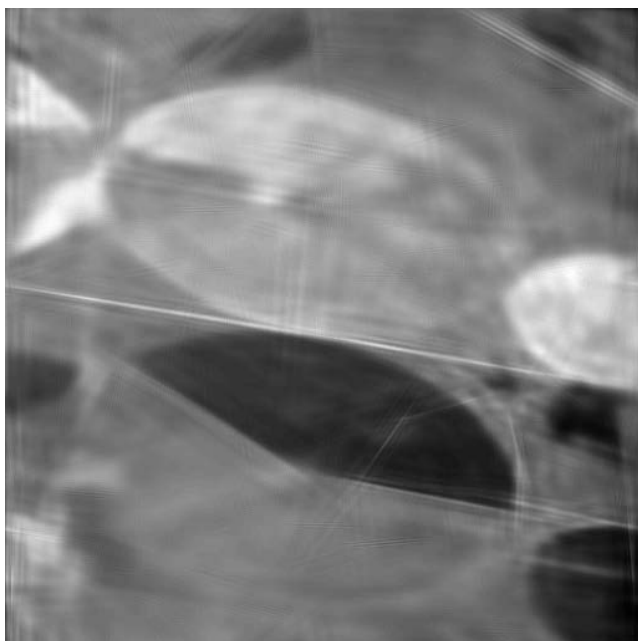
Noisy  $K = 10$



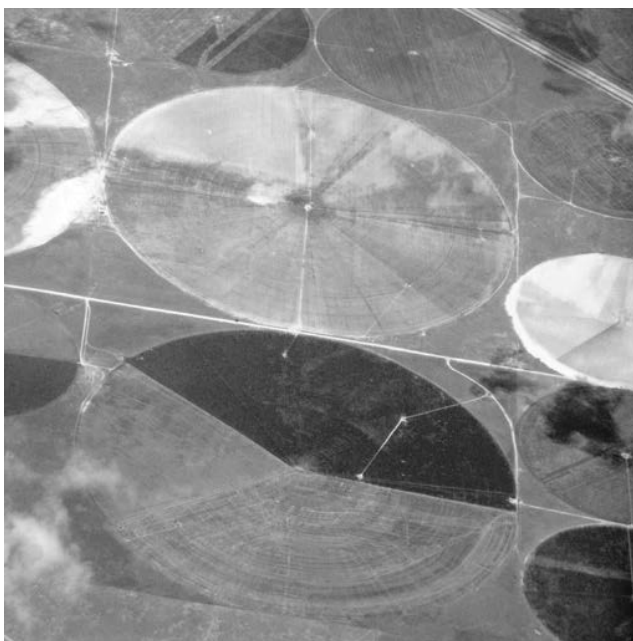
SO: PSNR=25.36, MAE=25.14



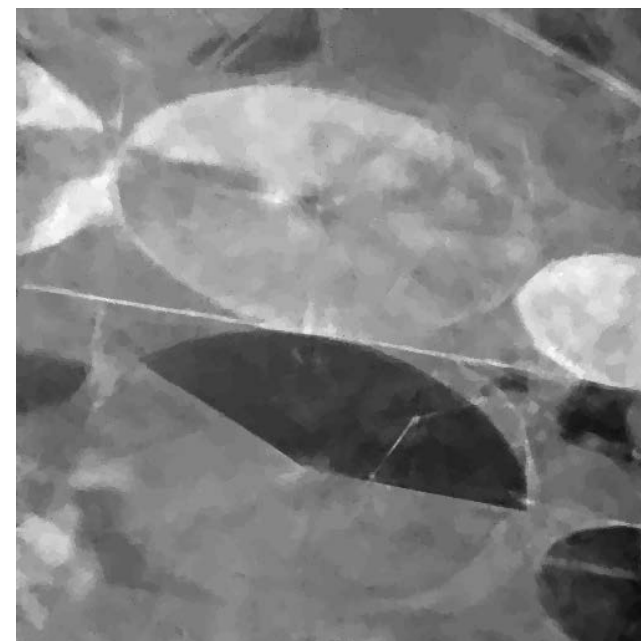
AA: PSNR=17.13, MAE=65.40



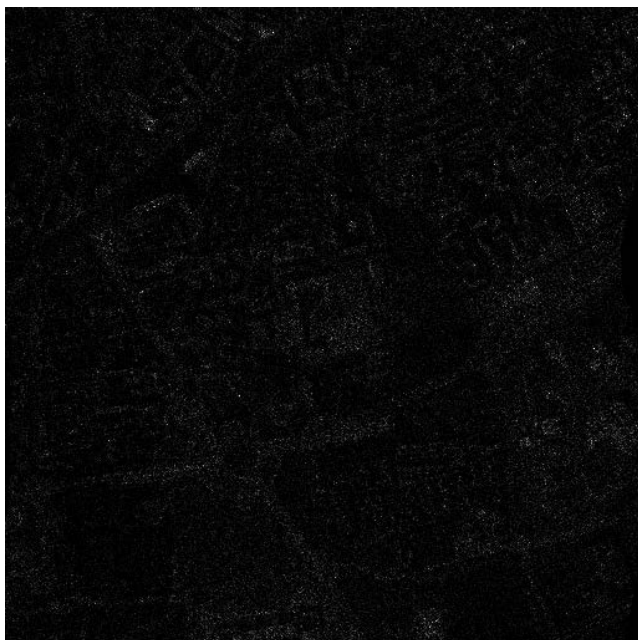
BS: PSNR=27.24, MAE=19.61



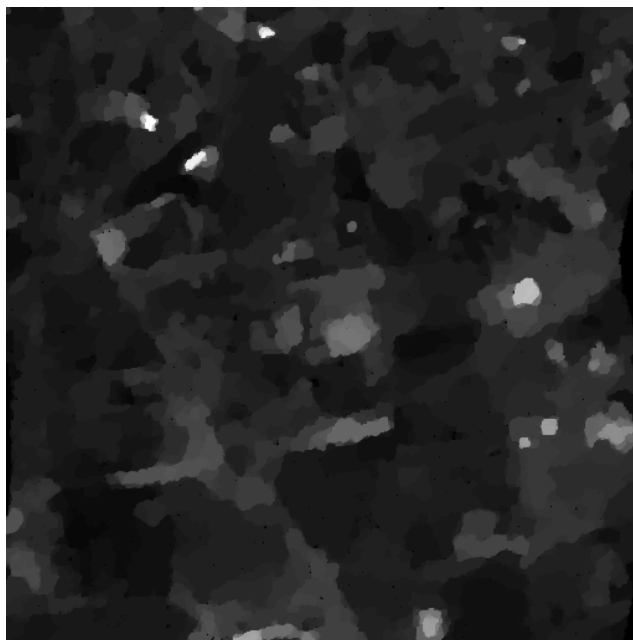
Fields (original)



Our: PSNR=28.04, MAE=18.19



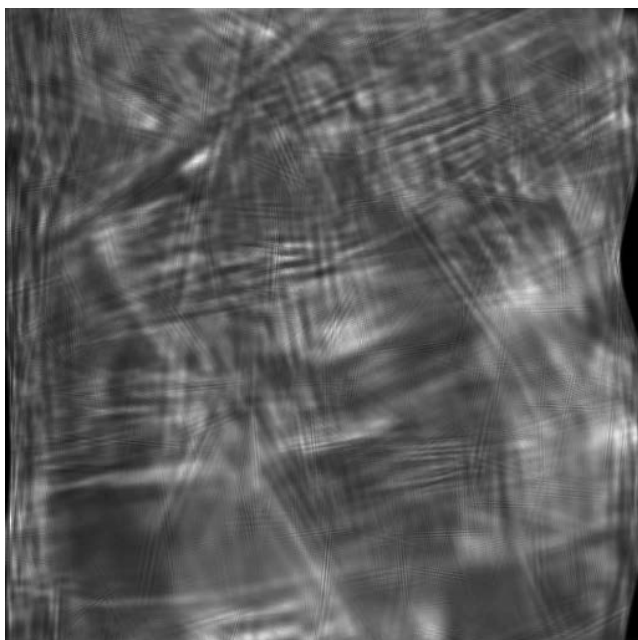
Noisy City  $K = 1$  (512×512)



SO: PSNR=18.39, MAE=24.08



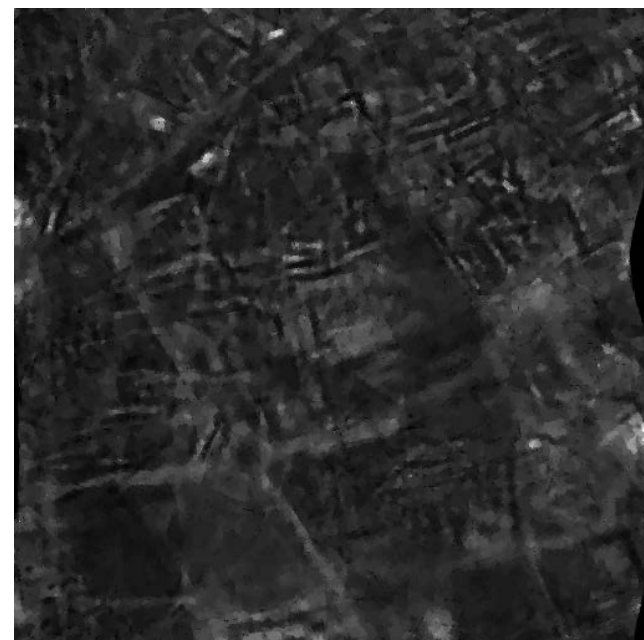
AA: PSNR=22.18, MAE=13.71



BS: PSNR=22.25, MAE=13.96



City (original)



Our: PSNR=22.64, MAE=13.39





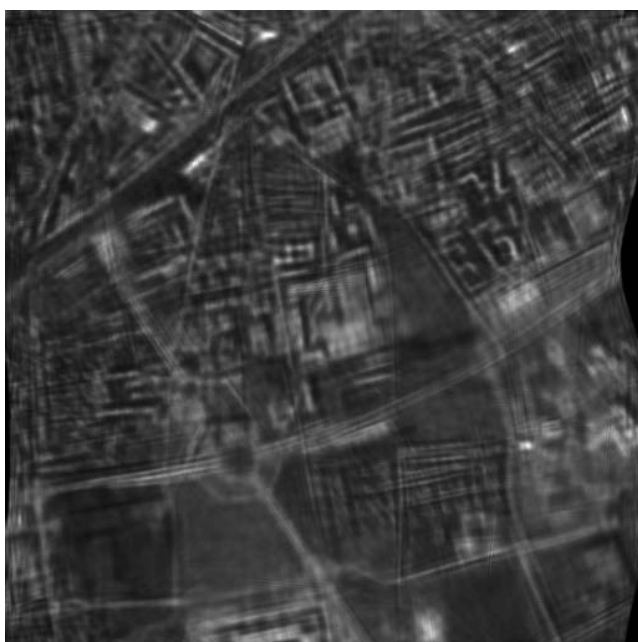
Noisy  $K = 4$



SO: PSNR=24.40, MAE=10.76



AA: PSNR=24.55, MAE=10.06



BS: PSNR=24.92, MAE=9.87



City (original)

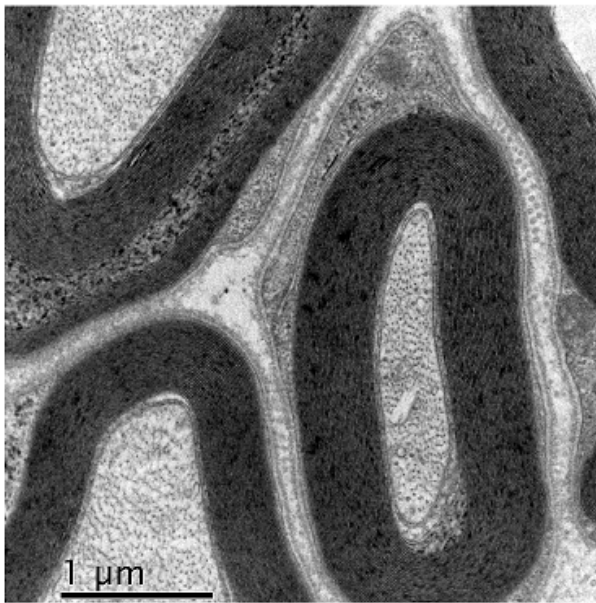


Our: PSNR=25.84, MAE=9.09

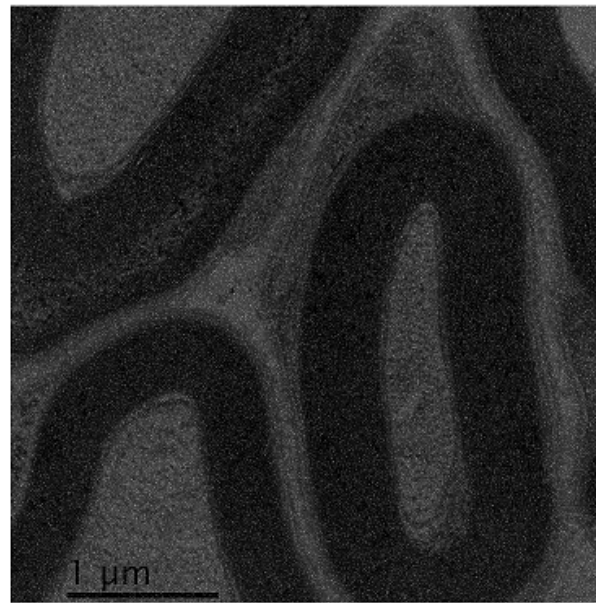
C. Clason, B. Jin, K. Kunisch

“Duality-based splitting for fast  $\ell_1$  – TV image restoration”, 2012,  
<http://math.uni-graz.at/optcon/projects/clason3/>

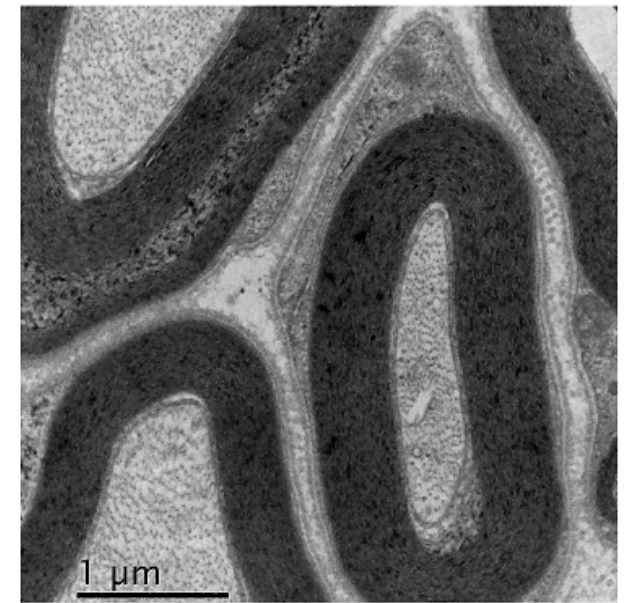
Scanning transmission electron microscopy ( $2048 \times 2048$  image)



true image



noisy image



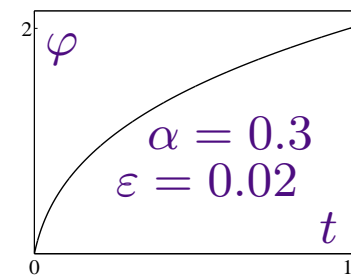
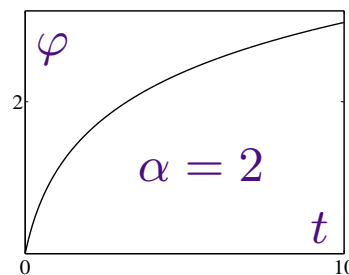
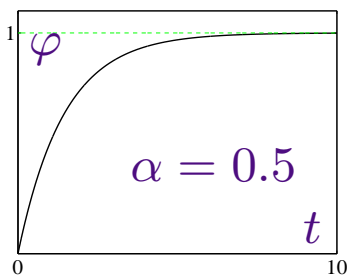
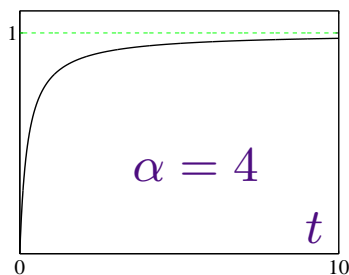
restoration

$$\mathcal{F}_v(u) = \sum_{i \in I} |a_i u - v[i]| + \beta \sum_{j \in J} \varphi(\|G_j u\|_2), \quad \varphi'(0^+) > 0, \quad \varphi''(t) < 0, \quad \forall t \geq 0$$

$$I = \{1, \dots, q\}, \quad J = \{1, \dots, r\}$$

$\varphi$  is strictly concave on  $[0, +\infty)$ .

$$\varphi(t) \quad \left\| \begin{array}{l} \frac{\alpha t}{\alpha t + 1} \quad \left| \quad 1 - \alpha^t, \alpha \in (0, 1) \quad \left| \quad \ln(\alpha t + 1) \quad \left| \quad (t + \varepsilon)^\alpha, \alpha \in (0, 1), \varepsilon > 0 \quad \left| \quad (\dots) \end{array} \right. \right. \right. \right.$$



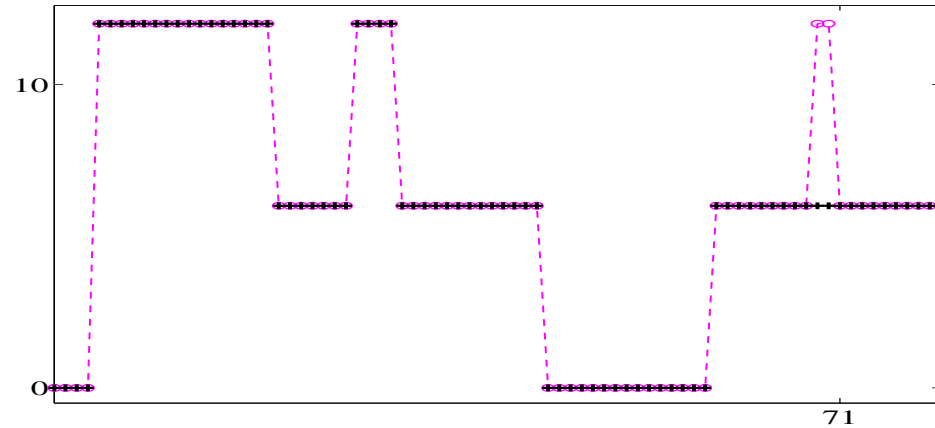
## Motivation

- This family of objective functions has never been considered before
- $\mathcal{F}_v$  can be seen as an extension of  $L1 - TV$
- $\hat{u}$ —(local) minimizer of  $\mathcal{F}_v \quad \xRightarrow{?}$  many  $i, j$  such that  $a_i \hat{u} = v[i]$  and  $G_j \hat{u} = 0$

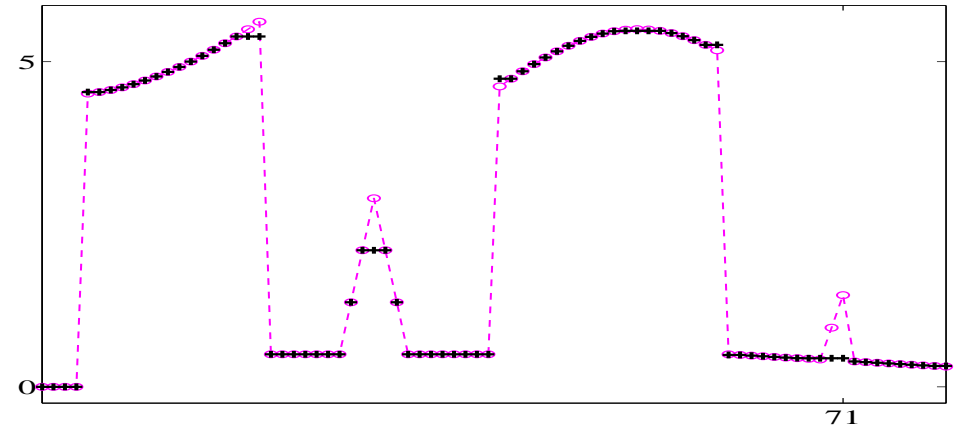


Minimizers of  $\mathcal{F}_v(u) = \|u - v\|_1 + \beta \sum_{i=1}^{p-1} \varphi(|u[i+1] - u[i]|)$

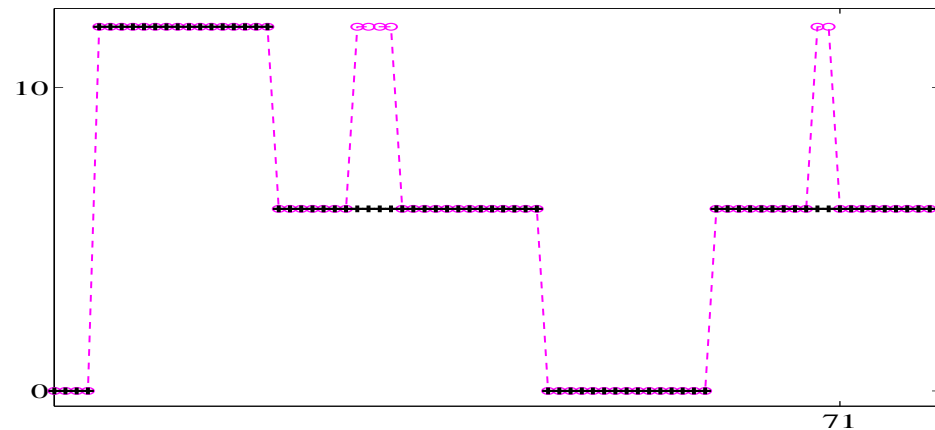
$$\varphi(t) = \frac{\alpha t}{\alpha t + 1} \text{ for } \alpha = 4$$



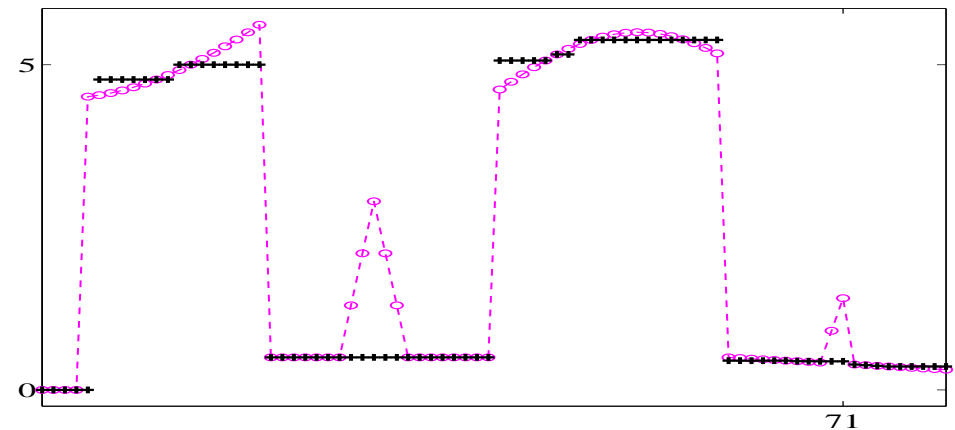
$$\varphi(t) = \ln(\alpha t + 1) \text{ for } \alpha = 2$$



$$\beta \in \{78, \dots, 156\}$$



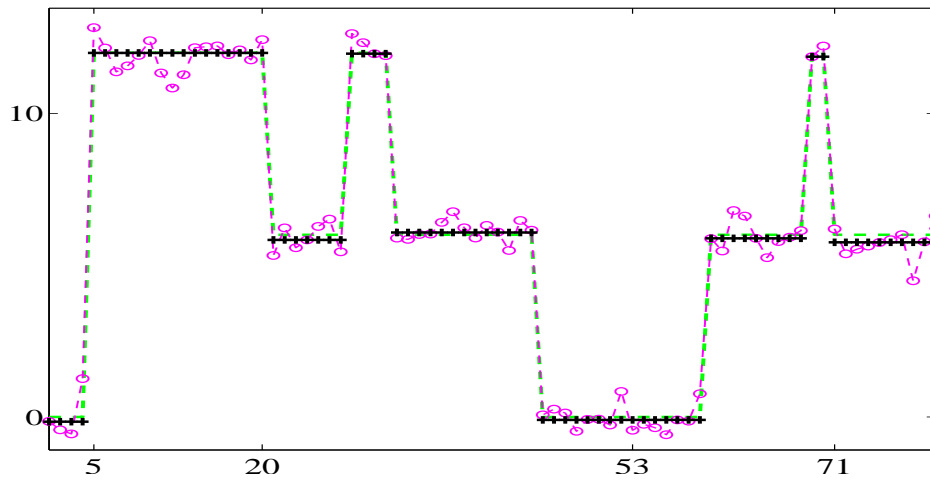
$$\beta \in 0.1 \times \{10, \dots, 14\}$$



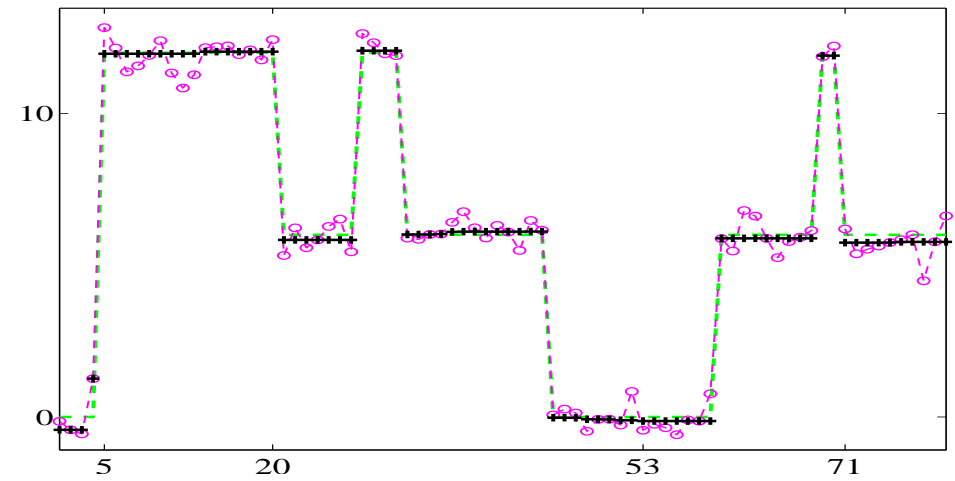
$$\beta \in \{157, \dots, 400\}$$

$$\beta \in 0.1 \times \{16, \dots, 30\}$$

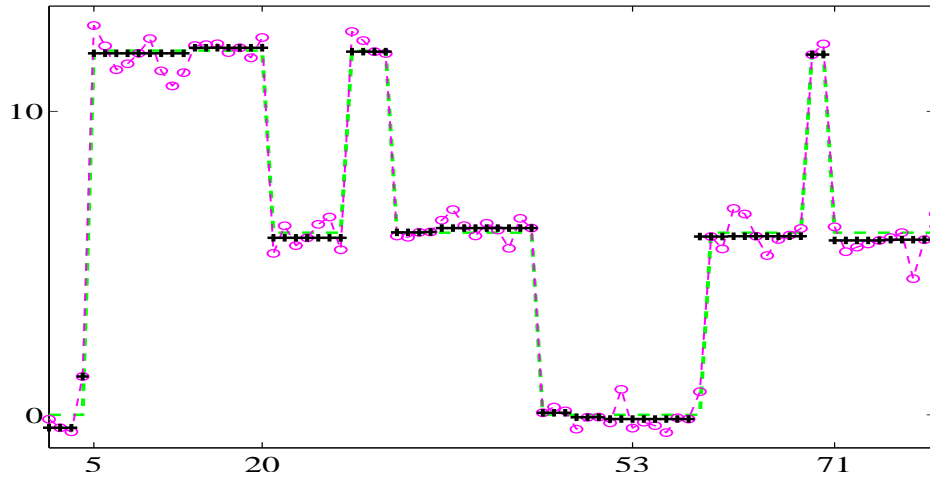
Data samples (ooo), Minimizer samples  $\hat{u}[i]$  (+++).



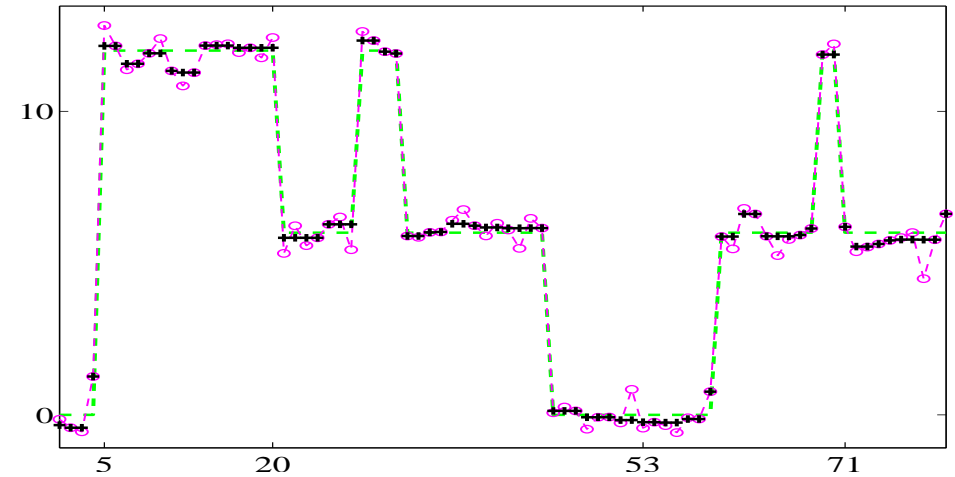
(a)  $\varphi(t) = \frac{\alpha t}{\alpha t + 1}$ ,  $\alpha = 4$ ,  $\beta = 3$



(b)  $\varphi(t) = 1 - \alpha^t$ ,  $\alpha = 0.1$ ,  $\beta = 2.5$



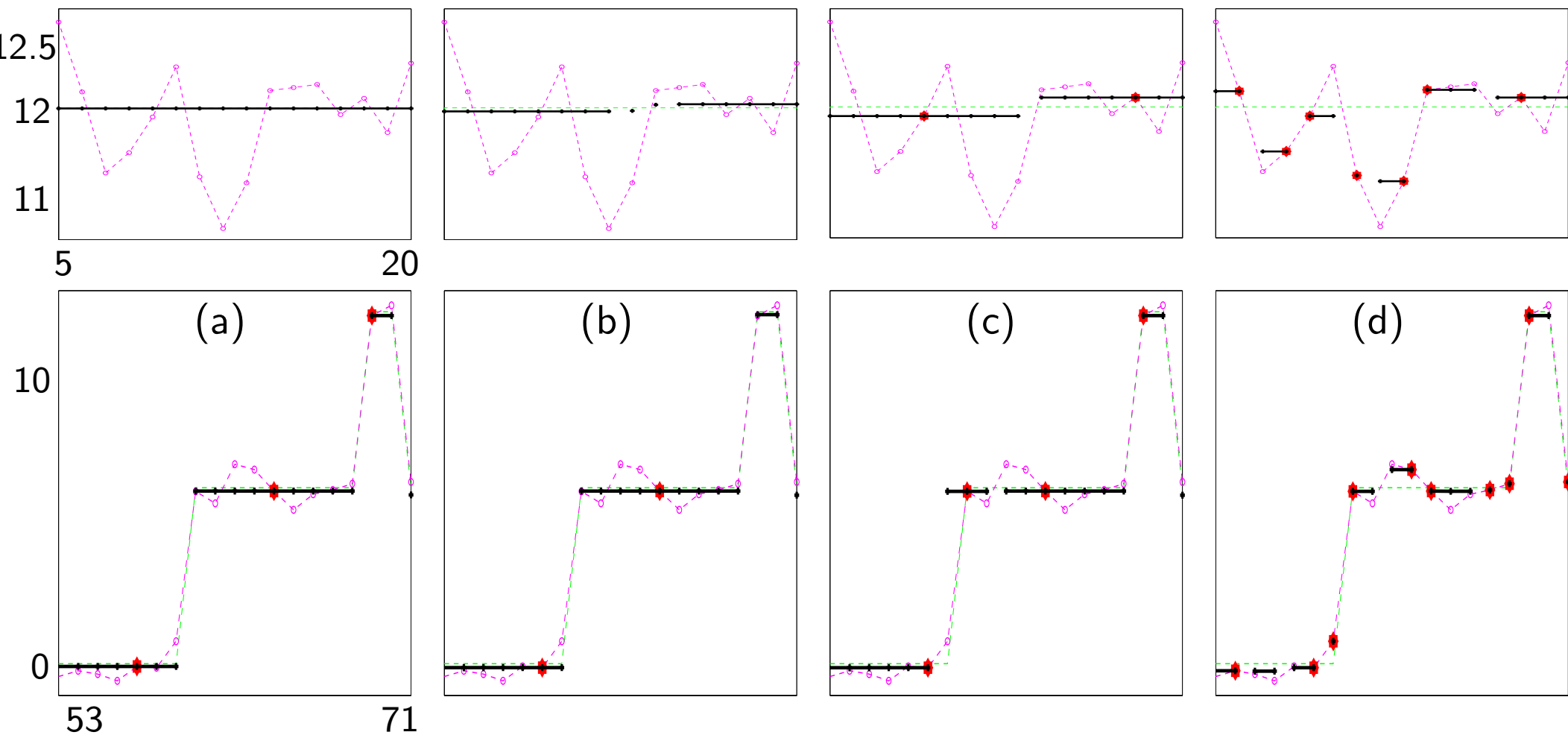
(c)  $\varphi(t) = \ln(\alpha t + 1)$ ,  $\alpha = 2$ ,  $\beta = 1.3$



(d)  $\varphi(t) = (t + 0.1)^\alpha$ ,  $\alpha = 0.5$ ,  $\beta = 1.4$

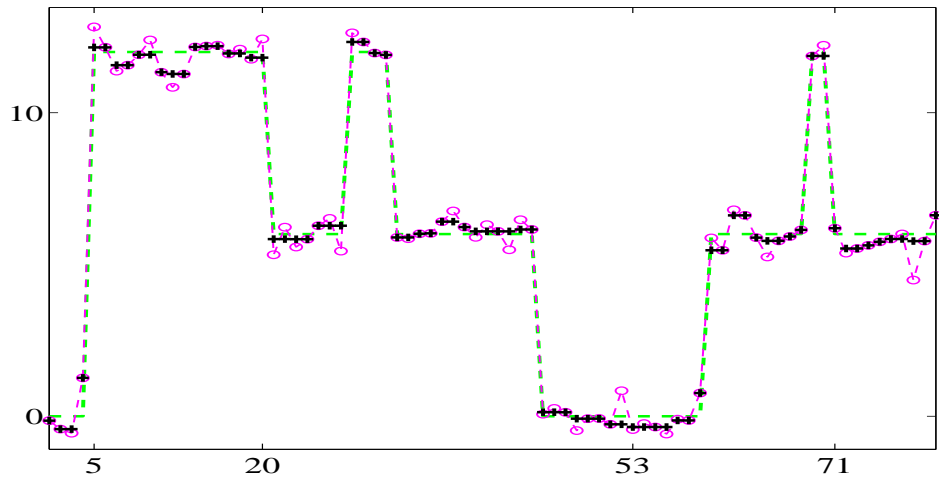
**Denoising:** Data samples (○○○) are corrupted with Gaussian noise. Minimizer samples  $\hat{u}[i]$  (+++). Original (---).  $\beta$ —the largest value so that the gate at 71 survives.

## Zooms



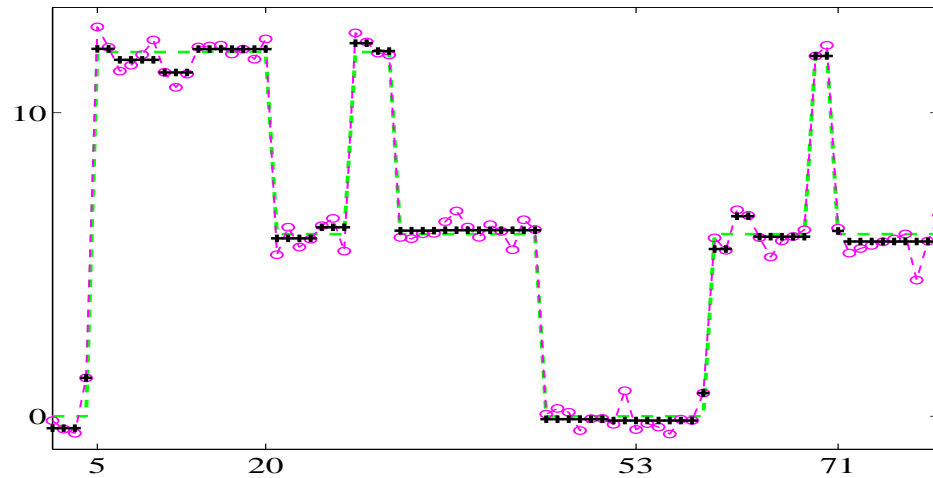
Constant pieces—solid black line.

Data points  $v[i]$  fitted exactly by the minimizer  $\hat{u}$  ( $\blacklozenge$ ).



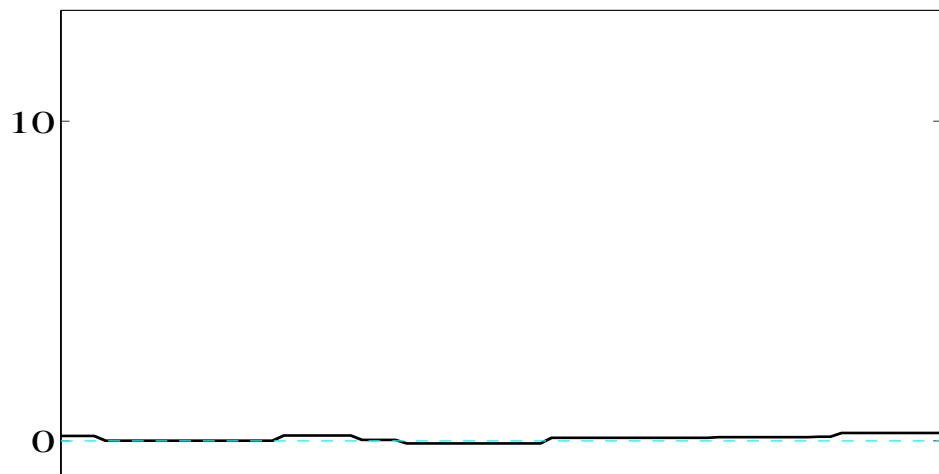
$\varphi(t) = t, \beta = 0.8 \quad (\ell_1 - \text{TV})$

the convex relaxation of  $\mathcal{F}_v$



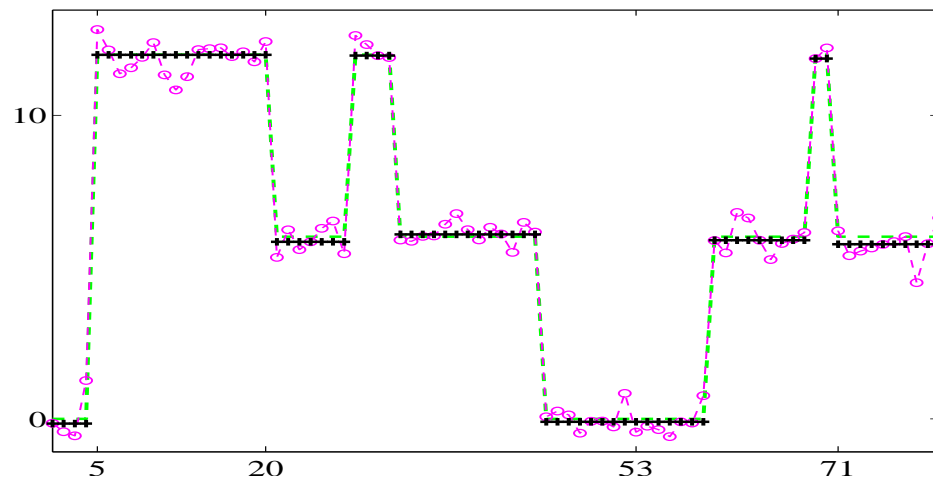
the minimizer for  $\varphi(t) = \frac{\alpha t}{\alpha t + 1}, \alpha = 4, \beta = 3$

closest to  $(\ell_1 - \text{TV})$



error for  $\varphi(t) = \frac{\alpha t}{\alpha t + 1}, \alpha = 4, \beta = 3$

$\|\text{original} - \hat{u}\|_\infty = 0.24$



$\varphi(t) = \frac{\alpha t}{\alpha t + 1}, \alpha = 4, \beta = 3$

original  $\in [0, 12]$ , data  $v \in [-0.6, 12.9]$

On the figures,  $\hat{u}$  are global minimizers of  $\mathcal{F}_v$  (Viterbi algorithm)

**Question 31** Can you sketch the main properties of the minimizers of  $\mathcal{F}_v$ ?

**Question 32** What seems being the role of the asymptotic of  $\varphi$ ?

Numerical evidence:

critical values  $\beta_1, \dots, \beta_n$  such that

- $\beta \in [\beta_i, \beta_{i+1}) \Rightarrow$  the minimizer remains unchanged
- $\beta \geq \beta_{i+1} \Rightarrow$  the minimizer is simplified

Result proven (under conditions) for the minimizers of  $L_1 - \text{TV}$  in [Chan, Esedoglu 2005]



Given  $v \in \mathbb{R}$  consider the function

$$\mathcal{F}_v(u) = |u - v| + \beta\varphi(|u|) \quad \text{for } \varphi(u) = \frac{\alpha u}{1 + \alpha u} \quad u \in \mathbb{R}, \quad \beta > 0$$

**Question 33** Does  $\mathcal{F}_v$  have a global minimizer for any  $v$ ? Explain.

**Question 34** Determine  $\varphi''(u)$  for  $u \in \mathbb{R} \setminus \{0\}$ .

**Question 35** Show that  $\forall v \in \mathbb{R}$ , any minimizer  $\hat{u}$  of  $\mathcal{F}_v$  obeys  $\hat{u} \in \{0, v\}$ .

**Question 36** Can you extend this result to the other  $\varphi$  on p. 71?

- $\mathcal{F}_v$  does have global minimizers, for any  $\{a_i\}$ , for any  $v$  and for any  $\beta > 0$ .
- Let  $\hat{u}$  be a (local) minimizer of  $\mathcal{F}_v$ . Set

$$\begin{aligned}\hat{I}_0 &= \{i \in I : a_i \hat{u} = v[i]\} \\ \hat{J}_0 &= \{j \in J : G_j \hat{u} = 0\}\end{aligned}$$

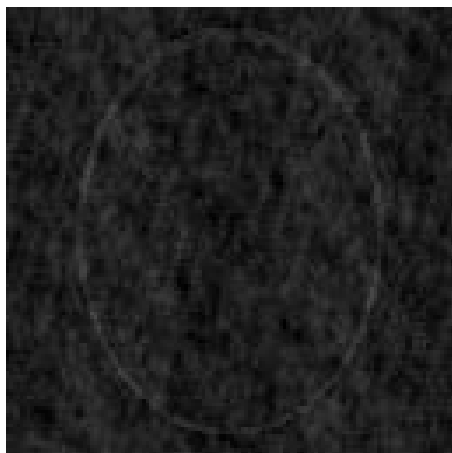
$\hat{u}$  is the unique point solving the linear system

$$\begin{cases} a_i \hat{u} = v[i] & \forall i \in \hat{I}_0 \\ G_j \hat{u} = 0 & \forall j \in \hat{J}_0 \end{cases}$$

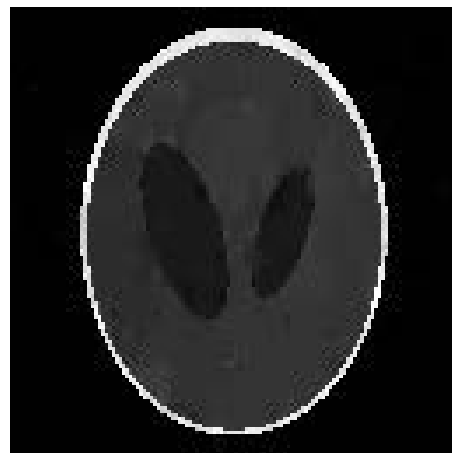
Each pixel of a (local) minimizer  $\hat{u}$  of  $\mathcal{F}_v$  is involved in (at least) one equation  $a_i \hat{u} = v[i]$ , or in (at least) one equation  $G_j \hat{u} = 0$ , or in both types of equations.

- “Contrast invariance” of (local) minimizers
- The matrix with rows  $(a_i, \forall i \in \hat{I}_0, G_j, \forall j \in \hat{J}_0)$  has full column rank
- All (local) minimizers of  $\mathcal{F}_v$  are strict

# MR Image Reconstruction from Highly Undersampled Data



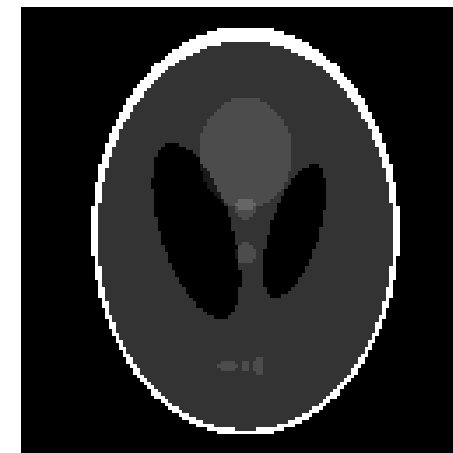
0-filling Fourier



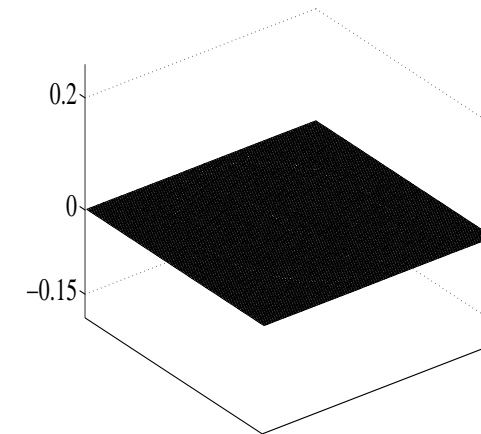
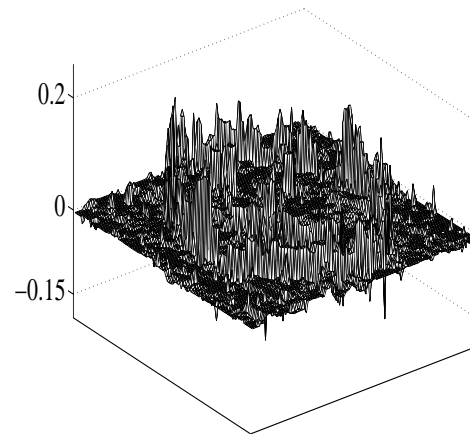
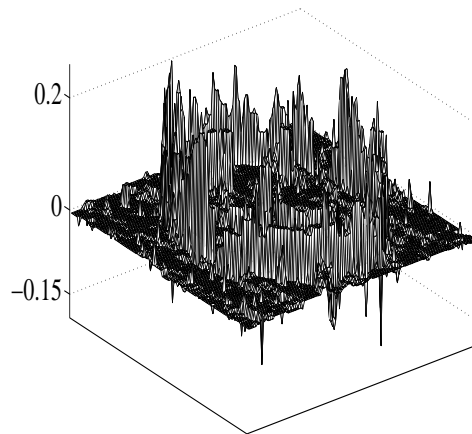
$\|\cdot\|_2 + \text{TV}$



$\|\cdot\|_1 + \text{TV}$



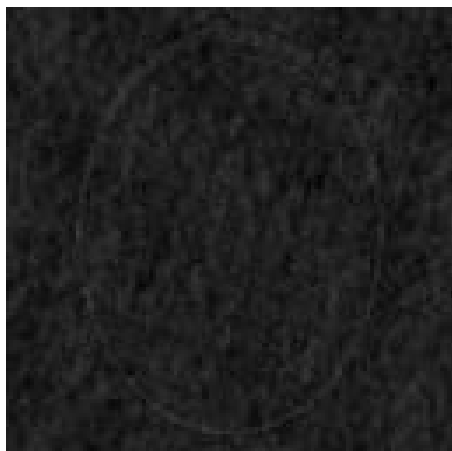
Our method



Reconstructed images from **7% noisy** randomly selected samples in the  $k$ -space.

Our method for  $\varphi(t) = \frac{\alpha t}{\alpha t + 1}$ .

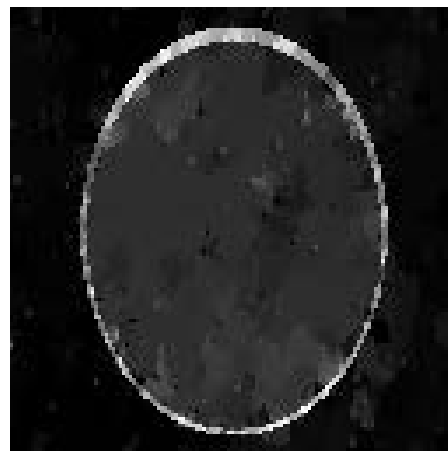
# MR Image Reconstruction from Highly Undersampled Data



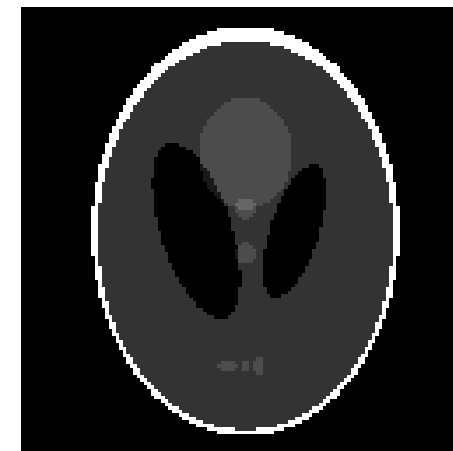
0-filling Fourier



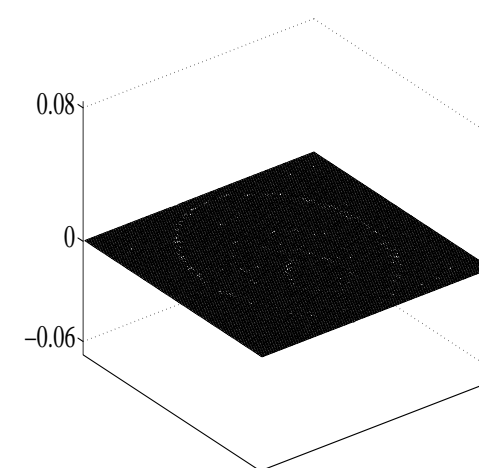
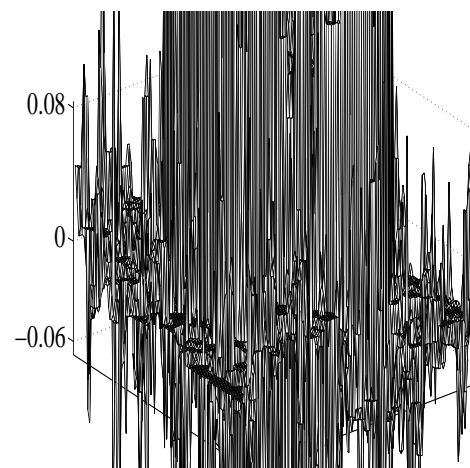
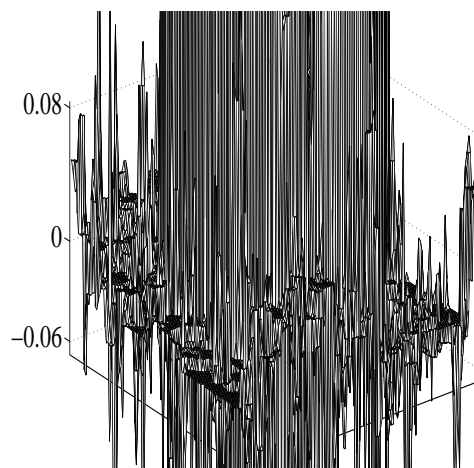
$\|\cdot\|_2 + \text{TV}$



$\|\cdot\|_1 + \text{TV}$



Our method



Reconstructed images from **5% noisy** randomly selected samples in the  $k$ -space.

Our method for  $\varphi(t) = \frac{\alpha t}{\alpha t + 1}$ .

## Cartoon



Observed



$\ell_1$ -TV



Our method,  $\varphi(t) = \frac{\alpha t}{\alpha t + 1}$

## Summer School 2014: Inverse Problem and Image Processing

### Tutorial: Inverse modeling in inverse problems using optimization

#### Outline

1. Energy minimization methods (p. 7)
2. Regularity results (p. 17)
3. Non-smooth regularization – minimizers are sparse in a given subspace (p. 26)
4. Non-smooth data-fidelity – minimizers fit exactly some data entries (p. 35)
5. Comparison with Fully Smooth Energies (p. 51)
6. Non-convex regularization – edges are sharp (p. 54)
7. Nonsmooth data-fidelity and regularization – peculiar features (p. 62)
8. Fully smoothed  $\ell_1$ –TV models – bounding the residual
9. Inverse modeling and Bayesian MAP – there is distortion (p. 98)
10. Some References (p. 103)

## 8. Fully smoothed $\ell_1$ – TV

$$\mathcal{F}_v(\mathbf{u}) = \Psi(\mathbf{u}, \mathbf{v}) + \beta \Phi(\mathbf{u}), \quad \beta > 0$$

$$\Psi(\mathbf{u}, \mathbf{v}) = \sum_{i=1}^p \psi(\mathbf{u}[i] - \mathbf{v}[i]) \quad \text{and} \quad \Phi(\mathbf{u}) = \sum_i \varphi(|\mathbf{G}_i \mathbf{u}|)$$

$$\psi(\cdot) := \psi(\cdot, \alpha_1)$$

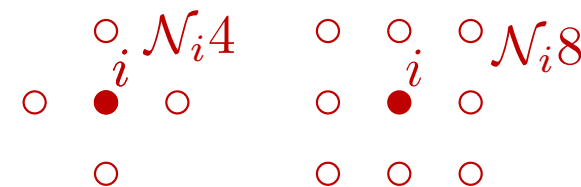
$$\varphi(\cdot) := \varphi(\cdot, \alpha_2)$$

$$(\alpha_1, \alpha_2) > 0$$

$\{G_i \in \mathbb{R}^{1 \times p}\}$  – forward discretization:

$\mathcal{N}_4$  Only vertical and horizontal differences;

$\mathcal{N}_8$  Diagonal differences are added.



$(\psi, \varphi)$  belong to the *family of functions*  $\theta(\cdot, \alpha) : \mathbb{R} \rightarrow \mathbb{R}$  satisfying

**H1** For any  $\alpha > 0$  fixed,  $\theta(\cdot, \alpha)$  is  $\mathcal{C}^{s \geq 2}$ -continuous, even and  $\theta''(t, \alpha) > 0, \forall t \in \mathbb{R}$ .

**H2** For any  $\alpha > 0$  fixed,  $|\theta'(t, \alpha)| < 1$  and for  $t > 0$  fixed, it is strictly decreasing in  $\alpha > 0$

$$\alpha > 0 \quad \Rightarrow \quad \lim_{t \rightarrow \infty} \theta'(t, \alpha) = 1 \quad \theta'(t, \alpha) := \frac{d}{dt} \theta(t, \alpha)$$

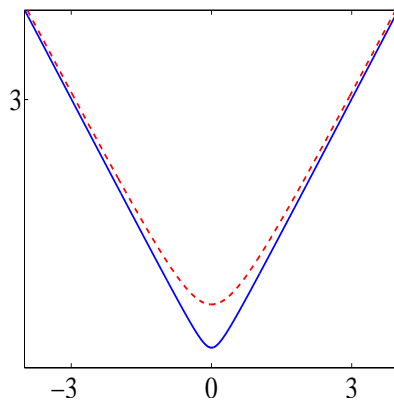
$$t \in \mathbb{R} \quad \Rightarrow \quad \lim_{\alpha \rightarrow 0} \theta'(t, \alpha) = 1 \quad \text{and} \quad \lim_{\alpha \rightarrow \infty} \theta'(t, \alpha) = 0 .$$

$\Rightarrow \mathcal{F}_v$  is a fully smoothed  $\ell_1$  – TV energy.

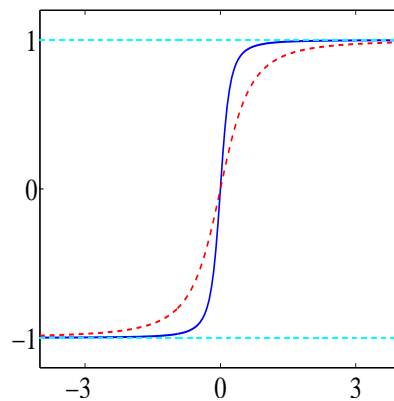


	$\theta$	$\theta'$
f1	$\sqrt{t^2 + \alpha}$	$\frac{t}{\sqrt{t^2 + \alpha}}$
f2	$\alpha \log \left( \cosh \left( \frac{t}{\alpha} \right) \right)$	$\tanh \left( \frac{t}{\alpha} \right)$
f3	$ t  - \alpha \log \left( 1 + \frac{ t }{\alpha} \right)$	$\frac{t}{\alpha +  t }$

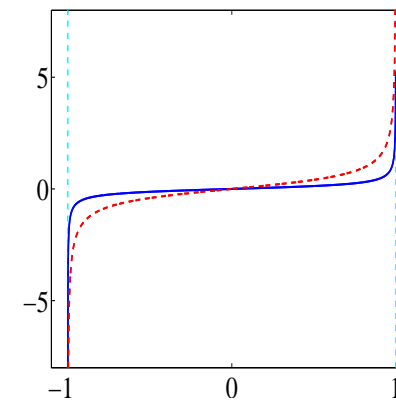
Choices for  $\theta(\cdot, \alpha)$  obeying H1 and H2. When  $\alpha \searrow 0$ ,  $\theta(\cdot, \alpha)$  becomes stiff near the origin.



$$\theta(t) = \sqrt{t^2 + \alpha}$$



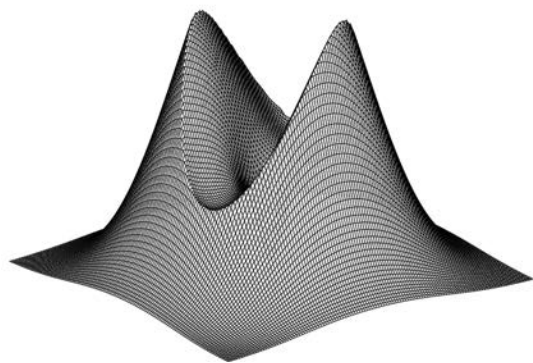
$$\theta'(t) = \frac{t}{\sqrt{t^2 + \alpha}}$$



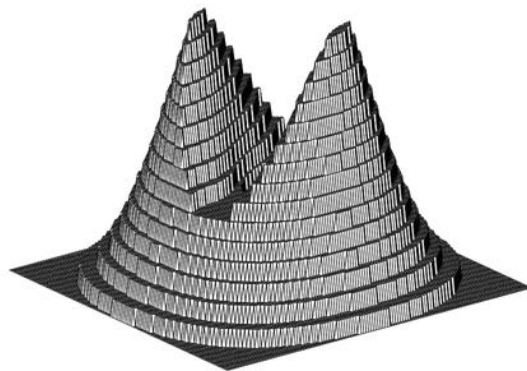
$$(\theta')^{-1}(y) = y \sqrt{\frac{\alpha}{1 - y^2}}$$

Plots of f1 for  $\alpha = 0.05$  (—) and for  $\alpha = 0.5$  (---).

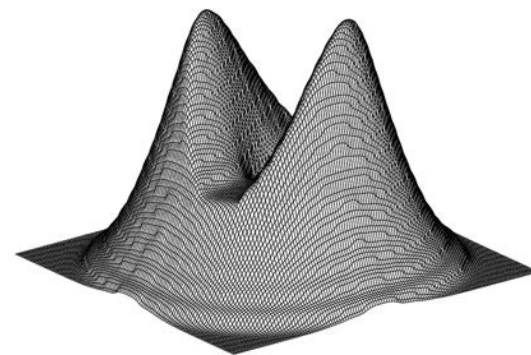
The minimizers  $\hat{u}$  of  $\mathcal{F}_v$  can decrease the quantization noise



Real-valued original



$v$  quantized on  $\{0, \dots, 15\}$



Restored  $\hat{u}$

- For any  $\beta > 0$ ,  $\mathcal{F}_v(\mathbb{R}^p)$  has a unique minimizer function  $\mathcal{U} : \mathbb{R}^p \rightarrow \mathbb{R}^p$  which is  $\mathcal{C}^{s-1}$ .

$$\text{Define } \mathcal{G} := \bigcup_{i=1}^p \bigcup_{j=1}^p \left\{ g \in \mathbb{R}^{1 \times p} : g[i] = -g[j] = 1, i \neq j, g[k] = 0 \text{ if } k \notin \{i, j\} \right\}$$

All difference operators  $G_i$  belong to  $\mathcal{G}$ .

$$N_{\mathcal{G}} := \bigcup_{g \in \mathcal{G}} \left\{ v \in \mathbb{R}^p : g\mathcal{U}(v) = 0 \right\} \quad \text{and} \quad N_I := \bigcup_{i=1}^p \bigcup_{j=1}^p \left\{ v \in \mathbb{R}^p : \mathcal{U}_i(v) = v[j] \right\}$$

**Question 37** How to interpret the sets  $N_{\mathcal{G}}$  and  $N_I$ ?

- The sets  $N_{\mathcal{G}}$  and  $N_I$  are closed in  $\mathbb{R}^p$  and obey

$$\mathbb{L}^p(N_{\mathcal{G}}) = 0 \quad \text{and} \quad \mathbb{L}^p(N_I) = 0$$

The property is true for any  $\beta > 0$  and  $(\alpha_1, \alpha_2) > 0$ .

- $\mathbb{R}^p \setminus (N_G \cup N_I)$  is open and dense in  $\mathbb{R}^p$ .

The elements of  $(N_G \cup N_I)$  are highly exceptional in  $\mathbb{R}^p$ .

- The minimizers  $\hat{u}$  of  $\mathcal{F}_v$  generically satisfy  $\hat{u}[i] \neq \hat{u}[j]$  for any  $(i, j)$  such that  $i \neq j$  and  $\hat{u}[i] \neq v[j]$  for any  $(i, j)$ .

**The minimizers  $\hat{u}$  of  $\mathcal{F}_v$  have pixel values that are different from each other and different from any data pixel.**

**Question 38** Describe the consequences if  $\ell_1 - \text{TV}$  is approximated by a smooth function like  $\mathcal{F}_v$ .

Recall the illustration on p. 24 and the results in section 3 (p. 26) and section 4 (p. 35).

Further...

[Bauss, Nikolova, Steidl 13]

- For any  $\alpha_1 > 0$  fixed, there is an inverse function  $(\psi')^{-1}(\cdot, \alpha_1) : (-1, 1) \rightarrow \mathbb{R}$  which is odd,  $\mathcal{C}^{s-1}$  and strictly increasing.

$\alpha_1 \mapsto (\psi')^{-1}(y, \alpha_1)$  is also strictly increasing on  $(0, +\infty)$ , for any  $y \in (0, 1)$ .

- Set  $\eta := \|G\|_1$ . Then

$$\beta\eta < 1 \quad \Rightarrow \quad \|\hat{u} - v\|_\infty \leq (\psi')^{-1}(\beta\eta, \alpha_1) \quad \forall v \in \mathbb{R}^p$$

- Also,  $\|\hat{u} - v\|_\infty \nearrow (\psi')^{-1}(\beta\eta, \alpha_1)$  as  $\alpha_2 \searrow 0$ .

**Full control on the bound  $\|\hat{u} - v\|_\infty$ .**

**Question 39** Can you suggest applications where the properties of  $\mathcal{F}_v$  are important?

## Exact histogram specification

- $v$  – input digital gray value  $m \times n$  image / stored as an  $p := mn$  vector
- $v[i] \in \{0, \dots, L - 1\} \quad \forall i \in \{1, \dots, p\}$       8-bit image  $\Rightarrow L = 256$
- Histogram of  $v$ :  $H_v[k] = \frac{1}{p} \#\{v[i] = k : i \in \{1, \dots, p\}\} \quad \forall k \in \{0, \dots, L - 1\}$
- Target histogram:  $\zeta = (\zeta[1], \dots, \zeta[L])$
- Goal of histogram specification (HS): convert  $v$  into  $\hat{u}$  so that  $H_{\hat{u}} = \zeta$

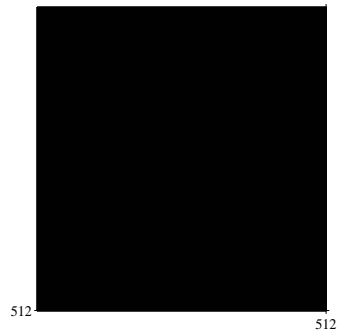
order the pixels in  $v$ :  $i \prec j$  if  $v[i] < v[j]$

$$\underbrace{i_1 \prec i_2 \prec \dots \prec i_{\zeta[1]}}_{\zeta[1]} \prec \dots \prec \underbrace{i_{p-\zeta[L]+1} \prec \dots \prec i_p}_{\zeta[L-1]}$$

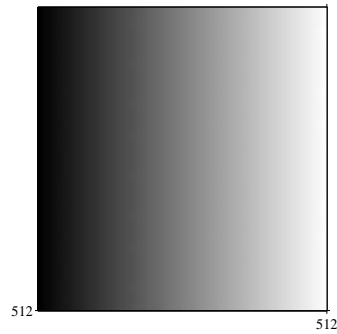
- Ill-posed problem for digital (quantized) images since  $p \gg L$
- An issue: obtain a **meaningful** total strict ordering of all pixels in  $v$

Histogram equalization is a particular case of HS where  $\zeta[k] = p/L \quad \forall k \in \{0, \dots, L - 1\}$

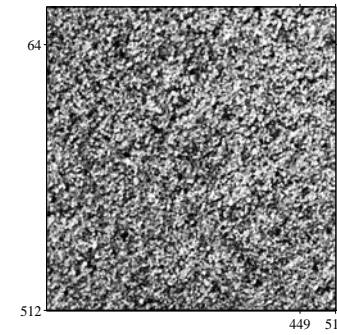
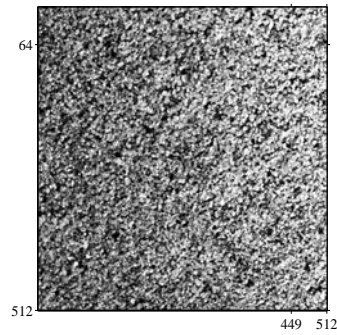
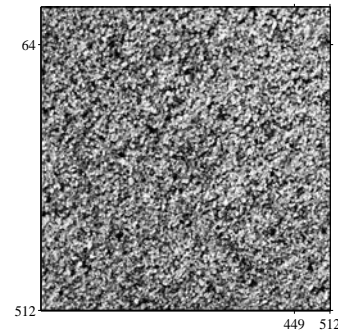
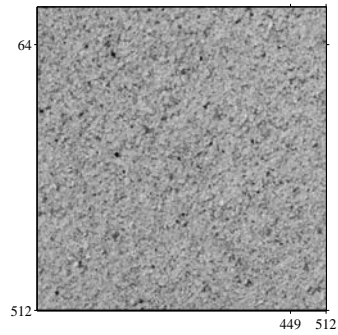
# Histogram Equalization (HE) using Matlab and our ordering



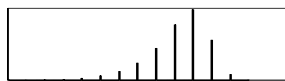
input image



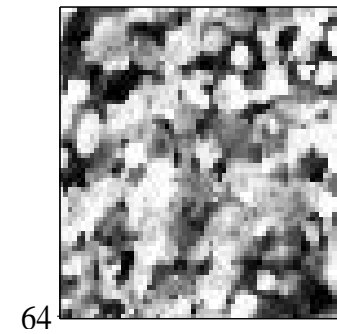
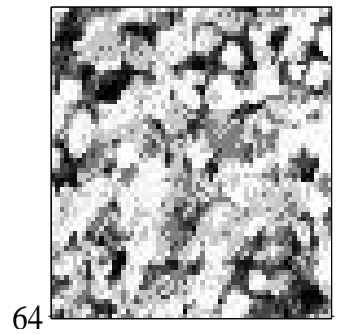
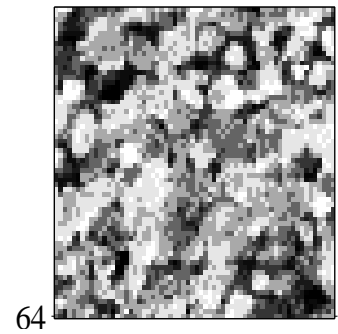
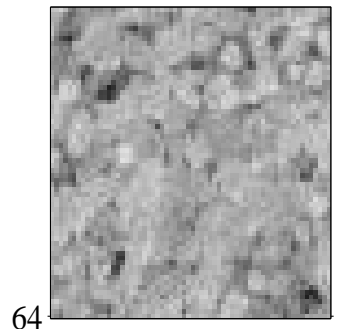
HE by "histeq"



histograms



zooms





## Modern sorting algorithms

For any pixel  $v[i]$ , extract  $K$  auxiliary information,  $a_k[i]$ ,  $k \in \{1, \dots, K\}$ , from  $v$ . Set  $a_0 := v$ . Then

$$i \prec j \quad \text{if} \quad v[i] \leq v[j] \quad \text{and} \quad a_k[i] < a_k[j] \quad \text{for some} \quad k \in \{0, \dots, K\}.$$

### Local Mean Algorithm (LM)

[Coltuc, Bolon, Chassery 06]

- If two pixels are equal and their local mean is the same, take a larger neighborhood.
- The procedure smooths edges and sorting often fails.

### Wavelet Approach (WA)

[Wan, Shi 07]

- Use wavelet coefficients from different subbands to order the pixels.
- Heavy and high level of failure.

### Specialized variational approach (SVA)

[Nikolova, Wen and R. Chan 12]

- Minimize  $\mathcal{F}_v$  for a parameter choice yielding  $\|\hat{u} - v\|_\infty \lesssim 0.1$ .
- Almost no failure, faithful order and fast algorithm.

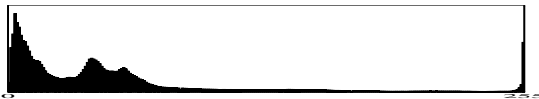
[Nikolova 13]

## Some results using $\mathcal{F}_v$ for color image enhancement

New fast histogram based color enhancement algorithm.

[Nikolova, Steidl 14]

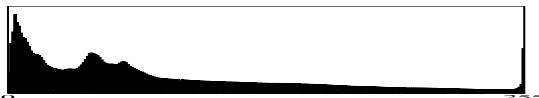
- [NS 14] M. Nikolova and G. Steidl, “Fast Hue and Range Preserving Histogram Specification: Theory and New Algorithms for Color Image Enhancement”, *IEEE Trans. Image Process.*, to appear.
- [HYL 11] J. H. Han, S. Yang, and B. U. Lee, A novel 3-D color histogram equalization method with uniform 1-D gray scale histogram, *IEEE Trans. Image Process.*, vol. 20, no. 2, pp. 506-512, Feb. 2011.
- [BCPR 07] M. Bertalmío, V. Caselles, E. Provenzi, and A. Rizzi, “Perceptual color correction through variational techniques”, *IEEE Trans. Image Process.*, vol. 16, no. 4, pp. 1058–1072, Apr. 2007.
- [APBC 09] R. Palma-Amestoy, E. Provenzi, M. Bertalmío, and V. Caselles, “A perceptually inspired variational framework for color enhancement”, *IEEE Trans. Pattern Analysis and Machine Intelligence*, vol. 31, no. 3, pp. 458–474, 2009.
- [ACE G 12] P. Gertreuer, “Automatic color enhancement (ACE) and its fast implementation”, *Image Processing On Line*, DOI: 10.5201/ipol.2012.g-ace, vol. 2012

*club* (1800 × 3200)

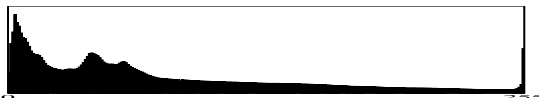
Hist.-based [NS 14]



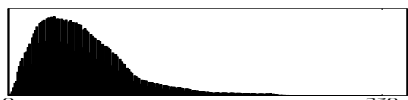
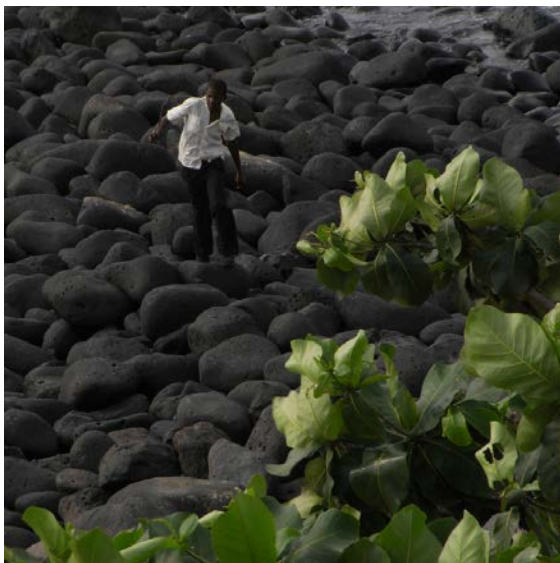
Hist.-based [NS 14]



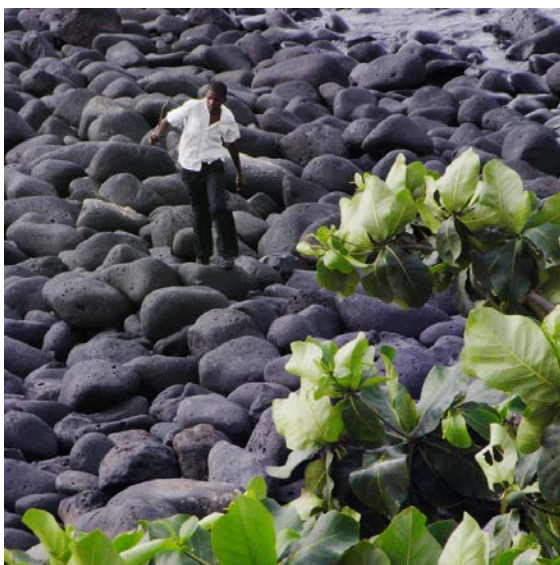
Perceptual [APBC 09]



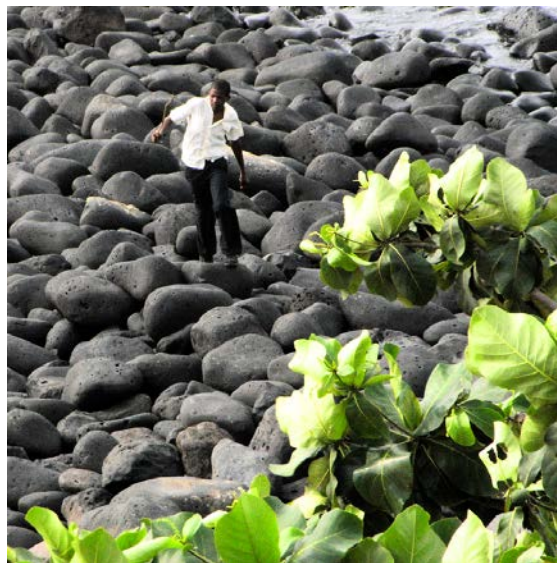


*boy-on-stones* (800 × 800)

Perceptual [BCPR 07]



Hist.-based [NS 14]



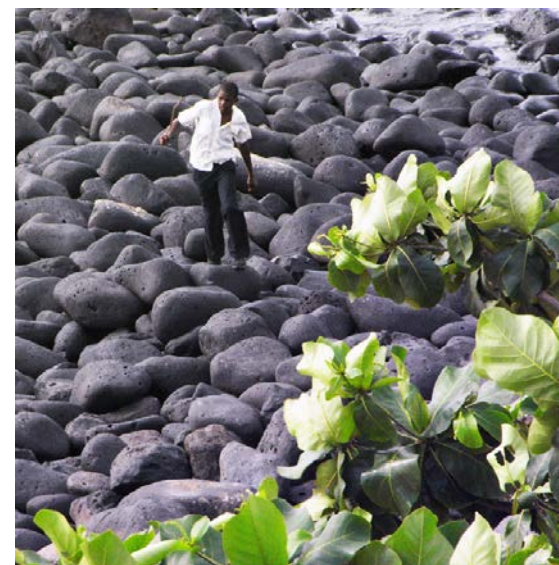
Perceptual [APBC 09]



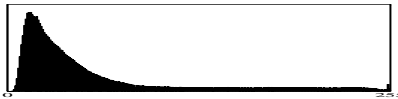
Hist.-based [HYL 11]



ACE [G 12]





*orchid* (768 × 1024)

Perceptual [APBC 09]



Hist.-based [NS 14]



Perceptual [BCPR 07]



Hist.-based [HYL 11]



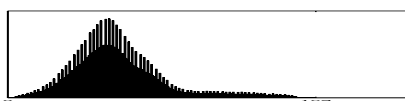
ACE [G 12]



Input “orchid” with a bad flashlight effect.



*snake* (1000 × 1000)



Hist.-based [HYL 11]



Hist.-based [NS 14]



Goal – enhance the snake.

## Summer School 2014: Inverse Problem and Image Processing

### Tutorial: Inverse modeling in inverse problems using optimization

#### Outline

1. Energy minimization methods (p. 7)
2. Regularity results (p. 17)
3. Non-smooth regularization – minimizers are sparse in a given subspace (p. 26)
4. Non-smooth data-fidelity – minimizers fit exactly some data entries (p. 35)
5. Comparison with Fully Smooth Energies (p. 51)
6. Non-convex regularization – edges are sharp (p. 54)
7. Nonsmooth data-fidelity and regularization – peculiar features (p. 62)
8. Fully smoothed  $\ell_1$ –TV models – bounding the residual (p. 83)
9. Inverse modeling and Bayesian MAP – there is distortion
10. Some References (p. 103)



## 9 Inverse modeling and Bayesian MAP

### MAP estimators to combine noisy data and prior

Bayesian approach:  $U, V$  random variables, events  $U = u, V = v$ .

Likelihood  $f_{V|U}(v|u)$ , Prior  $f_U(u) \propto \exp\{-\lambda\Phi(u)\}$ , Posterior  $f_{U|V}(u|v) = f_{V|U}(v|u)f_U(u)^{\frac{1}{Z}}$

**MAP**  $\hat{u}$  = the most likely solution given the recorded data  $V = v$ :

$$\begin{aligned}\hat{u} = \arg \max_u f_{U|V}(u|v) &= \arg \min_u ( - \ln f_{V|U}(v|u) - \ln f_U(u) ) \\ &= \arg \min_u ( \Psi(u, v) + \beta\Phi(u) )\end{aligned}$$

*MAP is the most frequent way to combine models on data-acquisition and priors*

**Realist models** for data-acquisition  $f_{V|U}$  and prior  $f_U$

$\Rightarrow \hat{u}$  must be coherent with  $f_{V|U}$  and  $f_U$

In practice one needs that:

$$\left\{ \begin{array}{l} U \sim f_U \\ AU - V \sim f_N \end{array} \right. \Rightarrow \left\{ \begin{array}{l} f_{\hat{U}} \approx f_U \\ f_{\hat{N}} \approx f_N, \quad \hat{N} \approx A\hat{U} - V \end{array} \right.$$

Our analytical results show that both models ( $f_{V|U}$  and  $f_U$ ) are violated in a MAP estimate

## Example: MAP shrinkage [Simoncelli99, Belge-Kilmer00, Antoniadis02]

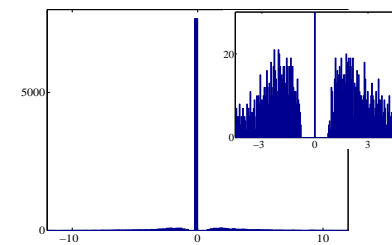
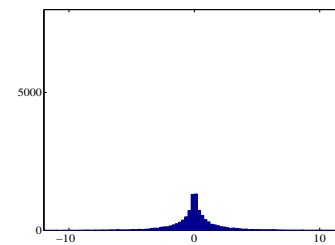
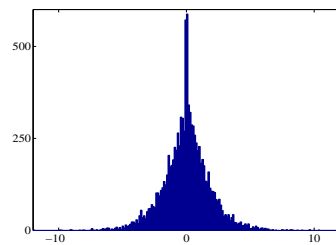
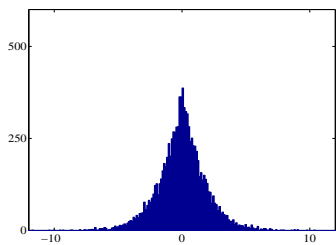
- Noisy wavelet coefficients  $y = Wv = Wu_o + n = x_o + n$ ,  $n \sim \mathcal{N}(0, \sigma^2 I)$
- Prior:  $x_o[i]$  are i.i.d.,  $f(x_o[i]) = \frac{1}{Z} e^{-\lambda |x_o[i]|^\alpha}$  (Generalized Gaussian, GG)

Experiments have shown that  $\alpha \in (0, 1)$  for many real-world images

- MAP restoration  $\Leftrightarrow \hat{x}[i] = \arg \min_{t \in \mathbb{R}} ((t - y[i])^2 + \lambda |t|^\alpha)$ ,  $\forall i$

$(\alpha, \lambda, \sigma)$  fixed—10 000 independent trials:

- (1) sample  $x \sim f_X$  and  $n \sim \mathcal{N}(0, \sigma^2)$ , (2) form  $y = x + n$ , (3) compute the true MAP  $\hat{x}$

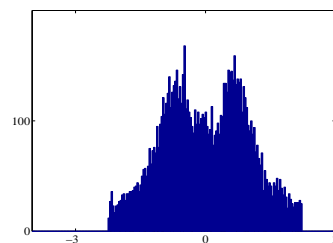
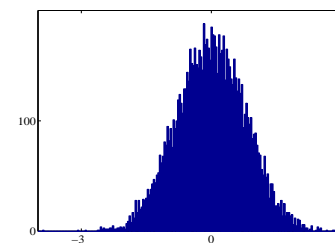
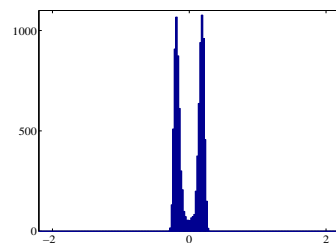
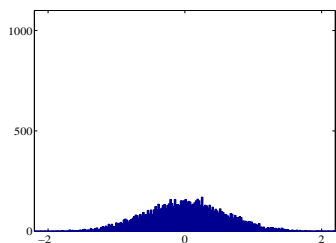


GG,  $\alpha = 1.2$ ,  $\lambda = \frac{1}{2}$

The true MAP  $\hat{x}$

GG,  $\alpha = \frac{1}{2}$ ,  $\lambda = 2$

True MAP  $\hat{x}$



Noise  $\mathcal{N}(0, \sigma^2)$

Noise estimate

Noise  $\mathcal{N}(0, \sigma^2)$

Noise estimate

## Theoretical explanations

$$V = AU + N \text{ and } f_{U|V} \text{ continuous} \Rightarrow \begin{cases} \Pr(G_i u = 0) = 0, \quad \forall i \\ \Pr(a_i u = v_i) = 0, \quad \forall i \\ \Pr(\theta_0 < \|G_i u\| < \theta_1) > 0, \quad \forall i \end{cases}$$

The analytical results on  $\hat{u} = \arg \min_u \mathcal{F}_v(u) = \text{MAP}$  yield:

- $f_U$  continuous and non-smooth at 0,  $\varphi'(0^+) > 0$  Ch. 3, p. 26

$$v \in \mathcal{O}_{\hat{h}} \Rightarrow [G_i \hat{u} = 0, \forall i \in \hat{h}] \Rightarrow \Pr(G_i \hat{u} = 0, \forall i \in \hat{h}) \geq \Pr(v \in \mathcal{O}_{\hat{h}}) > 0$$

The effective prior:  $G_i \hat{u} = 0$  for many  $i$ . (e.g. locally constant images)

- $f_N$  continuous and nonsmooth at 0,  $\psi'(0^+) > 0$  Ch. 4, p. 35

$$v \in \mathcal{O}_{\hat{h}} \Rightarrow [a_i \hat{u} = v_i, \forall i \in \hat{h}] \Rightarrow \Pr(a_i \hat{u} = v_i, \forall i \in \hat{h}) \geq \Pr(v \in \mathcal{O}_{\hat{h}}) > 0$$

The effective model: there are uncorrupted data entries.

- $-\ln f_U$  (resp.,  $\varphi$ ) continuous and nonconvex  $\Rightarrow \Pr(\theta_0 < \|G_i \hat{U}\| < \theta_1) = 0, \forall i$

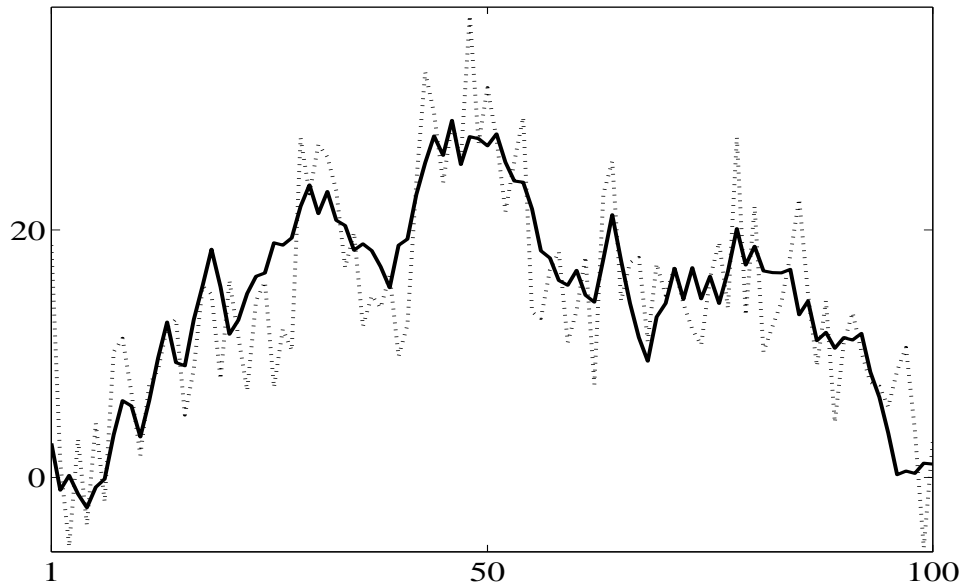
The effective prior: edges.

- $-\ln f_U$  nonconvex, nonsmooth at 0,  $\varphi'(0^+) > 0$  and  $\varphi'' \leq 0$  Ch. 6, p. 54

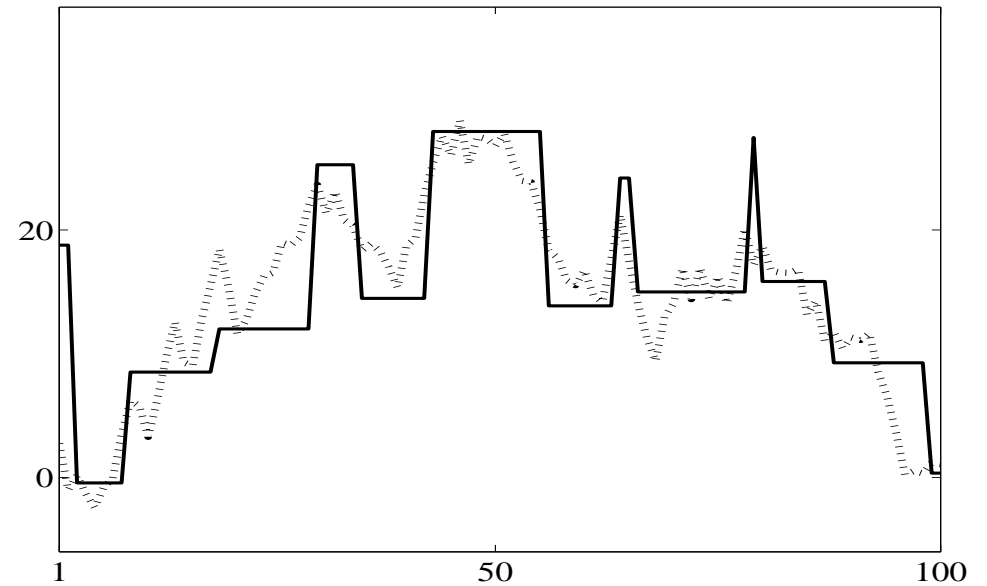
$$\Rightarrow \Pr(\|G_i \hat{u}\| = 0) > 0 \text{ and } \Pr(0 < \|G_i \hat{u}\| < \theta_1) = 0$$

## Illustration

Original differences  $U_i - U_{i+1}$  i.i.d.  $\sim f(t) \propto e^{-\lambda\varphi(t)}$  on  $[-\gamma, \gamma]$ ,  $\varphi(t) = \frac{\alpha|t|}{1+\alpha|t|}$



Original  $u_o$  (—) by  $f$  for  $\alpha = 10$ ,  $\lambda = 1$ ,  $\gamma = 4$   
 data  $v = u_o + n(\dots)$ ,  $N \sim \mathcal{N}(0, \sigma^2 I)$ ,  $\sigma = 5$ .



The true MAP  $\hat{u}$  (—),  $\beta = 2\sigma^2\lambda$   
 versus the original  $u_o$  ( $\dots$ ).

Knowing the true distributions, with the true parameters, is not enough.

**Combining models remains an open problem**

Knowledge on the features of the minimizers enables  
new energies yielding appropriate solutions to be conceived

‘ ‘ We’re in Act I of a digital revolution.’ ’

Jay Cassidy (film editor at Mathematical Technologies Inc.)

Thank you!

## 10 Some References

1. Alliney S (1992) Digital filters as absolute norm regularizers. *IEEE Trans Signal Process* SP-40:1548–1562
2. Ambrosio L, Fusco N, Pallara D (2000) *Functions of bounded variation and free discontinuity Problems*. Oxford Mathematical Monographs, Oxford University Press
3. Antoniadis A, Fan J (2001) Regularization of wavelet approximations. *J Acoust Soc Am* 96: 939–967
4. Aubert G, Kornprobst P (2006) *Mathematical problems in image processing*, 2nd edn. Springer, Berlin
5. Aubert G, Aujol J.-F. (2008) A variational approach to remove multiplicative noise, *SIAM J. on Appl. Maths.*, 68:925-946
6. Aujol J-F, Gilboa G, Chan T, Osher S (2006) Structure-texture image decomposition - modeling, algorithms, and parameter selection. *Int J Comput Vis* 67:111–136
7. Auslender A and Teboulle M. (2003) *Asymptotic Cones and Functions in Optimization and Variational Inequalities*. Springer, New York
8. Attouch, H., Bolte, J. and Svaiter, B. F. (2013) Convergence of descent methods for semi-algebraic and tame problems: proximal algorithms, forwardbackward splitting, and regularized GaussSeidel methods. *Math. Program.* 137:91-129
9. Bar L, Brook A, Sochen N, Kiryati N (2007) Deblurring of color images corrupted by impulsive noise. *IEEE Trans Image Process* 16:1101–1111
10. Bar L, Kiryati N, Sochen N (2006) Image deblurring in the presence of impulsive noise, *International. J Comput Vision* 70:279–298

11. Bar L, Sochen N, Kiryati N (2005) Image deblurring in the presence of salt-and-pepper noise. In Proceeding of 5th international conference on scale space and PDE methods in computer vision, ser LNCS, vol 3439, pp 107–118
12. Bae E, Yuan J, Tai X.-C. (2011) Global minimization for continuous multiphase partitioning problems using a dual approach, *Int. J. Comput. Vis.*, 92:112–129.
13. Baus F, Nikolova M, Steidl G. (2014) Fully smoothed  $\ell_1$ -TV models: Bounds for the minimizers and parameter choice, *J Math Imaging Vis* 48:295-307
14. Belge M, Kilmer M, Miller E (2000) Wavelet domain image restoration with adaptive edge-preserving regularization. *IEEE Trans Image Process* 9:597–608
15. Besag JE (1974) Spatial interaction and the statistical analysis of lattice systems (with discussion). *J Roy Stat Soc B* 36:192–236
16. Besag JE (1989) Digital image processing : towards Bayesian image analysis. *J Appl Stat* 16:395–407
17. Black M, Rangarajan A (1996) On the unification of line processes, outlier rejection, and robust statistics with applications to early vision. *Int J Comput Vis* 19:57–91
18. Blake A, Zisserman A (1987) *Visual reconstruction*. MIT Press, Cambridge
19. Bobichon Y, Bijaoui A (1997) Regularized multiresolution methods for astronomical image enhancement. *Exp Astron* 7:239–255
20. Bolte, J., Sabach, S. and Teboulle, M. (2013) Proximal alternating linearized minimization for nonconvex and nonsmooth problems, *Math. Program. Ser. A*, online
21. Bouman C, Sauer K (1993) A generalized Gaussian image model for edge-preserving map estimation. *IEEE Trans Image Process* 2:296–310



22. Bouman C, Sauer K (1996) A unified approach to statistical tomography using coordinate descent optimization. *IEEE Trans Image Process* 5:480–492
23. Bredies K, Kunich K, Pock T (2010) Total generalized variation. *SIAM J Imaging Sci* 3(3): 480–491.
24. Bredies K, and Holler, M. (2014) Regularization of linear inverse problems with total generalized variation. *J Inverse and Ill-posed Problems* DOI: 10.1515/jip-2013-0068.
25. Candès EJ, Donoho D, Ying L (2005) Fast discrete curvelet transforms. *SIAM Multiscale Model Simul* 5:861–899
26. Candès EJ, Guo F (2002) New multiscale transforms, minimum total variation synthesis. Applications to edge-preserving image reconstruction. *Signal Process* 82:1519–1543
27. Catte F, Coll T, Lions PL, Morel JM (1992) Image selective smoothing and edge detection by nonlinear diffusion (I). *SIAM J Num Anal* 29:182–193
28. Chambolle A (2004) An Algorithm for Total Variation Minimization and Application. *J. Math Imaging Vis* 20:89–98
29. Chan T, Esedoglu S, Nikolova M. (2006) Algorithms for finding global minimizers of image segmentation and denoising models. *SIAM J. Appl. Math.* 66:1632-1648
30. Chan T, Esedoglu S (2005) Aspects of total variation regularized  $L^1$  function approximation. *SIAM J Appl Math* 65:1817–1837
31. Chan TF, Wong CK (1998) Total variation blind deconvolution. *IEEE Trans Image Process* 7:370–375
32. Charbonnier P, Blanc-Féraud L, Aubert G, Barlaud M (1997) Deterministic edge-preserving regularization in computed imaging. *IEEE Trans Image Process* 6:298–311
33. Chellapa R, Jain A (1993) Markov random fields: theory and application. Academic, Boston

34. Chen X., M. Ng, Zhang C. (2012) Non-Lipschitz  $\ell_p$ -Regularization and Box Constrained Model for Image Restoration. *IEEE Trans Image Process* 21:4709–4721.
35. Chesneau C, Fadili J, Starck J-L (2010) Stein block thresholding for image denoising. *Appl. Comput. Harmon. Anal.* 28:67-88
36. Ciarlet PG (1989) Introduction to numerical linear algebra and optimization. Cambridge University Press, Cambridge
37. Coifman RR, Sowa A (2000) Combining the calculus of variations and wavelets for image enhancement. *Appl Comput Harmon Anal* 9:1–18
38. Do MN, Vetterli M (2005) The contourlet transform: an efficient directional multiresolution image representation. *IEEE Trans Image Process* 15:1916–1933
39. Dobson D, Santosa F (1996) Recovery of blocky images from noisy and blurred data. *SIAM J Appl Math* 56:1181–1199
40. Donoho DL, Johnstone IM (1994) Ideal spatial adaptation by wavelet shrinkage. *Biometrika* 81:425–455
41. Donoho DL, Johnstone IM (1995) Adapting to unknown smoothness via wavelet shrinkage. *J Acoust Soc Am* 90:1200–1224
42. Dontchev AL, Zollezi T (1993) Well-posed optimization problems. Springer, New York
43. Durand S, Froment J (2003) Reconstruction of wavelet coefficients using total variation minimization. *SIAM J Sci Comput* 24:1754–1767
44. Durand S, Nikolova M (2006) Stability of minimizers of regularized least squares objective functions I: study of the local behavior. *Appl Math Optim* 53:185–208, II: Study of the global behaviour. *Appl Math Optim* 53:259–277

45. Durand S, Nikolova M (2007) Denoising of frame coefficients using  $\ell^1$  data-fidelity term and edge-preserving regularization. *SIAM J Multiscale Model Simulat* 6:547–576
46. Durand S, Fadili J, Nikolova M. (2010) Multiplicative noise removal using L1 fidelity on frame coefficients. *J. Math Imaging and Vision*, 36:201-226
47. Duval V, Aujol J-F, Gousseau Y (2009) The TVL1 model: a geometric point of view. *SIAM J Multiscale Model Simulat* 8:154–189
48. Ekeland I, Temam R (1976) *Convex analysis and variational problems*. North-Holland/SIAM, Amsterdam
49. Fessler F (1996) Mean and variance of implicitly defined biased estimators (such as penalized maximum likelihood): applications to tomography. *IEEE Trans Image Process* 5:493–506
50. Fiacco A, McCormic G (1990) *Nonlinear programming*. Classics in applied mathematics. SIAM, Philadelphia
51. Geman D (1990) Random fields and inverse problems in imaging, vol 1427, *École d'Été de Probabilités de Saint-Flour XVIII - 1988*, Springer, Lecture notes in mathematics, pp 117–193
52. Geman D, Reynolds G (1992) Constrained restoration and recovery of discontinuities. *IEEE Trans Pattern Anal Mach Intell PAMI-14*:367–383
53. Geman D, Yang C (1995) Nonlinear image recovery with half-quadratic regularization. *IEEE Trans Image Process IP-4*:932–946
54. Geman S, Geman D (1984) Stochastic relaxation, Gibbs distributions, and the Bayesian restoration of images. *IEEE Trans Pattern Anal Mach Intell PAMI-6*:721–741
55. Green PJ (1990) Bayesian reconstructions from emission tomography data using a modified EM algorithm. *IEEE Trans Med Imaging MI-9*:84–93

56. Lustig M, Donoho D, Santos JM and Pauly LM (2008) Compressed Sensing MRI: a look how CS can improve our current imaging techniques: *IEEE Signal Proc. Magazine*. 25:72–82.
57. Haddad A, Meyer Y (2007) Variational methods in image processing, in “Perspective in Nonlinear Partial Differential equations in Honor of Haïm Brezis,” *Contemp Math (AMS)* 446:273–295
58. Hiriart-Urruty J-B, Lemaréchal C (1996) *Convex analysis and minimization algorithms*, vols I, II. Springer, Berlin
59. Hofmann B (1986) *Regularization for applied inverse and ill posed problems*. Teubner, Leipzig
60. Kak A, Slaney M (1987) *Principles of computerized tomographic imaging*. IEEE Press, New York
61. Keren D, Werman M (1993) Probabilistic analysis of regularization. *IEEE Trans Pattern Anal Mach Intell PAMI-15*:982–995
62. Li S (1995) *Markov random field modeling in computer vision*, 1st edn. Springer, New York
63. Li SZ (1995) On discontinuity-adaptive smoothness priors in computer vision. *IEEE Trans Pattern Anal Mach Intell PAMI-17*:576–586
64. Luisier F, Blu T (2008) SURE-LET multichannel image denoising: interscale orthonormal wavelet thresholding. *IEEE Trans Image Process* 17:482–492
65. Malgouyres F (2002) Minimizing the total variation under a general convex constraint for image restoration. *IEEE Trans Image Process* 11:1450–1456
66. Morel J-M, Solimini S (1995) *Variational methods in image segmentation*. Birkhäuser, Basel
67. Morozov VA (1993) *Regularization methods for ill posed problems*. CRC Press, Boca Raton
68. Moulin P, Liu J (1999) Analysis of multiresolution image denoising schemes using generalized Gaussian and complexity priors. *IEEE Trans Image Process* 45:909–919

69. Moulin P, Liu J (2000) Statistical imaging and complexity regularization. *IEEE Trans Inf Theory* 46:1762–1777
70. Mumford D, Shah J (1989) Optimal approximations by piecewise smooth functions and associated variational problems. *Commun Pure Appl Math* 42:577–684
71. Nashed M, Scherzer O (1998) Least squares and bounded variation regularization with nondifferentiable functional. *Numer Funct Anal Optim* 19:873–901
72. Nikolova M (2000) Local strong homogeneity of a regularized estimator. *SIAM J Appl Math* 61:633–658
73. Nikolova M (2000) Thresholding implied by truncated quadratic regularization. *IEEE Trans Image Process* 48:3437–3450
74. Nikolova M (2002) Minimizers of cost-functions involving nonsmooth data-fidelity terms. Application to the processing of outliers. *SIAM J Num Anal* 40:965–994
75. Nikolova M (2004) A variational approach to remove outliers and impulse noise. *J Math Imaging Vis* 20:99–120
76. Nikolova M (2004) Weakly constrained minimization. Application to the estimation of images and signals involving constant regions. *J Math Imaging Vis* 21:155–175
77. Nikolova M (2005) Analysis of the recovery of edges in images and signals by minimizing nonconvex regularized least-squares. *SIAM J Multiscale Model Simulat* 4:960–991
78. Nikolova M (2007) Analytical bounds on the minimizers of (nonconvex) regularized least- squares. *AIMS J Inverse Probl Imag* 1:661–677
79. Nikolova M (2007) Model distortions in Bayesian MAP reconstruction, *AIMS J Inverse Probl Imag*, 1:399–422

80. Nikolova M, Ng M, Tam CP (2013) On  $\ell_1$  Data Fitting and Concave Regularization for Image Recovery. *SIAM J. Sci. Comput* 35:397-430
81. Nikolova M (2009) One-iteration dejittering of digital video images, *J Vis Commun Image R*, 20:254–274
82. Nikolova M (2013) Description of the minimizers of least squares regularized with  $\ell_0$  norm. Uniqueness of the global minimizer. *SIAM J. Imaging Sci.*, 6: 904–937
83. Nikolova M, Wen YW, Chan R (2013) Exact histogram specification for digital images using a variational approach. *J Math Imaging Vis* 46: 309-325
84. Nikolova M, Steidl G (2014) Fast Hue and Range Preserving Histogram Specification: Theory and New Algorithms for Color Image Enhancement. *IEEE Trans Image Process* (to appear)
85. Papadakis N., Yildizoglu R., Aujol J-F. and Caselles V. (2013) High-dimension multi-label problems: convex or non convex relaxation? *SIAM J. Imaging Sci.* 6:2603–2639
86. Perona P, Malik J (1990) Scale-space and edge detection using anisotropic diffusion. *IEEE Trans Pattern Anal Mach Intell PAMI-12*:629–639
87. Potts R. B. (1952) Some generalized order-disorder transformations, *Proc. Cambridge Philos. Soc.*, 48:106–109
88. Rockafellar RT, Wets JB (1997) *Variational analysis*. Springer, New York
89. Rudin L, Osher S, Fatemi C (1992) Nonlinear total variation based noise removal algorithm. *Physica* 60 D:259–268
90. Robini, M. and Magnin, I. (2010) Optimization by stochastic continuation. *SIAM J. Imaging Sci.*, 3:1096-1121

91. Robini, M. and Reissman, P.-J. (2013) From simulated annealing to stochastic continuation: a new trend in combinatorial optimization. *J. Global Optim* 56:185–215
92. Sauer K, Bouman C (1993) A local update strategy for iterative reconstruction from projections. *IEEE Trans Signal Process* SP-41:534–548
93. Scherzer O, Grasmair M, Grossauer H, Haltmeier M, Lenzen F (2009) *Variational problems in imaging*. Springer, New York
94. Tautenhahn U (1994) Error estimates for regularized solutions of non-linear ill posed problems. *Inverse Probl* 10:485–500
95. Tikhonov A, Arsenin V (1977) *Solutions of ill posed problems*, Winston, Washington
96. Vogel C (2002) *Computational methods for inverse problems*. *Frontiers in applied mathematics series*, vol 23. SIAM, New York
97. Welk M, Steidl G, Weickert J (2008) Locally analytic schemes: a link between diffusion filtering and wavelet shrinkage. *Appl Comput Harmon Anal* 24:195–224
98. Winkler G (2006) *Image analysis, random fields and Markov chain Monte Carlo methods. A mathematical introduction*. *Applications of mathematics*, 2nd edn, vol 27. *Stochastic models and applied probability*. Springer, Berlin
99. Yuan J, Bae E, Tai X.-C. (2010) A study on continuous max-flow and min-cut approaches. *Comp Vis and Pattern Recognition*: 2217-2224
100. Yuan J, Bae E, Tai X.-C., Boykov Y. (2010) A continuous max-flow approach to Potts model. *Computer VisionECCV* 2010:379-392.